DRAFT

REVIEW OF THE LOWER ORDOVICIAN ELLENBURGER GROUP OF THE PERMIAN BASIN, WEST TEXAS

Robert Loucks

Bureau of Economic Geology
Jackson School of Geosciences
The University of Texas at Austin
Austin, TX

ABSTRACT

The Ellenburger Group of the West Texas Permian Basin is part of a Lower Ordovician carbonate platform that covered large areas of the United States. During the Lower Ordovician, the Permian Basin area was located on the southwest edge of the Laurentia plate between 20 to 30 degrees latitude. The equator crossed northern Canada situating Texas in a tropical to subtropical latitude. Texas was a shallow-water shelf with deeper water conditions to the south where it bordered the Iapetus Ocean.

Shallow-water carbonates were deposited on the shelf and deep-water shales and carbonates were deposited on the slope and in the basin. The interior of the shelf produced restricted environments, while the outer shelf produced open-marine conditions. The diagenesis of the Ellenburger Group is extremely complex and the processes that produced the diagenesis covered million of years. Three major diagenetic processes strongly affected the Ellenburger carbonates: (1) dolomitization, (2) karsting, and (3) tectonic fracturing. Pore networks in the Ellenburger are especially complex

because of the amount of brecciation and fracturing associated with karsting. The pore networks can consist of any combination of the following pore types depending on depth of burial: (1) matrix, (2) cavernous, (3) interclast, (4) crackle/mosaic breccia fractures, or (5) tectonic-related fractures.

The Ellenburger Group is an ongoing important exploration target in West Texas. The carbonate depositional systems within the Ellenburger Group are relatively simple; however, the diagenetic overprint is extremely complex producing strong spatial heterogeneity within the reservoir systems.

INTRODUCTION

The Ellenburger Group of the Permian Basin is part of a Lower Ordovician carbonate platform that covered large areas of the United States (Figures 1, 2) (Ross, 1976; Kerans, 1988, 1990). It is well known for being one of the largest shallow-water carbonate platforms in the geological record (covering thousands of square miles and up to 500 miles wide in West Texas), being extensively karsted at the Sauk unconformity, and its widespread hydrocarbon production. Hydrocarbon production ranges from as shallow as 856 ft in the West Era field in Cooke County to as deep as 25,735 ft in the McComb field in Pecos County. A review of the Ellenburger Group will aid in understanding the sedimentology and diagenesis that has lead to this widespread producing unit.

The first inclusive studies of the Ellenburger Group were completed by Cloud et al. (1945), Cloud and Barnes (1948, 1957) and Barnes et al. (1959). These studies covered many aspects of the group ranging from stratigraphy to diagenesis and chemistry. Much has been learned since then about carbonate sedimentology and diagenesis and these new concepts were integrated into later studies by Kerans (1988, 1989, and 1999). Kerans' studies covered regional geologic setting, depositional systems, facies analysis, depositional history, diagenesis, and paleokarsting. Many other papers have described the local geology of fields (e.g., Loucks and Anderson, 1980, 1985; Combs et al., 2003), outcrop areas (e.g., Goldhammer et al., 1992; Lucia, 1995, 1996; Loucks et al., 2004), or have elaborated on paleokarsting (e.g., Lucia, 1971, 1995, 1996;

Loucks and Anderson, 1985; Kerans, 1988, 1989, 1990; Loucks and Handford, 1992; Candelaria and Reed (1992); Loucks 1999; Loucks et al., 2004).

The major objectives of this paper are to review the: (1) regional geological setting and general stratigraphy, (2) depositional systems, facies analysis, and depositional history, (3) general regional diagenesis, (4) reservoir characteristics, and (5) petroleum system. Much of the data are from published literature, however, new insights can be derived from integrating these data.

REGIONAL GEOLOGICAL SETTING

At the global plate scale during the Lower Ordovician, the West Texas Permian Basin area was located on the southwest edge of the Laurentia plate between 20 to 30 degrees latitude (Figure 1) (Blakey, 2005a, 2005b). The equator crossed northern Canada (Figure 1) situating Texas in a tropical to subtropical latitude (Lindsay and Koskelin, 1993). Much of the United States was covered by a shallow sea. Most of Texas was a shallow-water shelf with deeper water conditions to the south where it bordered the Iapetus Ocean. The Texas Arch (Figures 2), a large land complex, existed in north Texas and New Mexico.

Ross (1976) and Kerans (1990) pointed out that the main depositional settings within the Permian Basin for the Ellenburger Group were the deeper water slope and the shallower water carbonate platform. In Figure 2, Ross (1976) showed the broad Lower Ordovician carbonate platform with the interior being dolomite and the outer area being limestone. Seaward of the limestone he showed black shale. Kerans (1990) interpreted Ross's map in terms of depositional settings (Figure 3). The dolomite being the restricted shelf interior and the limestone being an outer rim of more open-shelf deposits. Seaward of the platform was a deeper water slope system (shales), which Kerans (1990) stated is represented by the Marathon Limestone. The Ellenburger Group in the southern part of Texas, where the deeper water equivalent strata would have been, was strongly affected by the Ouachita Orogeny when the South American plate was thrusted against the North American plate (Figure 2). The basinal and slope facies strata were destroyed or

extensively structurally deformed. Ellenburger Group facies cannot be traced south of the slope setting in southwest Texas because of the Ouachita Orogeny.

Kerans (1990) recognized that several peripheral structural features affected the deposition of the Ellenburger sediments in the West Texas New Mexico area (Figure 4); however most of the platform was relatively flat. Major structural features in the area that formed after Early Ordovician time include the Middle Ordovician Toboas Basin and the Pennsylvanian Central Basin Platform (Galley, 1958).

Structural maps of the top Ellenburger Group (Figure 5) and top Precambrian intervals (Figure 6) show the Ellenburger Group at a structural low in the area of the Permian Basin. In the Midland Basin area, the top of Ellenburger carbonate is as deep as 11,000 ft, shallower over the Central Basin Platform, and as deep as 25,000 ft in the Delaware Basin. Isopach maps (Figure 4) by the Texas Water Development Board (1972), Wilson (1993), and Lindsay and Koskelin (1993) show thickening into the area of the Permian Basin.

GENERAL STRATIGRAPHY

The Ellenburger Group is equivalent to the El Paso Group in the Franklin Mountains, the Arbuckle Group in northeast Texas and Midcontinent, the Knox Group in the Eastern United States, and the Beekmantown Group of the northeast United States. In West Texas the Ellenburger Group overlies the Cambrian Bliss subarkosic sandstone (Loucks and Anderson, 1980). In the Llano area, Barnes et al. (1959) divided the Ellenburger Group from the bottom to the top into the Tanyard, Gorman, and Honeycut Formations. Kerans (1990) compared the Llano stratigraphic section to the subsurface stratigraphy of West Texas (Figure 7). A worldwide hiatus appeared at the end of Lower Ordovician deposition creating an extensive second-order unconformity (Sauk-Tippecanoe Supersequence Boundary defined by Sloss (1963); Figure 7). This unconformity produced extensive karsting throughout the United States and is discussed later in this report. In West Texas, the upper Middle Ordovician Simpson Group was deposited above this unconformity (Figure 7).

A general second-order sequence stratigraphic framework was proposed by Kupecz (1992) for the Ellenburger Group in West Texas (Figure 8). The contact between the Precambrian and the Lower Ordovician intervals represents a lowstand of sea level of unknown duration. The Bliss Sandstone sediments are in part lowstand erosional deposits (Loucks and Anderson, 1985). The lower second-order transgressive systems tract includes the Bliss Sandstone and the lower Ellenburger alluvial fan to interbedded shallow-subtidal paracycles. The second-order highstand systems tracts include the upper interbedded paracycles of peritidal deposits. The next second-order lowstand produced the Sauk-Tippecanoe sequence boundary.

The detailed sequence stratigraphy of the Lower Ordovician of West Texas (Figure 9) was worked out by Goldhammer et al. (1992), Goldhammer and Lehmann (1996), and Goldhammer (1996). Their work was in the Franklin Mountains in far West Texas. They compared their work to other areas including the Arbuckle Mountains in Oklahoma (Figure 9). They divided the general Lower Ordovician section, which they call the Sauk-C second-order supersequence, into nine third-order sequences (Figure 9) based upon higher order stacking patterns. Each third-order sequence had duration of 1-10 million years. Goldhammer et al. (1992) stated that the origin and control of third-order sequences in the Lower Ordovician remain problematic because this period of time lacks evidence for major glaciation.

In the Franklin Mountains, Goldhammer et al. (1992), Goldhammer and Lehmann (1996), and Goldhammer (1996) only recognized the lower seven sequences (Figure 9) and they included the Bliss Sandstone as the lowest sequence. The sequences in this area range form 2 to 6 million years in duration. Within the third-order sequences, they recognized numerous higher order sequences at the scale of fourth- and fifth-order parasequences. These higher order sequences are the detailed depositional units and consist of meter-scale aggradational or progradational depositional cycles. This is the stratigraphic architectural scale that is used for flow-unit modeling in reservoir characterization (Kerans et al., 1994).

DEPOSITIONAL FACIES AND DEPOSITIONAL SYSTEMS

Ellenburger Platform Systems

Loucks and Anderson (1980, 1985) presented depositional models (Figures 10, 11) for the Ellenburger section in the Puckett Field in Pecos County of West Texas. Their data consisted of two cores that provide ~1700 ft of overlapping, continuous coverage of the section (Figure 12). They defined the lower Ellenburger section as being dominated by alluvial fan/coastal sabkha paracycles, the middle Ellenburger as subtidal paracycles, and the upper Ellenburger as supratidal/intertidal paracycles. Numerous forth- and fifth-order cycles occur within this Puckett Ellenburger section. They recognized many solution-collapsed zones that they attributed to exposure surfaces of different duration (Figure 12).

Kerans (1990) completed the most detailed and complete regional Ellenburger depositional systems and facies analysis based on wireline log and core material. Much of the rest of this section is a summary of Kerans' work**.** See Kerans (1990) for complete description and interpretation of facies))**.** He recognized six general lithofacies (Figure 7):

(1) Litharenite: fan delta – marginal marine depositional system
(2) Mixed siliciclastic-carbonate packstone/grainstone: lower tidal-flat depositional system
(3) Ooid and peloid grainstone: high-energy restricted-shelf depositional system
(4) Mottled mudstone: low-energy restricted-shelf depositional system
(5) Laminated mudstone: upper tidal-flat depositional system
(6) Gastropod-intraclast-peloid packstone/grainstone: open shallow-water depositional system

Fan Delta – Marginal Marine Depositional System

Description: Kerans (1990) noted that this system contains two prominent facies: cross-stratified litharenite and massive to cross-stratified pebbly sandstone to

conglomerate. Sedimentary structures include thick trough and tabular crossbeds, parallel current lamination, and graded and massive beds. Clastic grains are composed of granite and quartzite rock fragments, feldspar, and quartz.

Interpretation: According to Kerans (1990) this unit was deposited as a fan delta – marginal marine depositional system. It is a basal retrogradational clastic deposit where the Ellenburger Group onlaps the Precambrian basement. Loucks and Anderson (1985) presented a similar interpretation of a fan-delta complex prograding into a shallow subtidal environment (Figure 11).

Lower Tidal-Flat Depositional System

Description: Kerans (1990) stated that the dominant facies are mixed siliciclastic-peloid packstone-grainstone, intraclastic breccia, stromatolitic boundstone containing silicified nodular anhydrite, ooid grainstone, and carbonate mudstone. These facies are mostly dolomitized. Kerans (1990) has noted that the siliciclastic content is related to the distribution of the sandstone below. Sedimentary structures include relict cross-stratification, scour channels, stromatolites, flat cryptalgal laminites, and silica replaced evaporate nodules.

Interpretation: According to Kerans (1990) this unit was deposited in a lower tidal-flat depositional system in close association with the fan delta depositional system (Figure 10). Upward in the section the carbonate tidal flats override the fan deltas. Kerans (1990) presented the idealized cycle within this system as an upward-shoaling succession. Tidal-flat complexes prograded across subtidal shoals and intervening lagoonal muds (Figure 10). The relic evaporate nodules indicate an arid sabkha climate (Loucks and Anderson, 1985; Kerans, 1990). Kerans (1990) pointed out that thin siliciclastic sand laminae in tidal-flat laminites represent eolian deposits, whereas thicker sand units represent periodic sheetflood deposits from adjacent alluvial fans. Loucks and Anderson (1985) also recognized the quartz sandstone units in the algal laminae.

High-Energy Restricted-Shelf Depositional System

Description: Kerans (1990) noted that this system is characterized by ooid grainstone, ooid-peloid packstone-grainstone, laminated, massive, and mottled mudstone, and minor cyanobacterial boundstone. Also contains coarse-crystalline white chert and rare gastropod molds. Coarse dolomite fabric is common. Depositional structures include cross-stratification, intraclastic breccias, small stromatolites, cryptalgal mats, and silicified relict nodular anhydrite.

Interpretation: According to Kerans (1990) this unit was deposited in a high-energy restricted-shelf depositional system. He stated that this system represents the period of maximum marine inundation during the Ellenburger transgression. He noted that extensive ooid shoals dominated the shelf and bioturbated mudstones formed in protected settings between shoals (Figure 11). Cryptalgal laminites and mudstones (tidal flats) with relic evaporate nodules may mark local shoaling cycles or more extensive upward shoaling events. Kerans (1990) noted that the lack of fauna suggests restricted circulation on the shelf produced by shoal-related restriction or by later destruction by dolomitization.

Low-Energy Restricted Shelf Depositional System

Description: Kerans (1990) described this widespread system as "remarkably homogeneous sequence of gray to dark-gray, fine- to medium-crystalline dolomite containing irregular mottling and lesser parallel-laminated mudstone and peloid wackestone." He noted a sparse fauna of a few gastropods and nautiloids. The facies is highly dolomitized.

Interpretation: According to Kerans (1990) this unit was deposited in a low-energy restricted-shelf depositional system (Figure 11). The mottling is considered to be the result of bioturbation. This is a restricted shelf deposit ranging from subtidal mudstones to shoaling areas with tidal flats. Kerans (1990) noted that seaward, this system interfingers with the open-marine, shallow-water shelf depositional system. This fits the model of Ross (1976) (Figure 2).

Upper Tidal-Flat Depositional System

Description: Kerans (1990) noted that the dominant facies in this system is smooth and parallel or irregular and crinkled laminated dolomite. Other facies include mottled mudstone, current-laminated dolostone, and beds of intraclastic breccia. Sedimentary structures include desiccation cracks, current laminations, nodular chert (relic evaporates?), and stromatolites.

Interpretation: According to Kerans (1990) this unit was deposited in an upper tidal-flat depositional system. A common cycle is composed of a basal bioturbated mudstone, passing through current-laminated mudstone, and into cryptalgal laminated mudstone with desiccation structures and intraclastic breccias (Figure 11). Kerans (1990) noted that the mottled and current-laminate mudstones intercalated with the laminites, are low-energy shelf deposits and intercalated ooid-peloid grainstone beds are storm deposits transported from high-energy shoals offshore (Figure 11). Kerans (1990) suggested that the upper tidal-flat depositional system consisted of a broad tidal-flat environment situated landward of the lagoon-mud shoal complex. This is similar to the model presented by Loucks and Anderson (1985) (Figure 11). This depositional system occurs near the top of the Ellenburger succession.

Open Shallow-Water Shelf Depositional System

Description: Kerans (1990) noted that the rocks in this system are mainly limestone which is in contrast to much of the other sections of the Ellenburger interval. Facies include peloid and ooid grainstones, mollusc-peloidal packstones, intraclastic breccias, cryptalgal laminated mudstones, digitate stromatolitic boundstones, bioturbated mudstones, and thin quartzarenite beds. Again, in general contrast to the other depositional systems, this system has abundant fossils including sponges, trilobites, gastropods, bivalves, and cephalopods. Kerans (1990) described the grainstones and packstones as massive or displaying parallel current laminations. He noted abundant desiccation cracks in the laminites as well as fenestral fabric.

Interpretation: According to Kerans (1990) this unit was deposited in an open shallow-water shelf depositional system. He described the depositional setting as a complex mosaic of tidal-flat subenvironments, shallow-water subtidal carbonate sand bars, and locally thin stromatolite bioherms and biostromes (Figure 11). He interpreted the greater diversity of fauna, lack of evaporate evidence, and presence of high-energy grainstones and packstones to suggest a moderate-current energy environment with open-marine circulation. He speculated that this system may have occurred close to the shelf edge or slope break.

Marathon Limestone Deeper Water System

The Marathon Limestone is the time equivalent, deeper water slope facies of the Ellenburger shallow-water platform facies (Berry, 1960; Young, 1968; Ross et al., 1982; Kerans, 1990). In West Texas, it occurs in the Marathon Basin (Young, 1968) and on the western margin of the Diablo Platform (Lucia, 1968, 1969).

Description: Kerans (1990) described the unit as containing graptolite-bearing shale, siliciclastic siltstone, lime grainstone and lime mudstone, and debris-flow megabreccia. Sedimentary structures consist of graded beds, horizontal laminations, sole marks, flute casts, and soft-sediment deformation structures (slump folds).

Interpretation: According to Kerans (1990) this unit was deposited in a more basinal setting than the laterally equivalent Ellenburger depositional systems. He defined the setting as a distally steepened ramp. He recognized that the thin-bedded shale, siltstone, and lime grainstone-mudstone packages are Bouma turbidite sequences produced by turbidity currents on a deeper water slope. Both Young (1968) and Kerans (1990) interpreted the massively bedded megabreccias as deeper water debris-flow deposits.

General Deposition History of the Ellenburger Group

Kerans (1990) summarized the depositional history of the Ellenburger Group in four stages (Figure 13).

Stage 1: Marked by retrogradational deposition of fan delta – marginal marine depositional system continuous with the Early Cambrian transgression (Kerans, 1990). Kerans (1990) described the interfingering of the basal siliciclastics with the overlying the tidal-flat and shallow-water subtidal deposits of the lower tidal-flat depositional system. This transition represents initial transgression and associated retrogradational sedimentation. Kerans (1990) noted that this stage was followed by the regional progradation and aggradation of peritidal carbonate facies. This stage of deposition filled in existing paleotopography resulting in a low-relief shelf.

Stage 2: Kerans (1990) documented rapid transgression and widespread aggradational deposition of the high-energy restricted-shelf depositional system across much of West and Central Texas during this stage. He noted that this transgression produced an extensive carbonate sand sheet over much of the platform. He interpreted a moderately hypersaline setting based on rare macrofauna, evidence of evaporites, and abundance of ooids.

Stage 3: Kerans (1990) stated that the upward transition from the high-energy restricted shelf depositional systems to the low-energy restricted-shelf depositional systems is evidence of a second regression across the Ellenburger shelf. The progradation during this stage is marked by the transition of landward upper tidal flats, to more seaward low-energy restricted subtidal to intertidal facies, to furthest seaward open-marine, shallow-water shelf facies. Kerans (1990) recognized that the laminated mudstones of the upper tidal-flat depositional system represent the maximum regression across the Ellenburger inner shelf.

Stage 4: Near the end of the Early Ordovician there was a worldwide eustatic lowstand. The timing of the lowstand is reported to be Whiterockian age (Sloss, 1963; Ham and Wilson, 1967). The length of exposure covered several million years. Throughout the United States, an extensive karst terrain formed on the Ellenburger platform carbonates (Kerans, 1988, 1989, 1990). During this long period of exposure, thick sections of cave development occurred resulting in extensive paleocave collapse breccias within the Ellenburger section (Lucia, 1971; Loucks and Anderson, 1980, 1985; Wilson, 1992; Kerans, 1988, 1989, 1990; Loucks 1999). The time equivalent, slope-deposited Marathon Limestone was not exposed during this sea-level drop (Kerans,

1990). The area appears to have had continuous deposition from the Lower Ordovician through the Middle Ordovician.

GENERAL REGIONAL DIAGENESIS

The diagenesis of the Ellenburger Group is extremely complex and the processes that produced the diagenesis covered millions of years (e.g., Folk, 1959; Lucia, 1971; Loucks and Anderson, 1985; Lee and Friedman, 1987; Kerans, 1988, 1989, 1990; Kupecz and Land, 1991; Amthor and Friedman, 1992; Loucks, 1999, 2003). Several studies have presented detailed diagenetic analysis of the Ellenburger (Kerans, 1990; Kupecz and Land, 1991; Amthor and Friedman, 1992). Several paragenetic charts are presented in Figures 14, 15. Three major diagenetic processes are important to discuss: (1) dolomitization, (2) karsting, and (3) tectonic fracturing. Other diagenetic features are present, but do not impact the appearance and reservoir quality of the Ellenburger as much as the three diagenetic events mentioned above. In the following discussion of these diagenetic processes, only an overview will be presented and the reader is referred to the literature on Ellenburger diagenesis for a complete and detailed discussion.

Understanding Diagenesis in the Ellenburger Group

As stated above, the diagenesis of the Ellenburger Group is complex. Detailed diagenesis can be worked out for any location, but trying to understand the complete diagenetic history for the entire Ellenburger carbonate section in West Texas may be beyond our reach because of relatively sparse subsurface data, long length of time (+/- 20 million years), thick stratigraphic section (possibly up to six third-order sequences), and the large area involved. It is important to keep in mind that carbonates generally undergo diagenesis very early in their history, especially if they are subjected to meteoric water. With the number of third-order sequences in the section and the time represented by each sequence (2 to 5 million years), extensive early and shallow diagenesis probably occurred but has been later masked by extreme dolomitization.

At the end of Early Ordovician time, a several million year hiatus occurred exposing the Ellenburger Group and subjecting it to meteoric karst processes. Several authors have demonstrated that the karst affected strata at least 300 to 1000 feet beneath the unconformity (e.g., Kerans 1988, 1989; Lucia, 1995; Loucks, 1999). With the occurrence of the Ouachita thrusting from Mississippian through Pennsylvanian, vast quantities of hydrothermal fluids moved though the available permeable pathways within the Ellenburger producing late stage diagenesis (e.g., Kupecz and Land, 1991). Following lithification, different parts of the Ellenburger Group were subjected to tectonic stresses and was fractured producing more late stage diagenesis that probably affected local areas (e.g., Loucks and Anderson, 1985; Kearns, 1990; Loucks, 2003).

Loucks (2003) presented an overview of the origins of fractures in Ordovician strata and concluded that in order to understand the complex diagenesis in these strata, one must sort all the events into a well documented paragenetic sequence. This is the most reliable method to delineate timing of events and features. He was able to demonstrate that karsting and paleocave collapse breccias and related fractures and some tectonic fractures occurred before the hydrothermal events that produced saddle dolomite. This was accomplished by establishing well documented paragenetic relationships.

Dolomitization

Of the several authors (Kerans, 1990; Kupecz and Land, 1991; Amthor and Friedman, 1992) that have attempted to understand the regional dolomite history, Kupecz and Land (1991) appear to have made the most progress. This section will mainly address the finding of Kupecz and Land (1991), but still include observations and conclusions from the other authors. Kupecz and Land's (1991) paragenetic sequence is presented in Figure 14. Their study covered a large area of West Texas as well as the Llano Uplift area in Central Texas. They used both cores and outcrop as a data source and combined petrography with carbon, oxygen, and strontium isotopes.

They recognized five general stages of dolomitization (Figure 14). The generations of dolomite were separated into early-stage dolomitization which predated the Sauk unconformity and late-stage dolomitization that post dated the Sauk

unconformity. They attribute 90 percent of the dolomite as early stage and 10 percent of the dolomite as late stage.

Kupecz and Land (1991) dolomite types:

(1) Stage 1 pre-karstification early-stage dolomite (Dolomite E1)
    a. Description: Crystal size ranges from 5 to 700 μ but varies by facies. In the cryptalgal laminites it comprises crystal sizes ranging from 5 to 100 μ. These euhedral crystals have planar interfaces. In millimeter-laminated facies the crystal size ranges from 5 to 70 μ and in the bioturbated mudstones the crystal size ranges from 5 to 700 μ. Kupecz and Land (1991) thought that some of the coarser crystals were a product of later recrystallization.
    b. Interpretation: Kupecz and Land (1991) documented that this dolomite replaced lime mud or mudstone and that the dolomite predated karstification because it is found in nonkarsted rock as well as in clasts created by karsting. Therefore, it must have formed before karsting to be able to be brecciated. Probable source of Mg for dolomitization is sea water (Kupecz and Land, 1991).
(2) Stage 2 post-karstification late-stage dolomite (Dolomite L1)
    a. Description: This replacement dolomite consists of coarse-crystalline euhedral rhombs with crystal size ranging from 200 to 2000 μ. Its homogeneous cathodoluminescence and homogeneous backscattered imaging suggest that this dolomite type has undergone recrystallization (Kupecz and Land, 1991). This stage of dolomitization is a regional event and is related to hydrothermal fluids.
    b. Interpretation: Late-stage origin is based on coarse-crystal size (Kupecz and Land, 1991).
(3) Stage 3 post-karstification late-stage dolomite (Dolomite L2)

a. Description: Crystals have planar interfaces and size ranges from 100 to 3500 μ and has subhedral to anhedral crystal shapes. Extinction ranges from straight to undulose.
b. Interpretation: It is a replacement type of dolomite (Kupecz and Land, 1991). Late origin is based on relationship to a later stage chert and its replacement of early-stage dolomite E1. Much of the grainstone facies is replaced by this stage of dolomitization. This stage of dolomitization is related to hydrothermal fluids. Probable source of Mg for dolomitization is dissolution of previous precipitated dolomite (Kupecz and Land, 1991).

(4) Stage 4 post-karstification late-stage dolomite (Dolomite C1)
a. Description: Crystals are subhedral with undulose extinction (saddle/baroque dolomite) and crystal size ranges from 100 to 5000 μ.
b. Interpretation: Pore-filling cement (Kupecz and Land, 1991). Paragenetic sequence is established by the fact that Dolomite C1 post dates Dolomite L2 and was corroded before Dolomite Cement 2 was precipitated. Probable source of Mg for dolomitization is dissolution of previous precipitated dolomite (Kupecz and Land, 1991). This stage of dolomitization is a regional event and is related to hydrothermal fluids.

(5) Stage 5 post-karstification late-stage dolomite (Dolomite C2)
a. Description: Subhedral white crystals with moderate to strong undulose extinction (saddle/baroque dolomite) and crystal size ranges from 100 to 7500 μ. Contain abundant fluid inclusions.
b. Interpretation: Pore-filling cement (Kupecz and Land, 1991). Occurred after corrosion of dolomite C1. Probable source of Mg for dolomitization is dissolution of previous precipitated dolomite (Kupecz and Land, 1991). This stage of dolomitization is related to hydrothermal fluids.

Kupecz and Land (1991) have provided the only integrated analysis of fluid-flow pathways and sources of Mg for the different dolomitizing events. The early-stage pre-karstification dolomite is associated with the muddier rocks and the source of Mg was probably sea water. Kerans (1990) similarly attributed these finer crystalline dolomites to

penecontemporaneous replacement of mud in tidal flats and to regionally extensive reflux processes during deposition.

The late-stage post-karstification dolomites are attributed by Kupecz and Land (1991) to warm, reactive fluids, which were expelled from basinal shales during the Ouachita Orogeny. The fluids are thought to have been corrosive as evidenced by corroded dolomite rhombs (Kupecz and Land, 1991). This corrosion provided the Mg necessary for dolomitization. The warm, overpressured fluids were episodically released and migrated hundreds of miles from the fold belt toward New Mexico (Figure 15). These fluids migrated through high-permeability aquifers of the Bliss sandstone, basal subarkose facies of the Ellenburger, as wall as grainstone facies and paleocave breccia zones. Figure 15 from Kupecz and Land (1991) shows the regional isotopic composition of late-stage dolomite L2. The pattern of lighter to heavier delta-O^{18} away from the fold belt to the south, suggests movement and cooling of fluids to the northwest. Kupecz and Land (1991) regional dolomitization model is displayed in Figure 15. Figure 16 show the tectonic setting that produced the hydrothermal fluids.

Kerans (1990) defined three major styles of dolomitization:

(1) Very fine crystalline dolomite that he considered as a replacement product penecontemporaneous with deposition in a tidal-flat setting.
(2) Fine- to medium-crystalline dolomite appearing in all facies and contributed to regionally extensive reflux processes during Ellenburger deposition.
(3) Coarse-crystalline replacement mosaic dolomite and saddle (baroque) dolomite associated with burial.

Kerans first two types of dolomite are probably equivalent to Kupecz and Land's (1991) early-stage Dolomite E1. His coarse-crystalline replacement mosaic dolomite and saddle dolomite are equivalent to Kupecz and Land's (1991) late-stage dolomites.

Amthor and Friedman (1992) also recognized early- to late-stage dolomitization of the Ellenburger Group (Figures 17, 18). Similar to Kerans (1990) and Kupecz and Land (1991), Amthor and Friedman (1992) described early-stage, low-temperature, fine-crystalline dolomites associated with lime muds where the Mg was supplied by diffusion from overlying seawater. Amthor and Friedman (1992) also describe medium- to coarse-

crystalline dolomite that replaces grains and matrix in the depth range of 1500 to 6000 ft. These dolomites are post-karstification and are probably replacement Dolomite L1 and L2 of Kupecz and Land (1991). Amthor and Friedman's (1992) last stage of dolomite is assigned a deep-burial origin (>6000 ft) and consists of coarse-crystalline saddle dolomite. Its occurrence as both pore filling and replacive. This is Dolomite L2, C1, and C2 of Kupecz and Land (1991). Amthor and Friedman (1992) also noticed extensive corrosion of previously precipitated dolomite and they invoked a similar fluid-flow model as Kupecz and Land (1991) from which the fluids were associated with the Ouachita Orogeny.

Overall, much of the Ellenburger is dolomitized. Dolomitization favors preserving open fractures and pores because it is mechanically and chemically more stable than limestone. Pores within dolomites are commonly preserved to deeper burial depths and higher temperatures than pores in limestone. Also, limestone breccia clasts tend to undergo extensive pressure solution at their boundaries and lose all interclast pores (Loucks and Handford, 1992), whereas dolomite breccia clasts are more chemically and mechanically stable with burial.

Karsting

Karsting is a complex and large-scale diagenetic event that strongly affected the Ellenburger Group. The process may affect only the surface of a carbonate terrain forming *terra rossa* or extensively dissolve the carbonate surface creating karst towers (Figure 19). It can also produce extensive subsurface dissolution in the form of dolines, caves, etc (Figure 19). The next several paragraphs are meant to provide background information on karst systems that are seen in the Ellenburger Group.

Review of caves and paleocaves

Loucks (1999) provided a review of paleocave carbonate reservoirs. He stressed that to understand the features of paleocave systems, an understanding of how paleocave systems form is necessary. The best approach to this understanding is to review how

modern cave systems form at the surface and evolve into coalesced, collapsed-paleocave systems in the subsurface. Loucks (1999) described this evolutionary process, and the review presented here is mainly from that investigation.

To describe the features or elements of both modern and ancient cave systems, Loucks (1999) proposed a ternary classification of breccias and clastic deposits in cave systems based on relationships between crackle breccia, chaotic breccia, and cave-sediment fill (Figure 20). Crackle breccias have thin fractures separating breccia clasts. Individual clasts can be fitted back together. Mosaic breccias are similar to crackle breccias, but displacement between clasts is greater and some clast rotation is evident. Chaotic breccias are characterized by extensive rotation and displacement of clasts. The clasts can be derived from multiple horizons, producing polymictic breccias. Chaotic breccias grade from matrix-free, clast-supported breccias to matrix-supported breccias.

Loucks (1999) also showed that paleocave systems have complex histories of formation (Figure 21). They are products of near-surface cave development, including dissolutional excavation of passages, breakdown of passages, and sedimentation in cave passages. This is followed by later-burial cave collapse, compaction, and coalescence.

Phreatic or vadose-zone dissolution create cave passages (Figures 19, 21). Passages are excavated where surface recharge is concentrated by preexisting pore systems, such as bedding planes or fractures (Palmer, 1991) that extend continuously between groundwater input, such as sinkholes, and groundwater output, such as springs (Ford, 1988).

Cave ceilings and walls are under stress from the weight of overlying strata. A tension dome, a zone of maximum shear stress, is induced by the presence of a cavity (White, 1988). Stress is relieved by collapse of the rock mass within the stress zone. The collapse of the ceiling and wall rock commonly starts in the vadose zone. In the phreatic zone, water supplies 40% of the ceiling support through buoyancy (White and White, 1969). The removal of this support in the vadose zone weakens the ceiling and can result in its collapse. Major products of collapsed ceiling and walls are chaotic breakdown breccia on the floor of the cave passage (Figures 19, 21). In addition, the stress release around cave passages produces crackle breccias in the cave-ceiling and cave-wall host rocks (Figures 19, 21).

Near-surface dissolutional excavation and cave sedimentation terminate as cave-bearing strata are buried into the subsurface. Extensive mechanical compacting begins, resulting in collapse of remaining passages and further brecciation of blocks and slabs (Figure 21). Multiple stages of collapse occur over a broad depth range, Foot-scale bit drops (cavernous pores) are not uncommon at depths of 6000 to 7000 ft (Loucks, 1999). The areal cross-sectional extent of brecciation and fracturing after burial and collapse is greater than that of the original passage (Figure 21). Collapsed, but relatively intact strata over the collapsed chamber are fractured and form burial cave-roof crackle and mosaic breccias with loosely to tightly fitted clasts (Figure 21). Sag feature and faults (suprastratal deformation) can occur over collapsed passages (Figure 21) (Lucia, 1971, 1995, 1996; Kerans, 1988, 1989, 1990; Hardage et al., 1996; Loucks, 1999, 2003).

The development of a large collapsed paleocave reservoir is the result of several stages of development (Figure 22). The more extensive coalesced, collapsed-paleocave system originated at composite unconformities where several cave system may overprint themselves during several million years of exposure to karst process (Figure 22) (Esteban 1991; Lucia, 1995; Loucks, 1999). As the multiple-episode cave system subsides into the deeper subsurface, wall and ceiling rock adjoining open passages collapse and form breccias that radiate out from the passage and may intersect with fractures from other collapsed passages and older breccias within the system. This process forms coalesced, collapsed paleocave systems and associated reservoirs that are hundreds to thousands of feet across, and thousands of feet long, and tens to hundreds of feet thick. Internal spatial complexity is high, resulting from the collapse and coalescing of numerous passages and cave-wall and cave-ceiling strata. These breccias and fractures are commonly the major reservoirs in the Ellenburger Group. The reader is referred to Kerans (1988, 1989, 1990), Loucks and Handford (1992), Hammes (1996), and Loucks (1999, 2001, 2003) for discussions about paleocave systems in the Ellenburger Group.

Loucks and Mescher (2001) have developed a classification of paleocave facies (Figure 23, Table 1). Six basic cave facies are recognized in a paleocave system and are classified by rock textures, fabrics, and structures: (1) undisturbed strata (undisturbed host rock), (2) disturbed strata (disturbed host rock), (3) highly disturbed strata (collapsed roof and

wall rock), (4) coarse chaotic breccia (collapsed-breccia cavern fill), (5) fine chaotic breccia (transported-breccia cavern fill), and (6) sediment fill (cave-sediment cavern fill). Each of paleocave facies can be distinct and adjoin sharply with adjacent facies, or they may show gradation into adjacent facies within the coalesced collapsed-paleocave system. Pore networks associated with paleocave reservoirs can consist of cavernous pores, interclast pores, crackle and mosaic breccia fractures, tectonic fractures, and less commonly, matrix pores. The paleocave facies classification, in conjunction with burial history data, can be used to describe the complex geology expressed in coalesced collapsed-paleocave systems and can be used to understand and predict pore-type distribution and magnitude of reservoir quality.

Ellenburger Karsting

In the Ellenburger Group, extensive cave systems formed at a composite unconformity (Sauk unconformity) that lasted several million years to several tens of million years. Many authors have recognized this karsting and associated features in the Ellenburger Group. Barnes et al. (1959) recognized solution collapse in the Ellenburger Group and stated that "… a matrix composed of material foreign to the formation indicates breccia formed by solution and collapse probably related to an erosional unconformity." Lucia (1971) was the first to promote that the extensive brecciation seen in the El Paso Group (equivalent to Ellenburger Group) was associated with karst dissolution and were not the result of tectonic brecciation. Loucks and Anderson (1980, 1985) in the Puckett Field in Pecos County also realized that many of the breccias in the Ellenburger Group were related to solution collapse (Figure 11). They associated them with exposed diagenetic terrains. Kerans (1988, 1989, 1990) strongly established karsting and cave development in the Ellenburger Group. He proposed paleocave models (Figure 24) that were immediately accepted and applied.

Lucia's (1971, 1995, 1996) work in the El Paso Group in the Franklin Mountains of far West Texas presented an excellent outcrop analog for coalesced, collapsed paleocave systems. He has mapped a large paleocave system that was developed in the upper 1000 ft of the El Paso Group during a 33 million year time gap (Figures 25, 26).

Large fracture systems and collapse breccia zones of 1000 ft thick and 1500 ft wide, and over a mile long mark the collapsed paleocave system. Lucia (1995) noted that the cavernous porosity could have been as high as 30% before infilling with cave-sediment fill and cement.

Within the southern Franklin Mountains, Lucia (1995) described the Great McKelligon Sag in McKelligon Canyon along the eastern face (Figure 27). The sag is ~1500 ft wide and ~150 ft deep. The sag formed by the collapse of paleocaves in the El Paso section after the Montoya and Fusselman units were deposited, buried, and lithified. This is an important feature representing the complete picture of a coalesced, collapsed paleocave system (Loucks, 1999). Loucks (2003) has stressed that the collapse of a coalesced paleocave system not only affects the karsted unit, but also strongly affects the units above (Figure 22). Loucks (2003) has called the deformation of the younger lithified units "suprastratal deformation." Besides the example of suprastratal deformation shown in the Great McKelligon Sag, examples of suprastratal deformation from seismic in the Ellenburger Group can be seen in Hardage et al. (1996) and Loucks (1999, 2003) and from wireline-log cross sections by Kerans (1999) (his Figure 25).

Kerans (1988, 1989, and 1990) presents an excellent overview of paleokarst in the Ellenburger Group. His paleocave models (Figure 24) were the first to define paleocave floor, paleocave sediment fill, and paleocave roof. Figures 28-32 presents several cores and associated core slabs from collapsed paleocave systems. These core descriptions emphasize Kerans' paleocave model. The paleocave terrigenous-bearing sediment fill is strikingly apparent from the gamma-ray, spontaneous potential, and resistivity logs (Kerans, 1988, 1989, 1990). These paleocave fabrics can be recognized on electrical imaging tools (Hammes, 1997). Kerans (1988, 1989) discussed several breccia types: (1) a laterally persistent breccia association formed in the upper phreatic zone (water-table) karst and (2) a laterally restricted breccia association formed by deep phreatic dissolution and collapse.

Kerans (1990) in his sequence of diagenetic events (his Figure 37) noted that the Ellenburger section was subjected to karsting during several periods of time. The main karst event was at the Early Ordovician Sauk-Tippecanoe Supersequence boundary. In local areas it was again karsted several more times. In the Llano area of Texas, Kupecz

and Land (1991) showed that the Ellenburger stayed near the surface until deep burial during later Pennsylvanian subsidence (Figure 33A). Loucks et al. (2000) recognized conodonts in cave-sediment fill from paleocaves in the Llano that would indicate exposure during the Middle to late Ordovician, Late Devonian, and Earliest Mississippian times. Also, they established other strong periods of karsting during the Pennsylvanian, Cretaceous, and Tertiary times. Combs et al. (2003) noted a second period of karsting in the Ellenburger interval in the Barnhart Field in Regan County where the Wolfcamp clastic overlies the Ellenburger Group. Their burial history diagram (Figure 33B) displays the two periods of karsting.

Tectonic Fracturing

In the past there has been controversy on the origin of many of the breccias and fractures in the Ellenburger Group. Some workers (e.g., Ijirighoi and Schreiber, 1986) wanted to assign most, if not all fractures, and breccias to a tectonic origin. They believed that faulting could produce these widespread breccias. The extensive size and shapes of most of the Ellenburger breccias and the inclusion of cave-sediment fill, speleothems, and younger conodonts, preclude a simple tectonic origin (Loucks, 2003).

However, several authors have noted tectonic fractures in the Ellenburger section (e.g., Loucks and Anderson, 1985; Kearns, 1989; Holtz and Kerans, 1992; Combs et al., 2003). Each of the authors recognized that the tectonic fractures cut across lithified breccias. Kerans (1989) noted the fractures cutting late saddle dolomite. Kerans (1989) suggested that the Pennsylvanian foreland deformation that affected much of West and Central Texas, as described by Budnik (1987), probably produced many tectonic related fractures. However, as pointed out by many authors, paleocave collapse also can produce fractures that are not associated with tectonic events. Kerans (1990), Lucia (1996), and Loucks (1999, 2003) showed that suprastratal deformation above collapsing paleocave systems can create sags, faults, and numerous fractures (Figure 22).

Kerans (1989) pointed out several distinct ways to separate karst-related fractures from tectonic-related fractures:

(1) Tectonic fractures are commonly the youngest fractures in the core and generally cross cut karst-related fractures.
(2) Tectonic fractures post-date saddle dolomite. In the Llano area, however, saddle dolomite fills in a well-developed Pennsylvanian fracture set (Loucks, 2003).
(3) Karst-related fractures are generally near the top of the Ellenburger section, whereas tectonic-related fractures can occur throughout the Ellenburger section.

Loucks and Mescher (1998) presented additional criteria for separating karst-related fractures from tectonic-related fractures:

(1) Tectonic fractures generally show a strong relationship to regional stress patterns and have well defined oriented sets of fractures, whereas karst-related fractures respond to near-field stresses and fracture orientation is more random than tectonic fractures.
(2) Regional tectonic fractures are usually spaced at greater than the inch scale and commonly at the foot or larger scale. Karst-related fractures (crackle breccia fractures can be very closely spaced only a fraction of an inch apart.
(3) Breccias associated with tectonic derived faults commonly from a narrow band around the fault only a few feet wide but may be tens of feet wide. Karst-related breccias can be thousands of feet wide and hundreds of feet thick, contain a large range of clast sizes, and show hydrodynamic sedimentary structures.
(4) Tectonic faults are linear or curved in map view. Karst-related faults are linear, curved, or cylindrical (Hardage et al., 1996; Loucks, 1999) in map view.

Tectonic- and karst-related fractures are both present in the Ellenburger section. Detailed analysis of the fractures usually can define their origin.

RESERVOIR CHARACTERISTICS

Pore Types

Pore networks in the Ellenburger are especially complex because of the amount of dolomitization, brecciation and fracturing associated with karsting, and regional tectonic deformation. The pore networks can consist of any combination of the following pore types depending on depth of burial (Loucks, 1999): (1) matrix, (2) cavernous, (3) interclast, (4) crackle/mosaic breccia fractures, or (5) tectonic-related fractures.

Loucks (1999) presented an idealized plot of how karst-related Ellenburger pore networks probably change with depth (Figure 34). Relative abundance of pore types and relative depth of burial are estimates based on review of near-surface modern cave systems and buried paleocave systems (see Table 2 in Loucks, 1999). Large voids may be preserved down to 8000 to 9000 feet of burial, but eventually collapse forming smaller interclast pores and fractures associated with crackle and mosaic breccias. Coarse-interclast pores between large clasts are reduced by rotation of clasts to more stable positions and by rebrecciation of clasts to smaller fragments (Figure 21). As passages and large interclast pores in the cave system collapse, fine-interclast pores first increases and then decreases, whereas fracture pore types become more abundant. Cave-sediment fill is commonly cemented tight during burial diagenesis in the Ellenburger carbonates, especially if it is terrigenous sediment or has a terrigenous sediment component. In the Ellenburger carbonates, matrix porosity is generally low (<5%) and consists of the common matrix pore types such as interparticle, moldic, intercrystalline, or micropores. See Table 1 (Loucks and Mescher, 2001) for a general estimate of reservoir quality by paleocave facies types.

Three-Dimensional Architecture of an Ellenburger Coalesced, Collapsed Paleocave System

The three-dimensional, interwell-scale architecture of a Lower Ordovician Ellenburger coalesced, collapsed paleocave system was constructed through the

integration of 7.8 miles of ground-penetrating radar (GPR), 29 shallow cores (~50-foot long), and outcrop data within a large quarry (McMechan et al., 1998, 2002; Loucks et al., 2000; Loucks et al., 2004). The data were collected near Marble Falls in Central Texas over an area (~2600 by ~3300 ft) that could cover several oil-well locations (~160 ac) typical of a region such as West Texas (Figure 35). Integration of core-based facies descriptions with GPR-reflection response identified several paleocave facies that can be deciphered and mapped with GPR data alone (Figure 36): (1) continuous reflections image the undisturbed strata, (2) relatively continuous reflections (over tens of feet) characterized by faults and folds image the disturbed strata, and (3) chaotic reflections having little to no perceptible continuity image heterogeneous cave-related facies recognized in core that cannot be individually resolved with the GPR data. These latter facies include the highly disturbed strata, coarse-clast chaotic breccia, fine-clast chaotic breccia, and cave-sediment fill.

The three-dimensional architecture of the coalesced, collapsed paleocave system based on core and GPR data indicates that there are trends of brecciated bodies that are as much as 1100 ft wide, greater than 3300 ft long, and tens of feet high (Figures 37, 38). These brecciated bodies are coalesced, collapsed paleocaves. Between the brecciated bodies are areas of disturbed and undisturbed host rock that are jointly as much as 660 ft wide. Representative cores from the study are presented in Figure 39.

As a cave system was buried, many structural features formed by mechanical compaction and these features were documented in the study by McMechan et al. (1998, 2002) and Loucks et al. (2004). These features include folds, sags, and faults. The folds and sags measure from ~10 ft to several hundred feet wide. The collapse-related faults are numerous and can have several feet of throw. Most are normal faults, but some reverse faults also occur. See Figures 40 to 43 for examples of collapsed paleocave features from GPR and outcrop data.

Megascale Architecture

Coalesced, collapsed paleocave systems are megascale geologic features that can have dimensions of hundreds to thousands of square miles laterally and several thousand

feet vertically (Loucks, 1999, 2003). Strata above and below the unconformity are affected by late collapse in the subsurface (Figure 22).

A coalesced, collapsed paleocave system can be divided into two parts: (1) a lower section of karsted strata that contains collapsed paleocaves and (2) an upper section of strata that is deformed to various degrees (suprastratal deformation) by the collapse and compaction of the lower section of paleocave-bearing strata (Figure 22). The collapse and compaction of cave systems provide the potential for the development of large-scale fracture/fault systems that can extend from the collapsed interval upward several thousand feet. These fracture/fault systems are not related to regional tectonic stresses.

Both Kerans (1990) and Loucks (1999) speculated that the regional pattern of karsted Ellenburger reservoirs probably follow a rectilinear pattern as a result of regional fractures controlling cave development. Loucks (1999) presented data from subsurface seismic and from mining areas that express the rectilinear pattern of paleocave systems (Figure 44). Lucia (1995) presented a map of the paleocave system in the El Paso Group that also displays a rectilinear pattern (Figure 26). The coalesced brecciated bodies mapped by Loucks et al. (2004) in the Marble Falls area are rectilinear (Figure 37). At a larger scale, Canter et al. (1993) showed a regional isopach map of Ellenburger paleocave-sediments over tens of square miles (Figure 45). The map has a strong rectilinear pattern. Also, a modified map of Hardage (1996) of rectilinear suprastratal deformation trends, associated with Ellenburger subsurface paleocave collapse, in Wise County, Texas line up in a rectilinear pattern (Figure 46). Therefore there is strong evidence that coalesced, collapsed paleocave systems have rectilinear patterns that may be associated with regional fracture systems. However, at the present time there is no definitive study that has shown the actual regional paleofracture system that has controlled these rectilinear patterns.

HYDROCARBON PRODUCTION

Holtz and Kerans (1992) estimated that the original in-place oil in the Lower Ordovician strata to be ~11 MMBOE of which 3.8 MMBOE was produced at the time of their article. Production from the Ellenburger since 1970 from the Texas Railroad

Commission files has been 488.5 million barrels of oil and 13.5 trillion cubic feet of gas (personal communication from Romulo Briceno). Total hydrocarbons produced are 2, 249 billion BOE.

Holtz and Kerans (1992) tabulated 149 oil and/or gas reservoirs that each has produced more than 1 million bbl of oil equivalent. According to the Texas Railroad Commission files there are approximately 700 fields of various sizes within the Ellenburger Group within Texas (personal communication from Romulo Briceno).

Holtz and Kerans (1992) divided the Ellenburger reservoirs into three groups (Figure 47):

(1) Karst-modified reservoirs: Reservoirs formed in the inner ramp depositional setting and affected by extensive dolomitization and karsting. Karst-related fractures and interclast pores are the main pore types with tectonic fractures secondary. These reservoirs are characterized by moderately thick net pay, low porosity, moderate permeability, low initial water saturation, and moderate residual oil saturation.

(2) Ramp carbonates: Reservoirs formed in middle to outer ramp depositional setting and were dolomitized to various degrees. Predominant pores types are intercrystalline and interparticle with tectonic and karst fractures being secondary. These reservoirs are characterized by thinnest net pay, highest porosity, moderate permeability, highest initial water saturation, and highest residual oil saturation.

(3) Tectonically fractured dolomites: Reservoirs formed in the inner ramp depositional environment, subsequently extensively dolomitized, karsted, and lastly extensively tectonically fractured. Tectonic-related fractures are the dominant pore type and the other pore types are commonly fractures. These reservoirs are characterized by the thickest net pay, lowest porosity, lowest permeability, and lowest initial water saturation.

Tables 1 and 2 from Holtz and Kerans (1992) summarized the geological and reservoir traits of each group. It is important to note that Ellenburger reservoirs generally have low porosities (a few percent) and fair permeabilities (one to a few hundred millidarcys). The low porosities and fair permeabilities are the result of the permeability

being related to fracture-type pores. Figure 48 shows field averages for porosity and permeability for a number of Ellenburger fields. The average porosities are low, whereas the permeabilities are fair. This relationship is the result of karst-related fracture pores. Figure 49 is a histogram of productive (past and present) wells drilled into the Ellenburger Group. Producing wells show a range from 856 ft (Originala Petroleum #1 Gensler well in Archer County, Texas) to 25,735 ft (Exxon Mobil McComb Gas Unit B well in Pecos County, Texas). A recent review of Texas oil fields by Dutton et al., (2005) summarized that the karst-modified reservoir play has produced ~1.5 billion barrels of oil and the Ellenburger ramp carbonate play has produced ~164 million barrels of oil up to 2005.

Figure 50 by Katz et al. (1994) is an event chart for the Simpson-Ellenburger petroleum system showing the temporal relationships of the essential elements and processes. Even though the source for the petroleum system is problematic, they believed that the source rocks are the shales within the Simpson Group. However, where the Simpson is absent, the Ellenburger oil appears to be sourced from the Woodford Shale or younger strata (Pennsylvanian or Permian) (Kvenvolden and Squires, 1967). Katz et al. (1994) mentioned that the level of organics within the Ellenburger section is too lean (<0.5% TOC) to be capable of generating commercial quantities of hydrocarbons. The Simpson has >1% TOC. Their ideas for reservoir rock type in the Ellenburger carbonates comes from the articles cited earlier in this paper and these reservoir rocks within this petroleum system are buried between 8,530 to 13,240 ft (Central Basin Platform area). Katz et al. (1994) stated that trap development was associated with the collisional event that subdivided the Permian basin into its major units around 290 ma years ago. The traps are predominately faulted anticlines (Figure 51). The seal rocks are the Simpson shales in the Central Basin Platform area. Traps formed about 50 my before peak generation at about 245 Ma (Figure 50). Katz et al. (1994) mentioned the API oil gravity ranges from 35 to 50 degrees which allows a recover factor of 40%.

COMMENTS ON APPROACHES TO EXPLORATION AND FIELD DEVELOPMENT

Exploration

The vast majority of Ellenburger fields are trapped in anticlinal or faulted anticlinal structures (Figure 51). The Ellenburger reservoirs are mainly structural plays, therefore, seismic is needed to define these structural prospects. Complexities of the structure must be delineated to focus on the correct trapping geometry. Stratigraphic trapping in the highly karsted and fractured Ellenburger carbonate is probably not common as there is generally some level of communication within the carbonate, however poor. After a structure is defined, the fault compartmentalization of the structure must be mapped. If 3-D seismic analysis is able to display the sag features produced by collapse of the cave system (Loucks, 1999), these collapsed zones may contain the highest reservoir quality (Purves et al., 1992).

Many wells testing the Ellenburger section only penetrate the top of the interval to prevent encountering water from drilling to deep (Kerans, 1990). Caution must be taken to ensure that the full prospective section is tested and that any vertical permeability barriers are penetrated (Loucks and Anderson, 1985; Kerans, 1990). Kerans (1990) provided an excellent example from the University Block 13 field in Andrews County, Texas where a series of wells drilled into the very top of the Ellenburger section were produced and then later deepened (Figure 52). The deepened wells encountered new hydrocarbons that were separated from the upper unit by paleocave fill and tight carbonate. The cave-fill-prone intervals are very distinctive on wireline logs. Is should be noted that a cave fill by itself cannot be a laterally continuous permeability barrier because its limited lateral extent is controlled by the size of the original cave itself (Loucks, 1999, 2001).

Kerans (1990), Loucks and Handford (1992), Hammes et al. (1996), and Loucks (1999) have stressed that karsted reservoirs can have stacked porous brecciated zones (Figure 29). These stacked reservoir zones are the results of multiple cave passages forming during base-level drop while a cave system is developing (Figure 19).

Commonly, each of the paleocave passage levels will be in contact with each other because of cave collapse and associated fracturing. However, as Kerans (1990) showed for the University Block 13 field, this is not always the case.

In any test of the Ellenburger section, a core or image log is necessary to properly evaluate the section. Commonly, the porosity will be low (<5%) as calculated from wireline logs, however, the permeability from karst-related fracturing may be in the hundreds of millidarcys. Core will provide the proper reservoir quality analysis and image logs will provide a description of the fractured pore network in the rock (Hammes, 1997).

Field Development

Field development of paleocave reservoirs should be based on integrated studies that include data from 3-D seismic surveys, cores, borehole image logs, conventional wireline logs, and engineering data (Loucks, 1999). In some cases it might be possible to identify cavernous or intraclast porosity from 3-D seismic data (Bouvier et al., 1990). Cores and borehole image logs are necessary to recognize and describe paleocave reservoir facies (Hammes, 1997). Whole-core data is recommended over core-plug data because of the scale and complexity of pore systems in paleocave reservoirs. Sags associated with cave collapse should be mapped because they may indicate location of the best coalesced reservoirs (Purves, 1992; Lucia, 1996; Loucks, 1999). Different cave passage levels of the paleocave system need to be identified and analyzed to determine whether they are separate reservoirs or in vertical communication with each other (Kerans, 1988, 1990). Because of the significant spatial complexity within coalesced paleocave systems, horizontal wells may be an option for improving recovery. Kerans (1988) stated that in the Mobil Block 36 lease of the Emma Ellenburger reservoir "Adjacent wells in this 40-acre-spaced reservoir have varied in production, one to the other, anywhere form 0 to 900,000 barrels of oil from the lower collapse zone." He noted, this variability is probably related to changes in paleocave facies. The details paleocave system maps provide by Loucks et al. (2004) would support this conclusion. Kerans (1988) lists other fields, such as the Shafter lake and Big Lake fields as showing strong

lateral reservoir heterogeneity. Other workers that addressed different aspects of exploration and development are Kerans (1990), Wright et al. (1991), Mazzulo and Mazzulo (1992), Lucia (1996), Hammes et al. (1996), Mazzulo and Chilingarian (1996) and Loucks (1999).

CONCLUSIONS

The Ellenburger Group of the Permian Basin is part of a Lower Ordovician carbonate platform that covered large areas of the United States. During the Lower Ordovician, the West Texas Permian Basin area was located on the southwest edge of the Laurentia plate between 20 to 30 degrees latitude. The equator crossed northern Canada situating Texas in a tropical to subtropical latitude. Texas was a shallow-water shelf with deeper water conditions to the south where it bordered the Iapetus Ocean. The Ellenburger Group in the southern part of the Permian Basin, where the deeper water equivalent strata would have been, was strongly affected by the Ouachita Orogeny. The basinal and slope facies strata were destroyed or extensively structurally deformed. A worldwide hiatus appeared at the end of Lower Ordovician deposition creating an extensive second order unconformity (Sauk-Tippecanoe Supersequence Boundary). This unconformity produced extensive karsting throughout the United States as well as in Texas.

The general depositional history of the Ellenburger was defined by Kerans (1990): (1) Marked by retrogradational deposition of fan delta – marginal marine depositional system continuous with the Early Cambrian transgression. This stage was followed by the regional progradation and aggradation of peritidal carbonate facies. (2) Rapid transgression and widespread aggradational deposition of the high-energy restricted-shelf depositional system across much of West and Central Texas during this stage. Interpreted as a moderately hypersaline setting based on rare macrofauna, evidence of evaporites, and abundance of ooids. (3) Upward transition from the high-energy restricted shelf depositional systems to the low-energy restricted-shelf depositional systems is evidence of a second regression across the Ellenburger shelf. The progradation during this stage is marked by the transition of landward upper tidal flats, to more

seaward low-energy restricted subtidal to intertidal facies, to furthest seaward open-marine, shallow-water shelf facies. (4) Near the end of the Early Ordovician there was a worldwide eustatic lowstand. The amount of exposure covered several million years. This exposed the Ellenburger platform in West Texas producing an extensive karst terrain.

The diagenesis of the Ellenburger Group is extremely complex and the processes that produced the diagenesis covered million of years. Three major diagenetic processes are important to recognize: (1) dolomitization, (2) karsting, and (3) tectonic fracturing. Five general stages of dolomitization were recognized by Kupecz and Land (1991). The generations of dolomite were separated into early stage dolomitization which pre-dated the Sauk unconformity and late stage dolomitization that post dated the Sauk unconformity. They attribute 90 percent of the dolomite as pre-karstification early stage dolomite and 10 percent of the dolomite as post-karstification late stage dolomite. The early-stage pre-karstification dolomite is associated with the muddier rocks and the source of Mg was probably sea water. The late-stage post-karstification dolomites are attributed to warm, reactive fluids, which were expelled from basinal shales during the Ouachita Orogeny. The fluids are thought to have been corrosive as evidenced by corroded dolomite rhombs. This corrosion provided the Mg necessary for dolomitization. These fluids migrated through high permeability aquifers of the Bliss sandstone, basal subarkose facies of the Ellenburger, as well as grainstone facies and paleocave breccia zones. In the Ellenburger Group, extensive cave systems formed at a composite unconformity (Sauk unconformity) that lasted several million years to several tens of million years. These cave systems collapsed with burial creating wide spread brecciated and fractured carbonate bodies that form many of the Ellenburger reservoirs. Up to a thousand feet of section can be affected, but more commonly only the top 300 feet are affected. The lithified strata above the karsted Ellenburger are also affected by suprastratal deformation. The West Texas area has been periodically tectonic active following Ellenburger deposition producing faults and fractures associated with these tectonic periods.

Pore networks in the Ellenburger are especially complex because of the amount of brecciation and fracturing associated with karsting. The pore networks can consist of any combination of the following pore types depending on depth of burial (Loucks, 1999): (1)

matrix, (2) cavernous, (3) interclast, (4) crackle/mosaic breccia fractures, or (5) tectonic-related fractures. The pore network evolved with burial and diagenesis.

Coalesced, collapsed paleocave systems are megascale geologic features that can have dimensions of hundreds to thousands of square miles laterally and several thousand feet vertically. Strata above and below the unconformity are affected by late collapse in the subsurface. A coalesced collapsed paleocave system can be divided into two parts: (1) a lower section of karsted strata that contains collapsed paleocaves and (2) an upper section of strata that is deformed to various degrees (suprastratal deformation) by the collapse and compaction of the lower section of paleocave-bearing strata. The regional pattern of karsted Ellenburger reservoirs probably follows a rectilinear pattern as a result of regional fractures controlling original cave-system development.

The Ellenburger Group is an ongoing important exploration target in West Texas. The structural play covers a depth interval of over 25,000 ft. The carbonate depositional systems with the Ellenburger Group are relatively simple; however, the diagenetic overprint is extremely complex. This complex diagenetic overprint produces strong spatial heterogeneity within the reservoir systems.

REFERENCES

Amthor, J. E., and Friedman, G. M., 1989, Petrophysical character of Ellenburger karst facies: Stateline (Ellenburger) field, Lea County, southeastern New Mexico, *in* Cunningham, B. K., and Cromwell, D. W., eds., The Lower Paleozoic of West Texas and southern New Mexico; Modern exploration concepts: Permian Basin Section-Society of Economic Paleontologists and Mineralogists Publication No. 89-31, p.133-144.

Amthor, J. E., and Friedman, G. M., 1991, Dolomite-rock textures and secondary porosity development in Ellenburger Group carbonates (Lower Ordovician), West Texas and southeastern New Mexico: Sedimentology, v. 38, p. 343-362.

Barnes, V. E., Cloud, P. E., Jr., Dixon, L. P., Folk, R. L., Jonas, E. C., Palmer, A. R., and Tynan, E. J., 1959, Stratigraphy of the pre-Simpson Paleozoic subsurface rocks of

Texas and southeast New Mexico: The University of Texas at Austin, Bureau of Economic Geology Publication 5924, 294 p.

Berry, W. B. N., 1960, Graptolite faunas of the Marathon region, West Texas: The University of Texas at Austin, Bureau of Economic Geology Publication 6005, 179 p.

Blakey, R., 2005a, Regional paleogeographic views of earth history; paleogeographic globes: web site: http://jan.ucc.nau.edu/~rcb7/RCB.html.

Blakey, R., 2005b, Paleogeography and geologic evolution of North America; Images that track the ancient landscapes of North America: web site: http://jan.ucc.nau.edu/~rcb7/RCB.html.

Bouvier, J. D., Gevers, E. C.A., and Wigley, P. L., 1990, #-D seismic interpretation and lateral prediction of the Amposta Marino field (Spanish Mediterranean Sea): Geologie en Mijnbouw, v. 69, P. 105-120.

Budnik, T. T., 1987, Left-lateral intraplate deformation along the Ancestral Rocky Mountains: implications for late Paleozoic plate motions: Tectonophysics, v. 132, p. 195-214.

Candelaria, M. P., and Reed (eds.), C. L., 1992, Paleokarst, karst related diagenesis and reservoir development: Examples from Ordovician-Devonian age strata of West Texas and the Mid-Continent: Permian Basin Section-Society of Economic Paleontologists and Mineralogists Publication No. 92-33, 202 p.

Canter, K. L., Stearns, D. B., Geesaman, R. C., and Wilson, J. L., 1993, Paleostructural and related paleokarst controls on reservoir development in the Lower Ordovician Ellenburger Group, Val Verde Basin, *in* Fritz, R. D., Wilson, J. L., and D. A. Yurewicz, D. A., eds., Paleokarst related hydrocarbon reservoirs: SEPM Core Workshop No. 18, New Orleans, April 25, 1993, p. 61-101.

Cloud, P. E., and Barnes, V. E., 1948, the Ellenburger Group of Central Texas: The University of Texas at Austin, Bureau of Economic Geology Publication 4621, 473 p.

Cloud, P. E., and Barnes, V. E., 1957, Early Ordovician sea in Central Texas: Geological Society of American Memoir 67, P. 163-214.

Cloud, P. E., Barnes, V. E., and Bridge, J. 1945, Stratigraphy of the Ellenburger Group in Central Texas—a progress report: The University of Texas at Austin, Bureau of Economic Geology Publication 4301, 133-161.

Combs, D. M., Loucks, R. G., and Ruppel, S. C., 2003, Lower Ordovician Ellenburger Group collapsed paleocave facies and associated pore network in the Barnhart field, Texas, *in* Hunt, T. J., and Lufholm, P. H., The Permian Basin: back to basics: West Texas Geological Society Fall Symposium: West Texas Geological Society Publication #03-112, p. 397–418.

Custer, M. A., 1957, Polar field, Kent County, Texas, *in* Heard, F. A., ed., Occurrence of oil and gas in West Texas: The University of Texas at Austin, Bureau of Economic Geology Publication No. 5716, p. 200-282.

Dutton, S. P., Kim, E. M., Broadhead, R. F., Breton, C. L., Raatz, W. D., Ruppel, S. C., and Kerans, Charles, 2005, Play analysis and digital portfolio of major oil reservoirs in the Permian Basin: The University of Texas at Austin, Bureau of Economic Geology Report of Investigations No. 271, 287 p., CD-ROM.

Entzminger, D. J., 1994, Shafter Lake (Ellenburger), *in* Oil & gas fields in West Texas: West Texas Geological Society Publication 94-96, v. 4, p. 247-250.

Folk, R. L., 1959, Thin-section examination of Pre-Simpson Paleozoic rocks, in Barnes, V. E., Cloud, P. E., Jr., Dixon, L. P., Folk, R. L., Jonas, E. C., Palmer, A. R., and Tynan, E. J.: Stratigraphy of the pre-Simpson Paleozoic subsurface rocks of Texas and southeast New Mexico: The University of Texas at Austin, Bureau of Economic Geology Publication. 5924, p. 95-130.

Ford, D. C., 1988, Characteristics of dissolutional cave systems in carbonate rocks, *in* James, N. P., and Choquette, P. W., eds., Paleokarst: Springer-Verlag, p. 25–57.

Esteban, M., 1991, Palaeokarst: practical applications, *in* Wright, V. P., Esteban, M., and Smart, P. L., eds., Palaeokarst and palaeokarstic reservoirs: Postgraduate Research for Sedimentology, University of Reading, PRIS Contribution No. 152, p. 89–119.

Galley, J. E., 1958, Oil and geology in the Permian Basin of Texas and New Mexico, *in* Weeks, W. L., ed., Habitat of oil, American Association of Petroleum Geologists Special Publication, p. 395-446.

Goldhammer, R. K., 1996, Facies architecture, cyclic and sequence stratigraphy: the Lower Ordovician El Paso Group, West Texas, *in* Stoudt, E. L., ed., Precambrian-Devonian geology of the Franklin Mountains, West Texas - Analogs for exploration and production in Ordovician and Silurian karsted reservoirs in the Permian basin: West Texas Geological Society 1996 Annual Field Trip Guidebook, WTGS Publication No. 96-100, p. 71-98.

Goldhammer, R. K., Lehmann, P. J., and Dunn, P. A., 1992, Third-order sequence boundaries and high frequency cycle stacking pattern in Lower Ordovician platform carbonates, El Paso Group (Texas): Implications for carbonate sequence stratigraphy, *in* Candelaria, M. P., and Reed, C. L., eds., Paleokarst, karst related diagenesis and reservoir development: examples from Ordovician-Devonian age strata of West Texas and the Mid-Continent: Permian Basin Section, (Society for Sedimentary Geology), Publication No. 92–33, p. 59-92.

Goldhammer, R. K., and Lehmann, P. J., 1996, Chaos in El Paso, *in* Stoudt, E. L., ed., Precambrian-Devonian geology of the Franklin Mountains, West Texas - Analogs for exploration and production in Ordovician and Silurian karsted reservoirs in the Permian basin: West Texas Geological Society 1996 Annual Field Trip Guidebook, WTGS Publication No. 96-100, p. 125-140.

Hardage, B. A., Carr, D. L., Lancaster, D. E., Simmons, J. L., Jr., Elphick, R. Y., Pendleton, V. M., and Johns, R. A., 1996, 3-D seismic evidence of the effects of carbonate karst collapse on overlying clastic stratigraphy and reservoir compartmentalization: Geophysics, v. 61, p. 1336-1350.

Ham, W. E., and Wilson, J. L., 1967, Paleozoic epeirogeny and orogeny in the central United States: American Journal of Science, v. 265, issue 5, p. 332-407.

Hammes, Ursula, Lucia, F. J., and Kerans, Charles, 1996, Reservoir heterogeneity in karst-related reservoirs: Lower Ordovician Ellenburger Group, West Texas, *in* Stoudt, E. L., ed., Precambrian–Devonian geology of the Franklin Mountains, West Texas—analogs for exploration and production in Ordovician and Silurian karsted reservoirs in the Permian Basin: West Texas Geological Society, Publication No. 96-100, p. 99–117.

Hammes, U., 1997, Electrical imaging catalog: microresistivity images and core photos from fractured, karsted, and brecciated carbonate rocks: The University of Texas at Austin, Bureau of Economic Geology Geological Circular 97-2, 40 p.

Hardwick, J. V., 1957, Block 32 field, Crane County, Texas, *in* Heard, F. A., ed., Occurrence of oil and gas in West Texas: The University of Texas at Austin, Bureau of Economic Geology Publication No. 5716, p. 40-46.

Holland, R. R., 1966, Puckett, Ellenburger, Pecos County, Texas: in Oil and gas fields in West Texas—A Symposium: West Texas Geological Society publication 66-52, p. 291-295.

Holtz, M. H., and Kerans, C., 1992, Characterization and categorization of West Texas Ellenburger reservoirs, *in* Candelaria, M. P., and Reed, C. L., eds., Paleokarst, karst related diagenesis and reservoir development: examples from Ordovician-Devonian age strata of West Texas and the Mid-Continent: Permian Basin Section SEPM Publication No. 92-33, p. 31-44.

Ijirighoi, B. T., and Schreiber, J. F., Jr., 1986, Origin and classification of fractures and related breccia in the Lower Ordovician Ellenburger Group, West Texas: West Texas Geological Society Bulletin, v. 26, p. 9-15.

Katz, B. J., Dawson, W. C., Robison, V. D., and Elrod, L. W., 1994, Simpson—Ellenburger(.) petroleum system of the Central Basin Platform, West Texas, U.S.A., *in* Magoon, L. B. and Dow, W. G., eds., The petroleum system—from source to trap: AAPG Memoir 60, p. 453-461.

Kerans, Charles, 1988, Karst-controlled reservoir heterogeneity in Ellenburger Group carbonates of West Texas: reply: American Association of Petroleum Geologists Bulletin, v. 72, p. 1160–1183.

Kerans, Charles, 1989, Karst-controlled reservoir heterogeneity and an example from the Ellenburger Group (Lower Ordovician) of West Texas: The University of Texas at Austin, Bureau of Economic Geology Report of Investigations No. 186, 40 p.

Kerans, Charles, 1990, Depositional systems and karst geology of the Ellenburger Group (Lower Ordovician), subsurface West Texas: The University of Texas at Austin, Bureau of Economic Geology Report of Investigations No. 193, 63 p., 6 pl.

Kerans, Charles., Lucia, F. J., and Senger, R. K., 1994, integrated characterization of carbonate ramp reservoirs using Permian San Andres outcrop analogs: American Association of Petroleum Geologists Bulletin, v. 78, 181-216.

Kvenvolden, K. A., and Squires, R. M., 1967, Carbon isotopic composition of crude oils from Ellenburger Group (Lower Ordovician), Permian basin, West Texas and eastern New Mexico: American Association of Petroleum Geologists Bulletin, v. 51, p. 1293-1303.

Kupecz, J. A., 1992, Sequence boundary control on hydrocarbon reservoir development, Ellenburger Group, Texas, *in* Candelaria, M. P., and Reed, C. L., eds., Paleokarst, karst related diagenesis and reservoir development: examples from Ordovician-Devonian age strata of West Texas and the Mid-Continent: Permian Basin Section, (Society for Sedimentary Geology), Publication No. 92–33, p. 55-58.

Kupecz, J. A., and L. S. Land, 1991, Late-stage dolomitization of the Lower Ordovician Ellenburger Group, West Texas: Journal of Sedimentary Petrology, v. 61, p. 551-574.

Lee, I. Y., and Friedman, G. M., 1998, Deep-burial dolomitization in the Ordovician Ellenburger Group carbonates, West Texas and southeastern New Mexico – Reply: Journal of Sedimentary Petrology, v. 58, p. 910-913.

Lindsay, R. F., and Koskelin, K. M., 1993, Arbuckle Group (Late Cambrian-early Ordovician) shallowing-upward parasequences and sequences, southern Oklahoma, *in* Keller, D. R. and Reed, C. L., eds., Paleokarst, karst related diagenesis and reservoir development: examples from Ordovician-Devonian age strata of West Texas and the Mid-Continent: Permian Basin Section SEPM Publication No. 92-33, p. 45-65.

Loucks, R. G., 1999, Paleocave carbonate reservoirs: origins, burial-depth modifications, spatial complexity, and reservoir implications, American Association of Petroleum Geologists Bulletin, v. 83, p. 1795–1834.

Loucks, R. G., 2001, Modern analogs for paleocave-sediment fills and their importance in identifying paleocave reservoirs: Gulf Coast Association of Geological Societies Transactions, v. 46, p. 195–206.

Loucks, R. G., 2003, Understanding the development of breccias and fractures in Ordovician carbonate reservoirs, *in* Hunt, T. J., and Lufholm, P. H., The Permian Basin: back to basics: West Texas Geological Society Fall Symposium: West Texas Geological Society Publication No. 03-112, p. 231–252.

Loucks, R. G., and J. H. Anderson, 1980, Depositional facies and porosity development in Lower Ordovician Ellenburger dolomite, Puckett Field, Pecos County, Texas, *in* Halley, R. B. and Loucks, R. G., eds., Carbonate reservoir rocks: SEPM Core Workshop No. 1, p. 1-31.

Loucks, R. G., and J. H. Anderson, 1985, Depositional facies, diagenetic terrains, and porosity development in Lower Ordovician Ellenburger Dolomite, Puckett Field, West Texas, *in* Roehl, P. O. and Choquette, P. W., eds., Carbonate petroleum reservoirs: Springer-Verlag, p. 19-38.

Loucks, R. G., and Handford, R. H., 1992, Origin and recognition of fractures, breccias, and sediment fills in paleocave-reservoir networks, *in* Candelaria, M. P., and Reed, C. L., eds., Paleokarst, karst related diagenesis and reservoir development: examples from Ordovician-Devonian age strata of West Texas and the Mid-Continent: Permian Basin Section, (Society for Sedimentary Geology), Publication No. 92–33, p. 31–44.

Loucks, R. G., and Mescher, P. A, 1998, Origin of fractures and breccias associated with coalesced collapsed paleocave systems (abs.), *in* Rocky Mountain Association Symposium on Fractured Reservoirs: Practical Exploration and Development Strategies, unpaginated.

Loucks, R. G., and Mescher, P., 2001, Paleocave facies classification and associated pore types: American Association of Petroleum Geologists, Southwest Section, Annual Meeting, Dallas, Texas, March 11–13, CD-ROM, 18 p.

Loucks, R. G., Mescher, P., and McMechan, G. A., 2000, Architecture of a coalesced, collapsed-paleocave system in the Lower Ordovician Ellenburger Group, Dean Word Quarry, Marble Falls, Texas: Final report prepared for the Gas Research Institute, GRI-00/0122, CD-ROM.

Loucks, R. G., Mescher, P. K., and McMechan, G. A., 2004, Three-dimensional architecture of a coalesced, collapsed-paleocave system in the Lower Ordovician

Ellenburger Group, Central Texas: American Association of Petroleum Geologists Bulletin, v. 88, no. 5, p. 545–564.

Lucia, F. J., 1971, Lower Paleozoic history of the western Diablo Platform, West Texas and south-central New Mexico, *in* Cys, J. M., ed., Robledo Mountains and Franklin Mountains-1971 Field Conference Guidebook: Permian Basin Section, SEPM, p. 174-214.

Lucia, F. J., 1968, Sedimentation and Paleogeography of the El Paso Group, *in* Stewart, W. J., ed., Delaware basin exploration: West Texas geological Society Guidebook No. 68-55, p. 61-75.

Lucia, F. J., 1969, Lower Paleozoic history of the western Diablo Platform of West Texas and south-central New Mexico, *in* Seewald, K. and Sundeen, D., eds., the geologic framework of the Chihuahua tectonic belt: West Texas Geological Society, p. 39-56.

Lucia, F. J., 1995, Lower Paleozoic cavern development, collapse, and dolomitization, Franklin Mountains, El Paso, Texas, *in* Budd, D. A., Saller, A. H., and Harris, P. M., eds., Unconformities and porosity in carbonate strata: AAPG Memoir 63, p. 279-300.

Lucia, F. J., 1996, Structural and fracture implications of Franklin Mountains collapse brecciation, *in* Stoudt, E. L., ed., Precambrian-Devonian geology of the Franklin Mountains, West Texas - Analogs for exploration and production in Ordovician and Silurian karsted reservoirs in the Permian basin: West Texas Geological Society 1996 Annual Field Trip Guidebook, WTGS Publication No. 96-100, p. 117-123.

McMechan, G. A., Loucks, R. G., Zeng, X., and Mescher, P. A., 1998, Ground penetrating radar imaging of a collapsed paleocave system in the Ellenburger dolomite, Central Texas: Journal of Applied Geophysics, v. 39, p. 1-10.

McMechan, G. A., Loucks, R. G., Mescher, P. A., and Zeng, Xiaoxian, 2002, Characterization of a coalesced, collapsed paleocave reservoir analog using GPR and well-core data: Geophysics, v. 67, no. 4, p. 1148–1158.

Mazzullo, S. J., and G. V. Chilingarian, 1996, Hydrocarbon reservoirs in karsted carbonate rocks, *in* G. V. Chilingarian, S. J. Mazzullo, and H. H. Rieke, eds.,

Carbonate reservoir characterization: a geologic - engineering analysis , Part II: Elsevier, p. 797-685.

Mazzullo, S. J., and Mazzullo, L. J., 1992, Paleokarst and karst-associated hydrocarbon reservoirs in the Fusselman Formation, West Texas, Permian basin, *in* Candelaria, M. P., and Reed, C. L., eds., Paleokarst, karst related diagenesis and reservoir development: examples from Ordovician-Devonian age strata of West Texas and the Mid-Continent: Permian Basin Section, (Society for Sedimentary Geology), Publication No. 92–33, p. 110-120.

Palmer, A. N., 1991, Origin and morphology of limestone caves: GSA Bulletin, v. 103, p. 1–21.

Ross, R. J., 1976, Ordovician sedimentation in the western United States, *in* Bassett, M. G., ed., The Ordovician System: proceedings of a Paleontological Association symposium: Birmingham, p. 73-105.

Ross, R. J., and others, 1982, The Ordovician System in the United States, correlation chart and explanatory note: proceedings of a Paleontological Association symposium: Birmingham, p. 73-105.

Ruppel, S. C., Jones, R. H., Breton, C. L., and Kane, J. A., 2005, Preparation of maps depicting geothermal gradient and Precambrian structure in the Permian Basin: The University of Texas at Austin, Bureau of Economic Geology, contract report prepared for the U.S. Geological Survey, under order no. 04CRSA0834 and requisition no. 04CRPR01474, 23 p + CD-ROM.

Sloss, L. L., 1963, Sequences in the cratonic interior of North America: Geological Society of America Bulletin, v. 74, p. 93-114.

Texas water Development Board, 1972, A survey of the subsurface saline water of Texas: Austin, TWDB, v. 1, 113 p.

Weiner, S. P., 1994, Martin (Ellenburger), *in* Oil & gas fields in West Texas: West Texas Geological Society Publication 94-96, v. 4, p.157-161.

White, W. B., 1988, Geomorphology and hydrology of karst terrains: New York, Oxford University Press, 464 p.

White, E. L., and White, W. B., 1968, Dynamics of sediment transport in limestone caves: National Speleothem Society Bulletin, v. 30, 115–129.

Wilson, J. L., R. L. Medlock, R. D. Fritz, K. L. Canter, and R. G. Geesaman, 1991, A review of Cambro-Orodovician breccias in North America, *in* Keller, D. R. and. Reed, C. L, eds., Paleokarst, karst related diagenesis and reservoir development: examples from Ordovician-Devonian age strata of West Texas and the Mid-Continent: Permian Basin Section SEPM Publication No. 92-33, p. 19-29.

Wright, V. P., M. Esteban, and P. L. Smart, (eds.), 1991, Palaeokarst and palaeokarstic reservoirs: Postgraduate Research for Sedimentology, University, PRIS Contribution No. 152, 158 p.

Young, L. M., 1968, Sedimentary petrology of the Marathon Formation, (Lower Ordovician), Trans-Pecos Texas: The University of Texas at Austin at Austin, Ph.D. dissertation, 234 p.

Table 1. Summary of general paleocave facies. From Loucks and Mescher (2001).

Description of Paleocave Facies

Cave Facies	Interpretation	Description	Pore System/ Reservoir Quality
Undisturbed Strata	Undisturbed host rock	Excellent bedding continuity for hundreds to thousands of feet.	Minor matrix and fracture pores. Ø < 3% to 5% K < few millidarcys
Disturbed Strata	Disturbed host rock	Bedding continuity is high but folded and offset by small faults. Commonly overprinted with crackle and mosaic brecciation.	Minor matrix pores and crackle to mosaic fracture pores. Ø < 5% K is as much as tens of millidarcys
Highly Disturbed Strata	Collapsed host rock (cave-roof and cave-wall rock) over passages	Highly disturbed, very discontinuously bedded strata with pockets and layers of chaotic breccia. Small-scale folding and faulting are common. Commonly overprinted with crackle and mosaic brecciation.	Localized pockets or layers of breccia might have porosities in the range of 5% to 15% and permeabilities in the tens to hundreds of millidarcys.
Coarse Chaotic Breccia	Collapsed-breccia cavern fill	Mass of very poorly sorted, granule- to boulder-sized chaotic breccia clasts 1 to 10 ft long. Commonly clast supported but can contain matrix material. Ribbon- to tabular-shaped body as much as 45 ft across and hundreds of meters long.	Abundant interclast pores. Porosity can exceed 20%, and permeability can be in the darcys.
Fine Chaotic Breccia	Transported-breccia cavern fill	Mass of clast-supported, moderately sorted, granule- to cobble-sized clasts with varying amounts of matrix. Clasts can be imbricated or graded. Ribbon- to tabular-shaped body as much as 45 ft across and hundreds of feet long.	Abundant interclast pores. Porosity can exceed 20%, and permeability can be in the darcys.
Sediment Fill	Cave-sediment cavern fill	Carbonate and/or siliciclastic debris commonly with sedimentary structures.	Siliciclastic fill is commonly tight. Carbonate fill might be permeable.

Table 2. Geologic characteristics of the three Ellenburger reservoir groups. From Holtz and Kerans (1992).

	Karst Modified	Ramp Carbonate	Tectonically Fractured Dolostone
Lithology	Dolostone	Dolostone	Dolostone
Depositional setting	Inner ramp	Mid- to outer ramp	Inner ramp
Karst facies	Extensive sub-Middle Ordovician	Sub-Middle Ordovician, sub-Silurian/Devonian, sub-Mississippian, sub-Permian/ Pennsylvanian	Variable intra-Ellenburger, sub-Middle Ordovician
Fault-related fracturing	Subsidiary	Subsidiary	Locally extensive
Dominant pore type	Karst-related fractures and interbreccia	Intercrystalline in dolomite	Fault-related fractures
Dolomitization	Pervasive	Partial, stratigraphic and fracture-controlled	Pervasive

Table 3. Petrophysical parameter of the three Ellenburger reservoir groups. From Holtz and Kerans (1992).

Parameter	Karst Modified	Ramp Carbonate	Tectonically Fractured Dolostone
Net pay (ft)	Avg. = 181, Range = 20 - 410	Avg. = 43 Range = 4 - 223	Avg. = 293, Range = 7 - 790
Porosity (%)	Avg. = 3 Range = 1.6 - 7	Avg. = 14 Range = 2 - 14	Avg. = 4 Range = 1 - 8
Permeability (md)	Avg. = 32 Range = 2 - 750	Avg. = 12 Range = 0.8 - 44	Avg. = 4 Range = 1 - 100
Initial water Saturation (%)	Avg. = 21 Range = 4 - 54	Avg. = 32 Range = 20 - 60	Avg. = 22, Range = 10 - 35
Residual oil Saturation (%)	Avg. = 31 Range = 20 - 44	Avg. = 36 Range = 25 - 62	NA

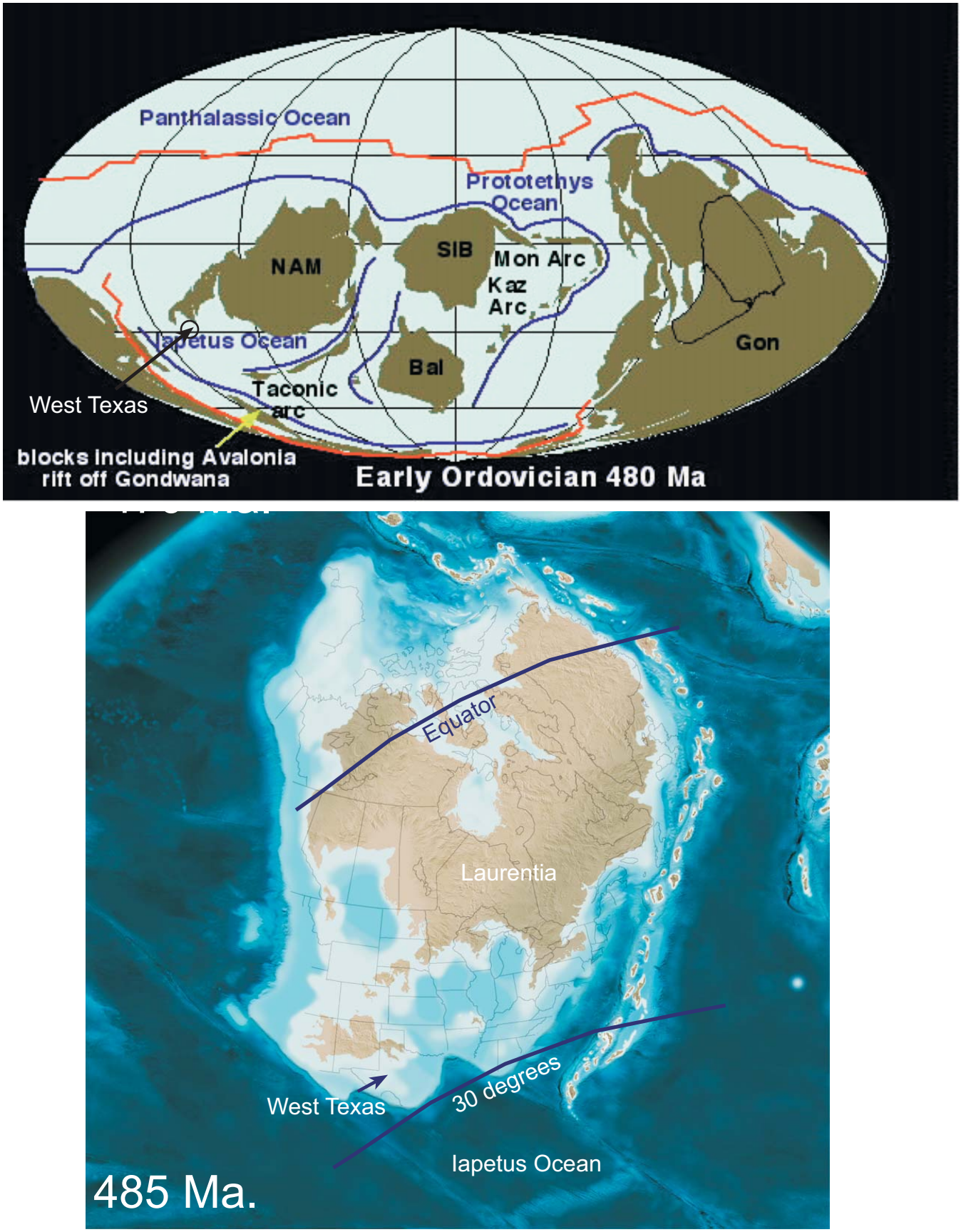

Figure 1. Reconstruction of Laurenia Plate for the Lower Ordovician (480 Ma at top and 485 Ma at bottom). West Texas was located at the southwest edge of the continent bordering the deep Iapetus Ocean. Upper map is from Blakey (2005a) and lower map is from Blakey (2005b). The lower map is slightly modified by present author. The location of the equator and 30 degrees latitude are estimated from the upper global diagram.

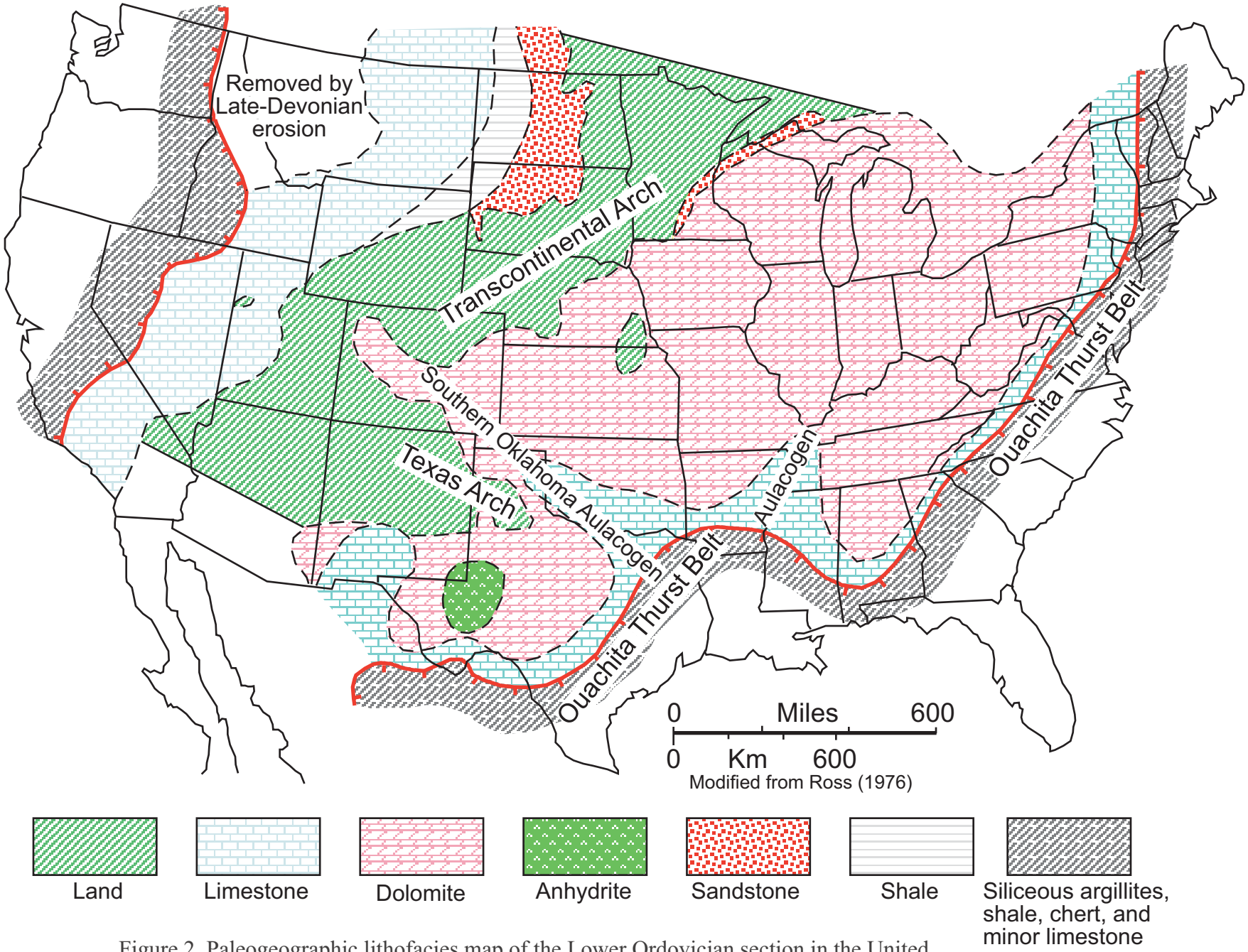

Figure 2. Paleogeographic lithofacies map of the Lower Ordovician section in the United States. From Ross (1976).

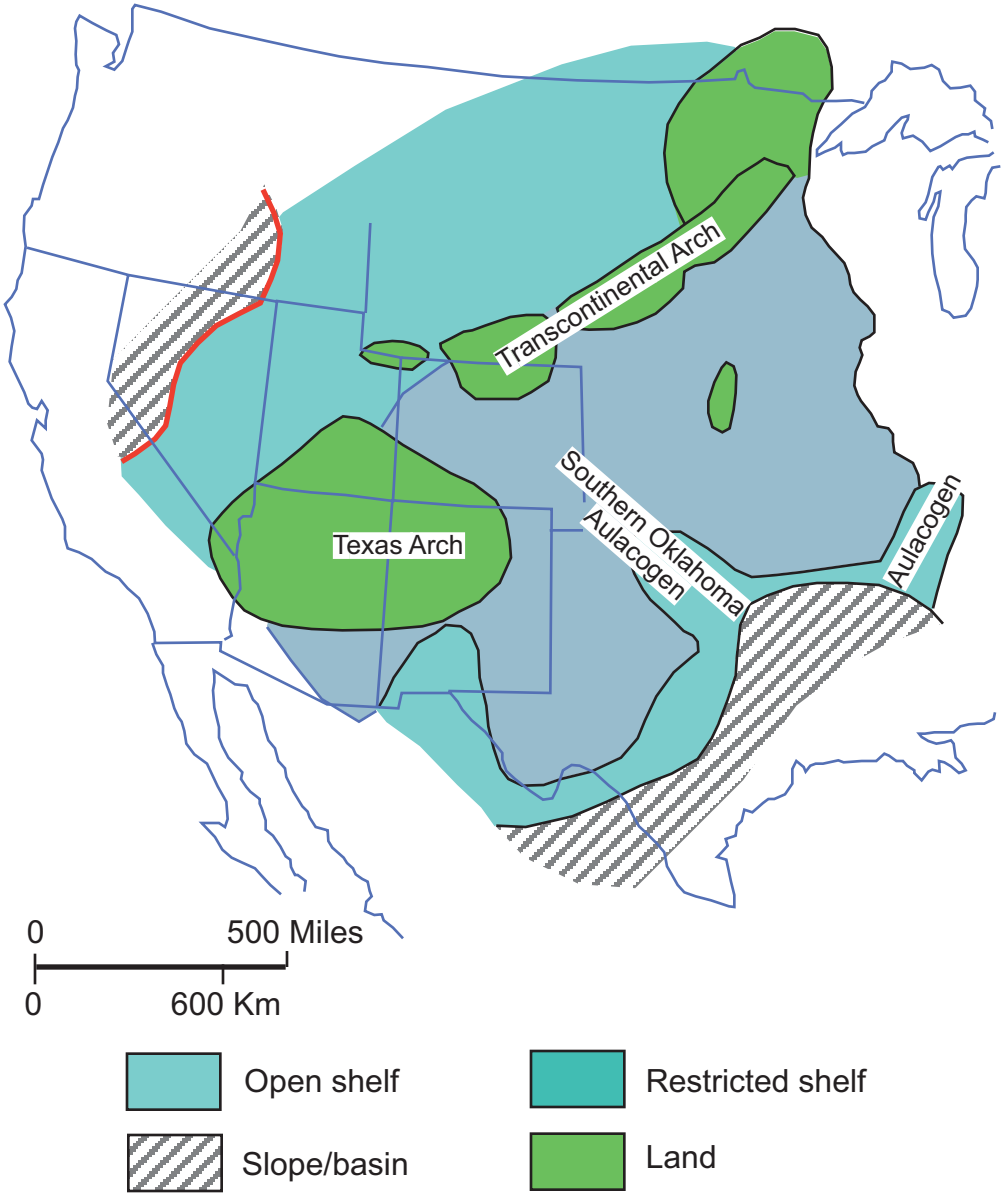

Figure 3. Interpreted regional depositional setting during Early Ordovician time. After Ross (1976) and Kerans (1990).

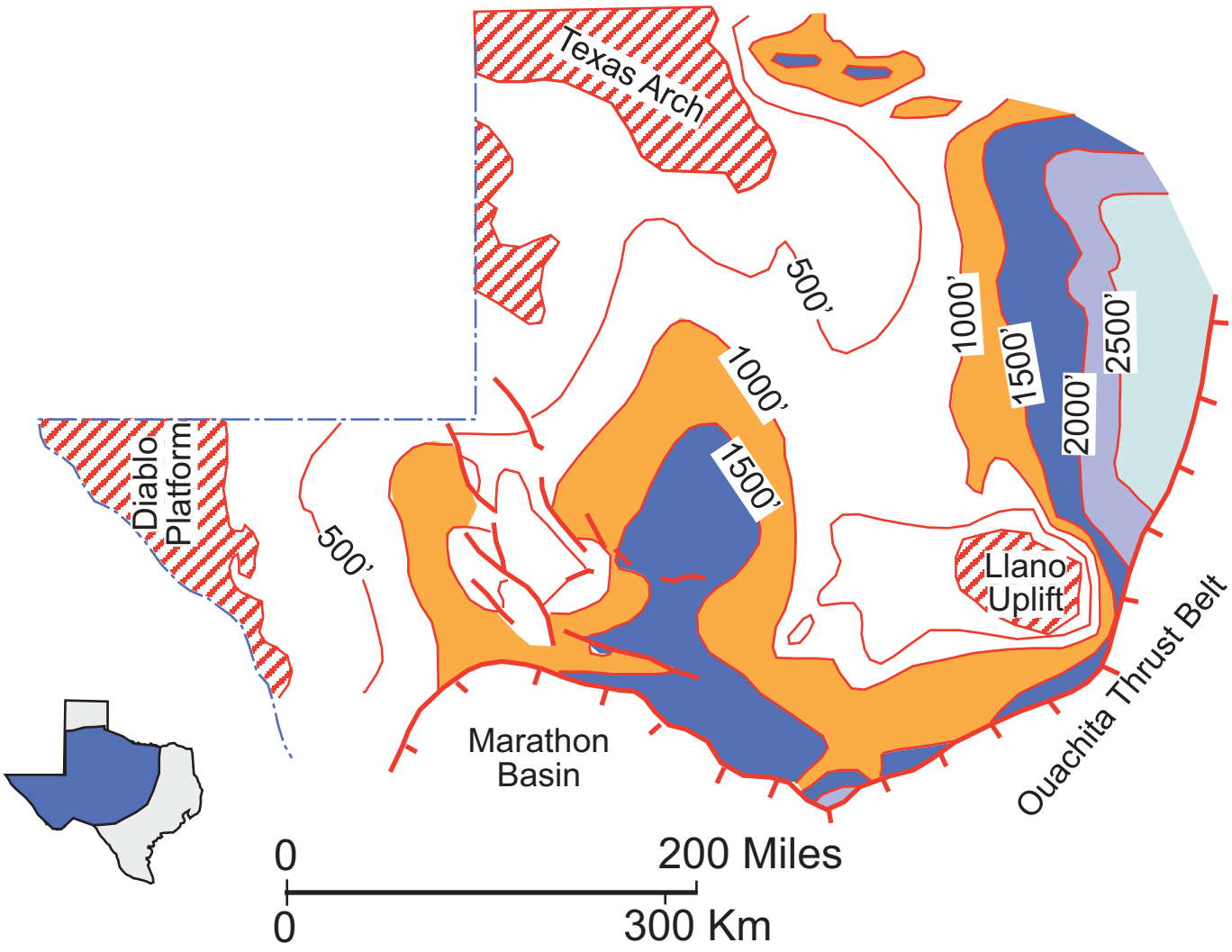

Figure 4. Generalized isopach map of the Ellenburger Group in West Texas. Thickest areas are colored. After Kerans (1972) who modified Texas Water Development Board (1972) figure.

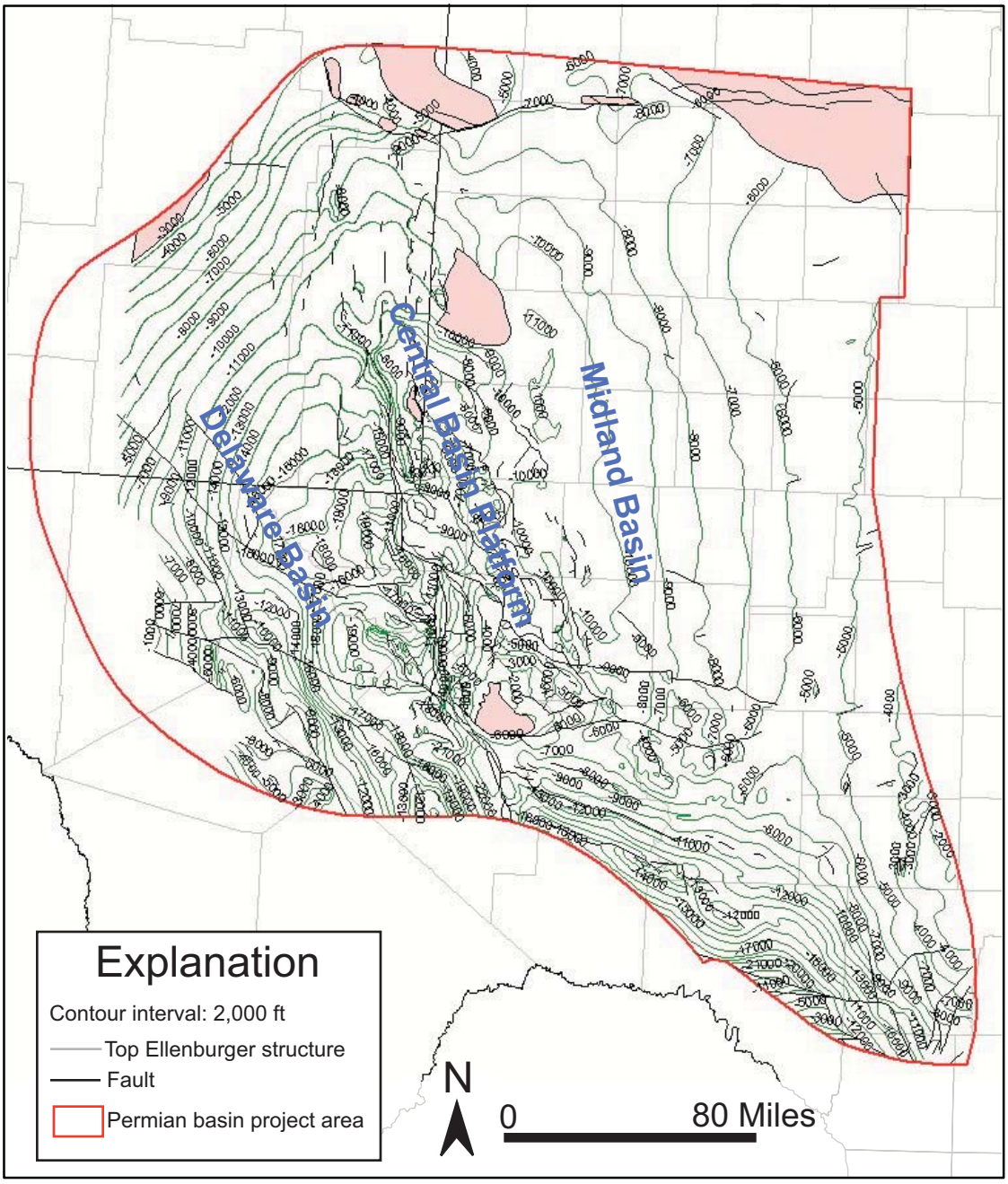

Figure 5. Structure map on top of Ellenburger Group from Ruppel et al. (2005). Contours are subsea depths.

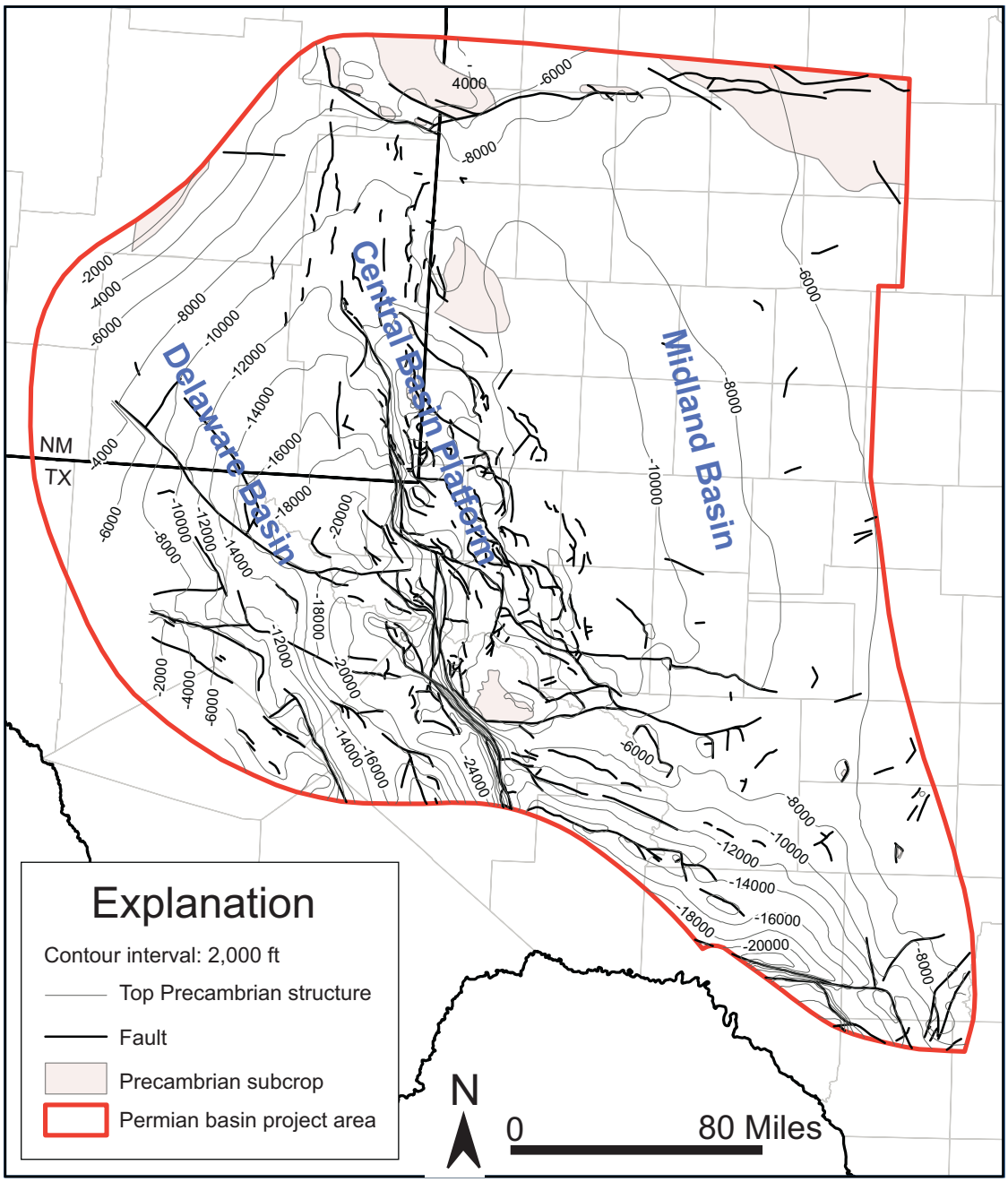

Figure 6. Structure map on top of Precambrian strata Ruppel et al. (2005). Contours are subsea depths.

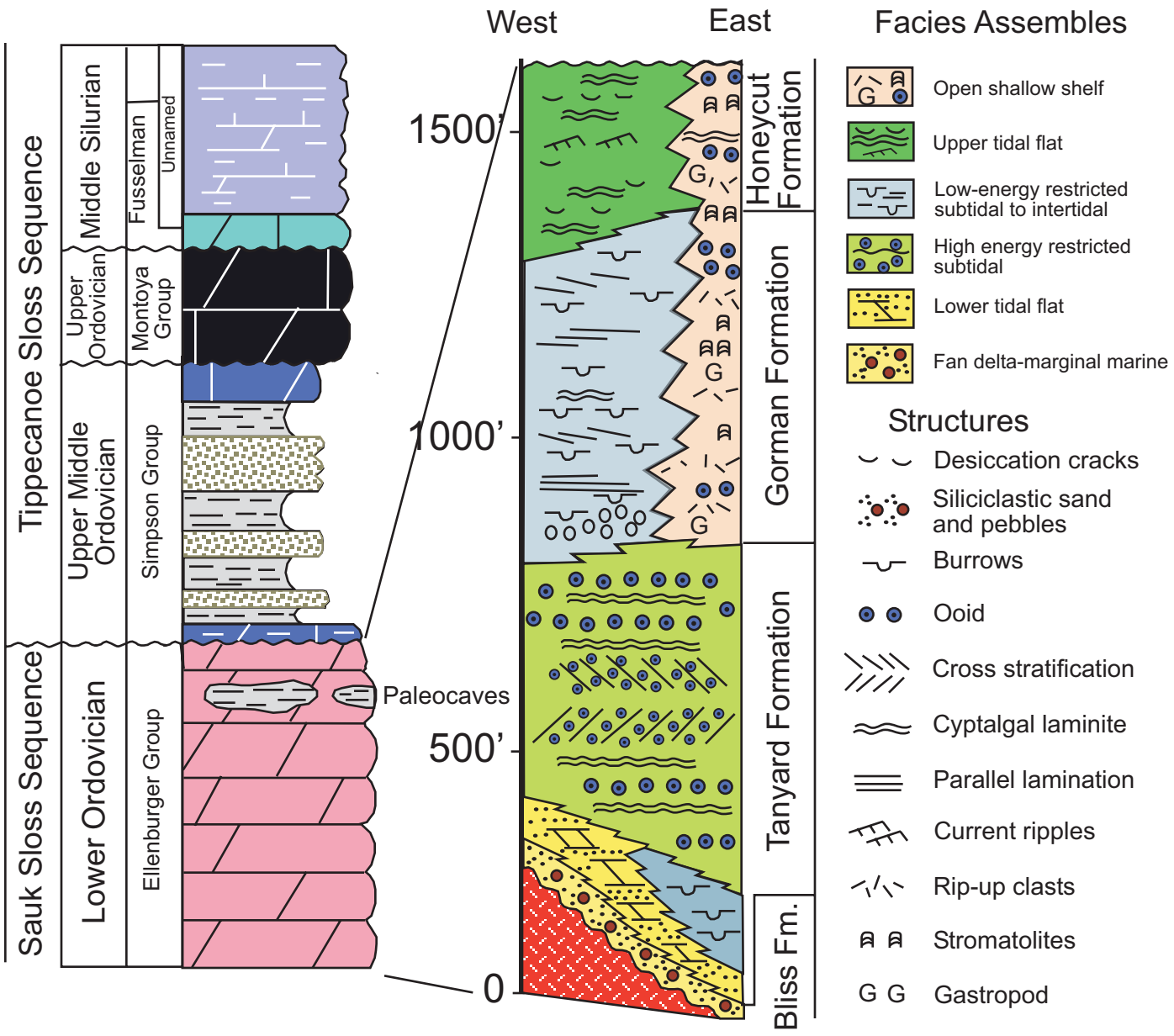

Figure 7. Schematic representation of Ellenburger depositional systems in West Texas compared with formalized Ellenburger stratigraphic units in the Llano area. Thickness of descriptive Ellenburger section is approximate. From Kerans (1990) with minor additions.

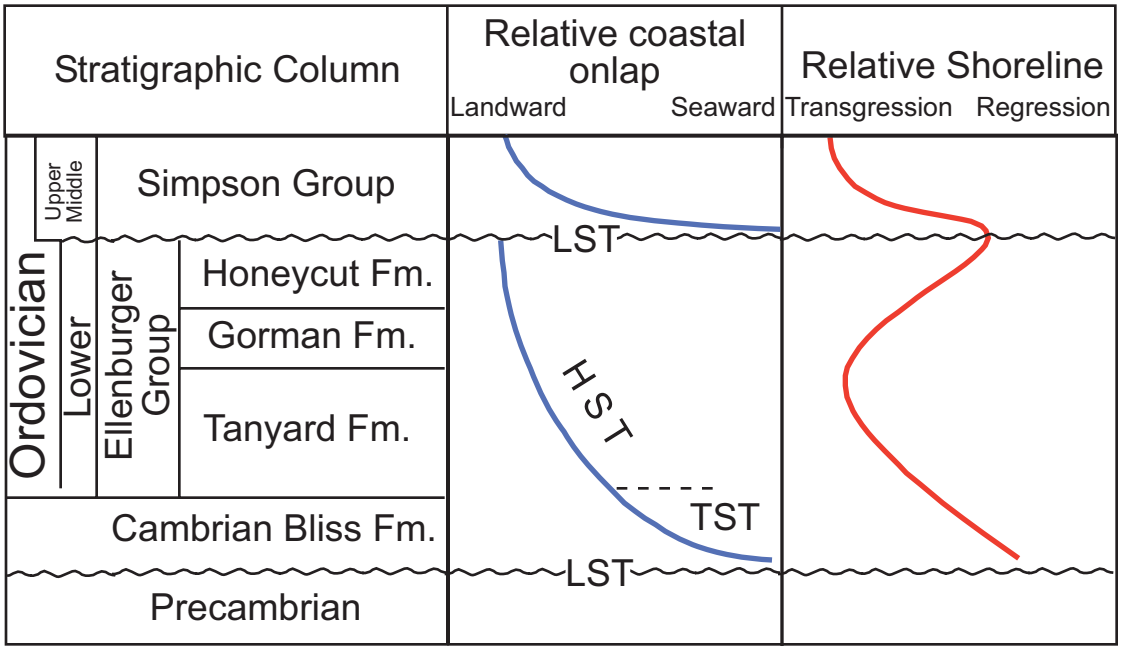

Figure 8. Interpretation of the second-order relative coastal and relative shoreline curves for the Ellenburger Group. Modified from Kupecz (1992).

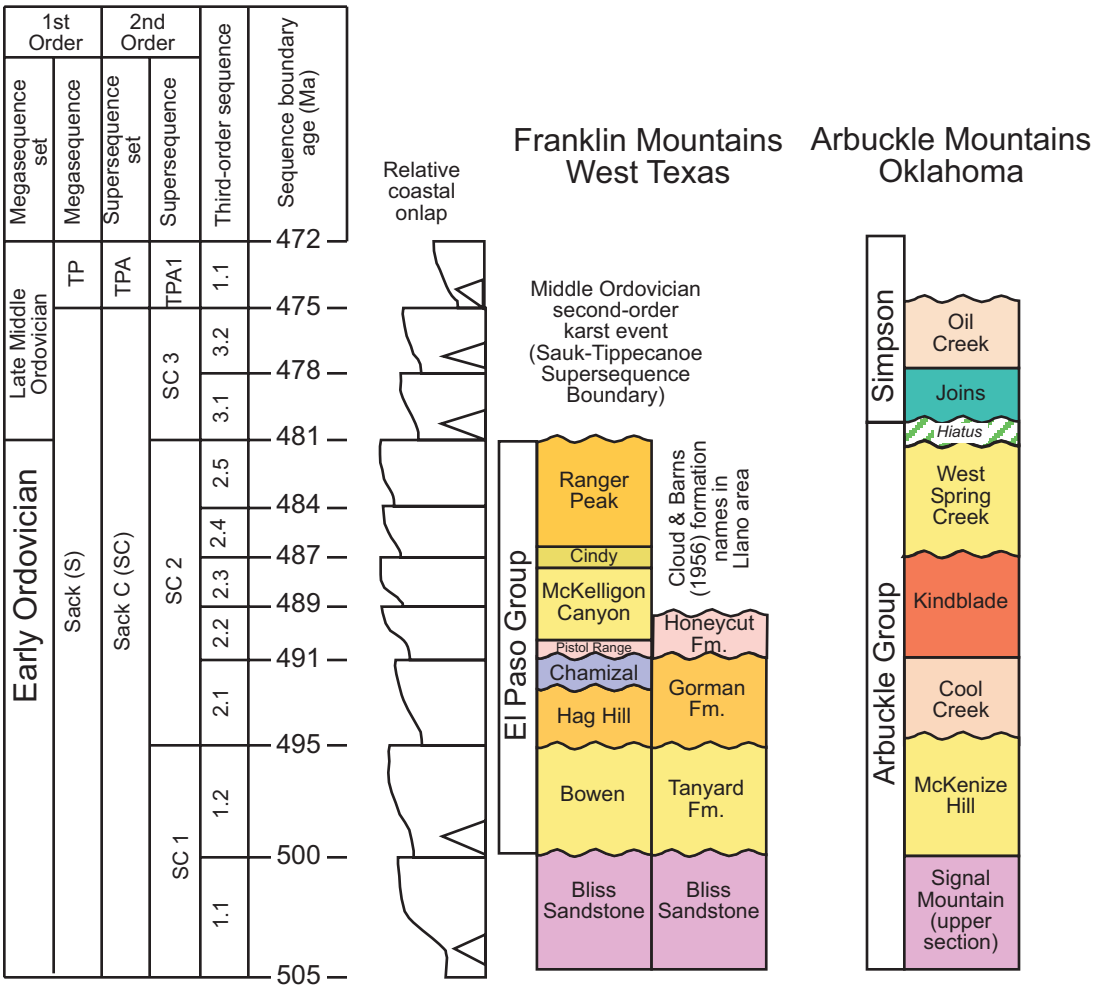

Figure 9. Chronostratigraphic summary of third-order depositional sequences in the Franklin Mountains of West Texas. Modified from Goldhammer et al. (1992).

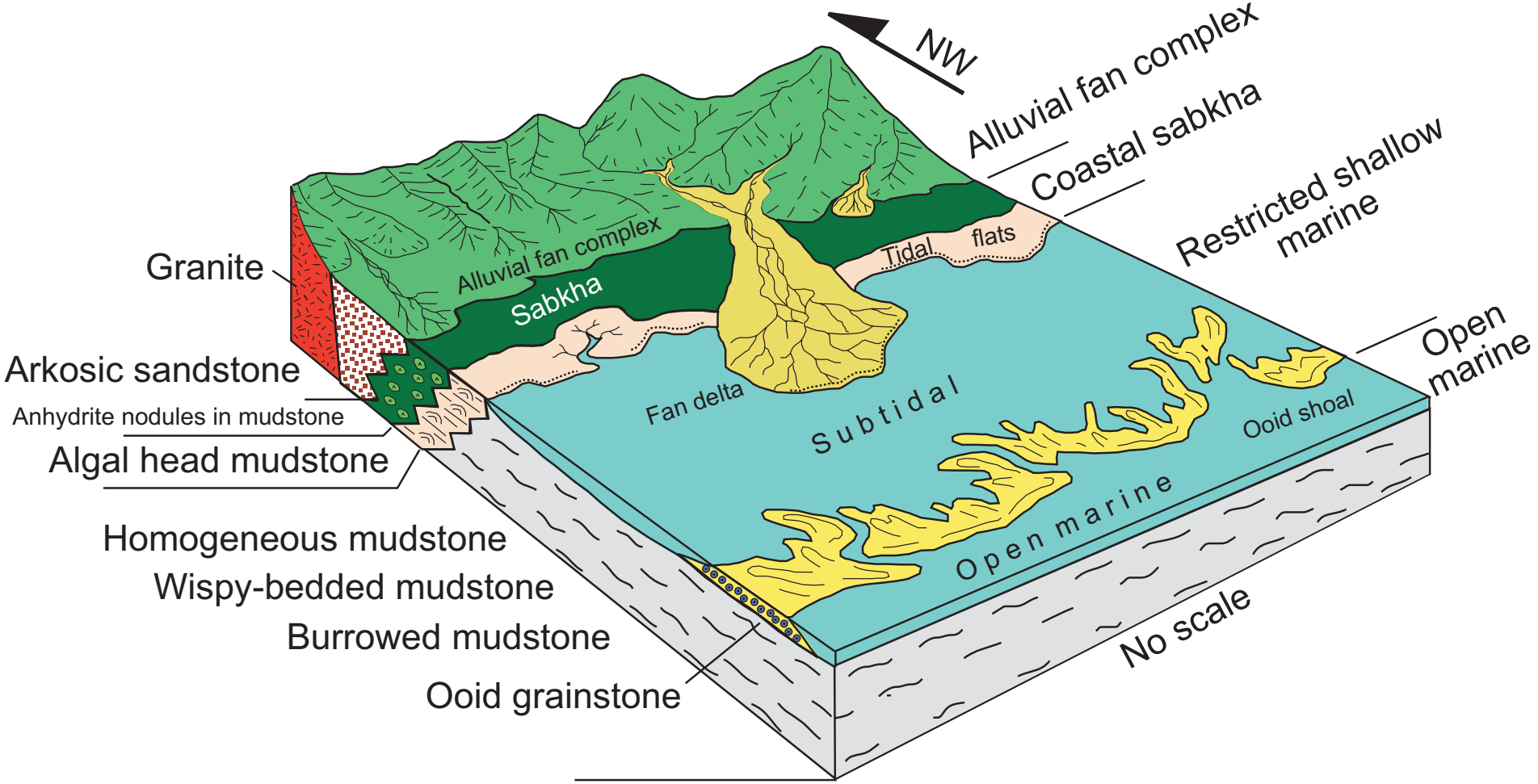

Figure 10. Depositional model for the Bliss and lower Ellenburger sections. Modified slightly from Loucks and Anderson (1985).

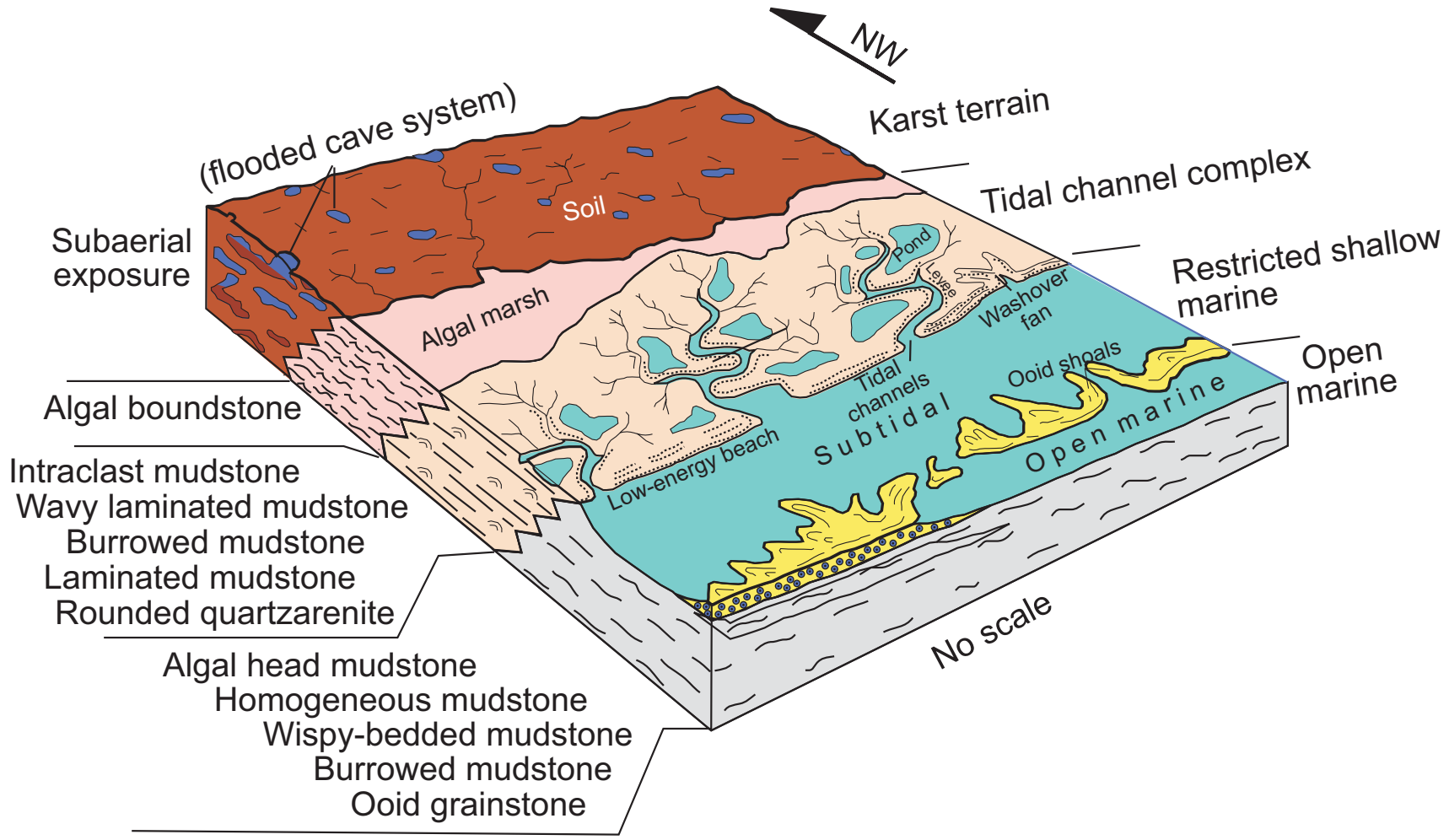

Figure 11. Depositional model for the middle and upper Ellenburger sections. Modified slightly from Loucks and Anderson (1985).

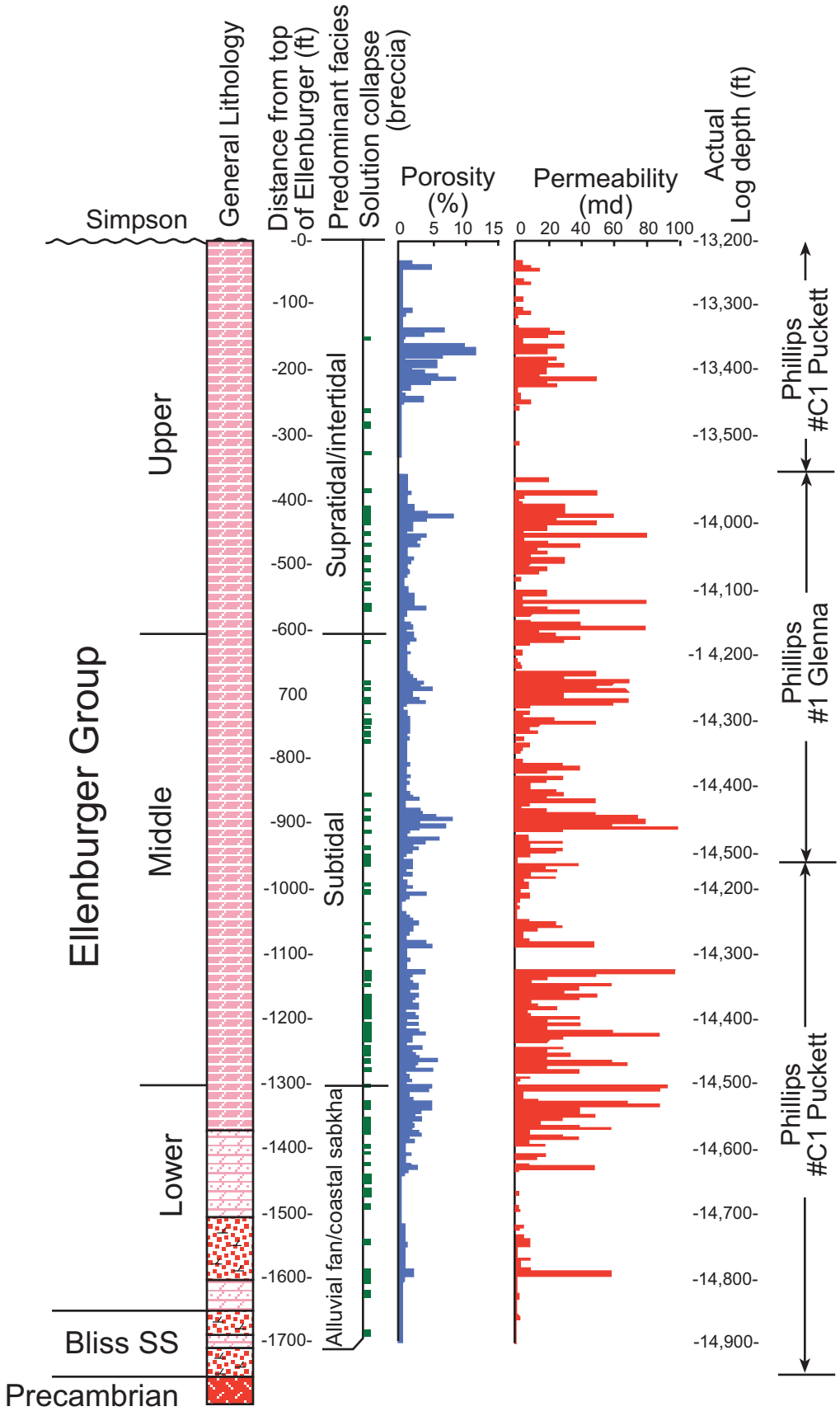

Figure 12. Profiles of porosity and permeability versus depth in the Phillips #C-1 Puckett and #1 Glenna wells. Both well-log depths and depth below top of Ellenburger section are shown. "Predominant facies" refers to the facies comprising largest proportions of individual cycles. From Loucks and Anderson (1980, 1985).

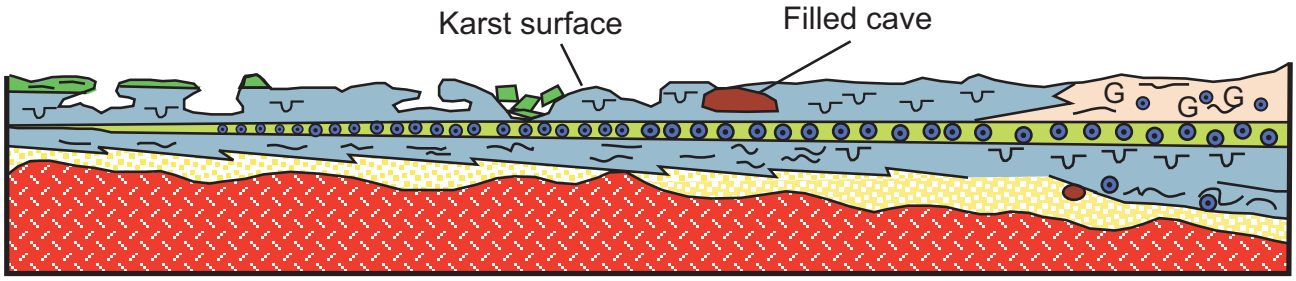

Stage 4. Exposure and erosion of the Ellenburger Group before the Middle Ordovician transgression formed a karst terrain.

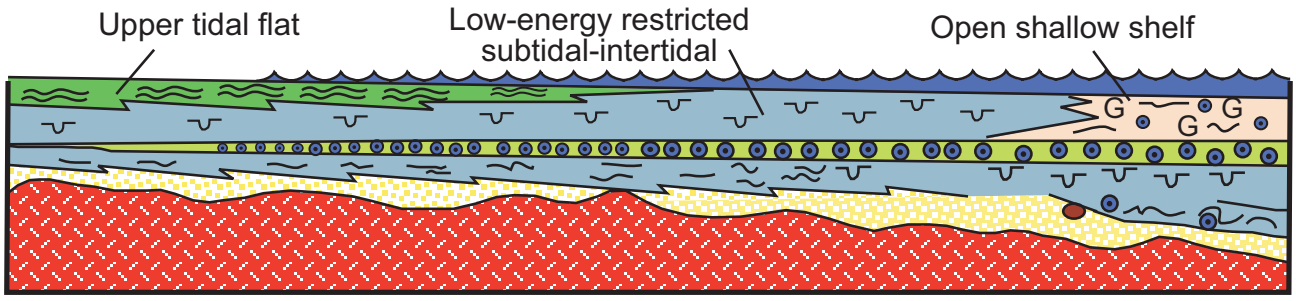

Stage 3. Regressive sedimentation with low-energy restricted-shelf and upper tidal-flat depositional systems prograding across the Ellenburger shelf, from northwest to east, southeast, and south. The open shallow-water shelf depositional system was deposited where more normal marine conditions prevailed, along the southern and eastern portions of the shelf.

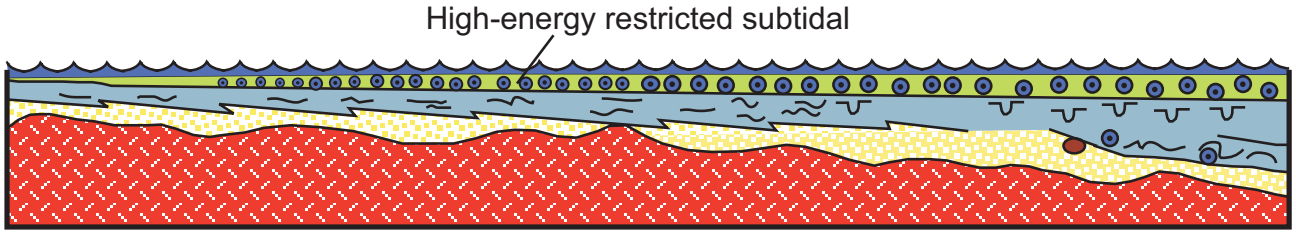

Stage 2. Rapid transgression and widespread aggradational deposition of the high-energy restricted-shelf depositional system across much of west and central Texas.

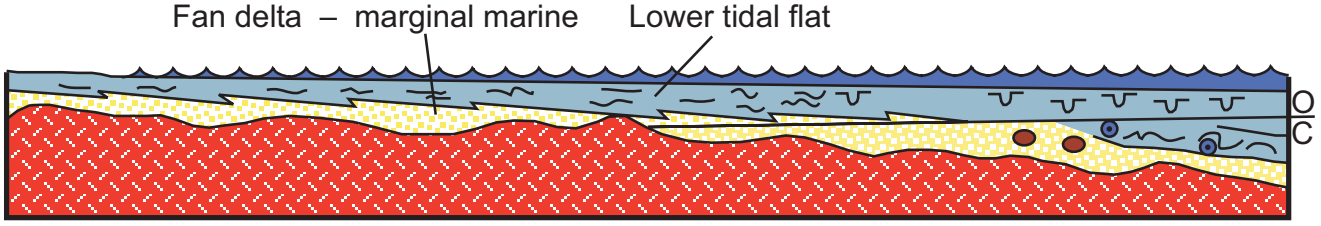

Stage 1. Regional depositional of fan delta – marginal marine depositional system continuous with the Early Cambrian transgression. Progradation of lower tidal-flat depositional system followed.

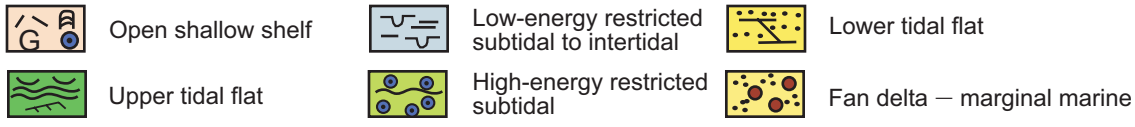

Figure 13. General depositional history of Ellenburger Group by stages. From Kerans (1990). Description of stages is taken directly from Kerans original figure caption.

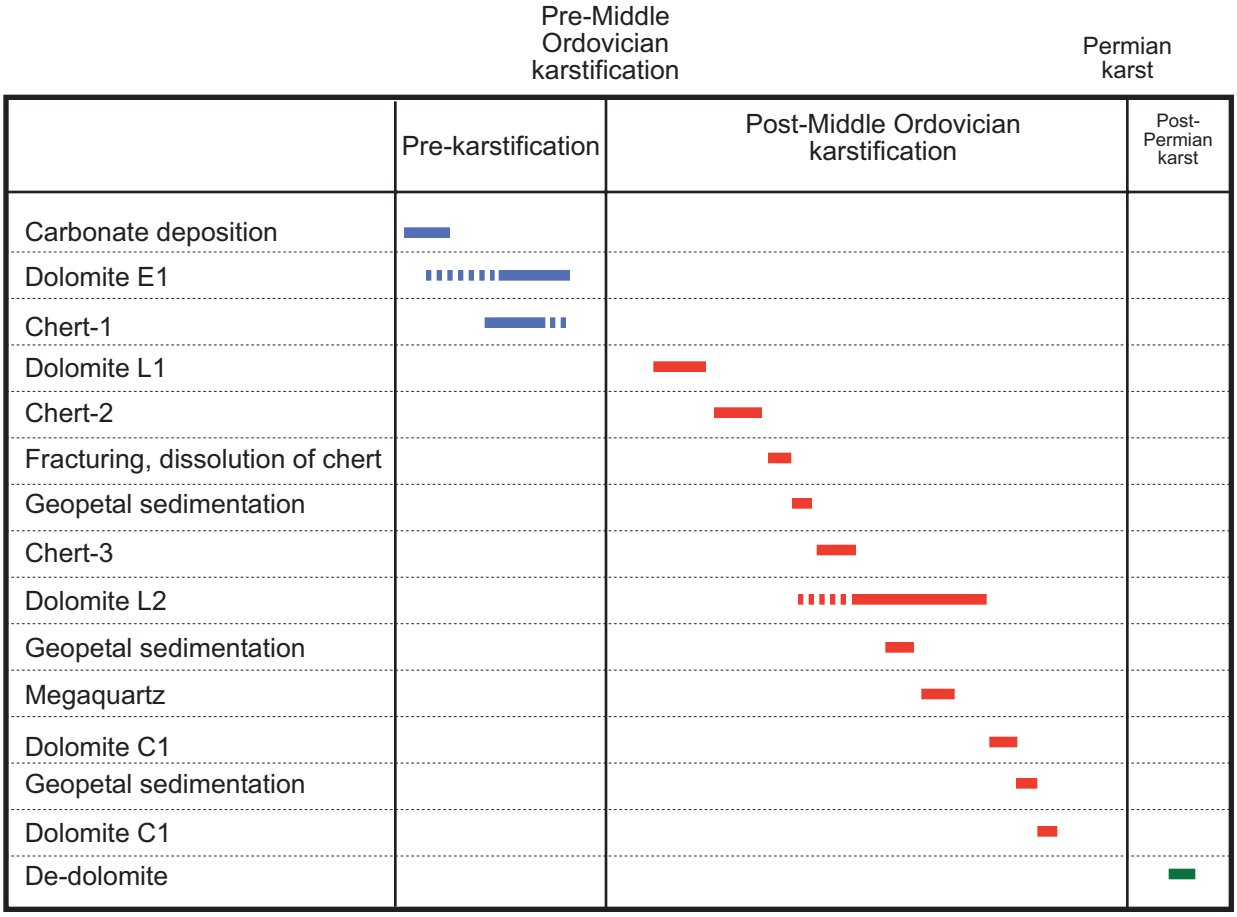

Figure 14. Paragenetic sequence of regional Ellenburger diagenesis by Kupecz and Land (1991). Figure from Kupecz and Land (1991).

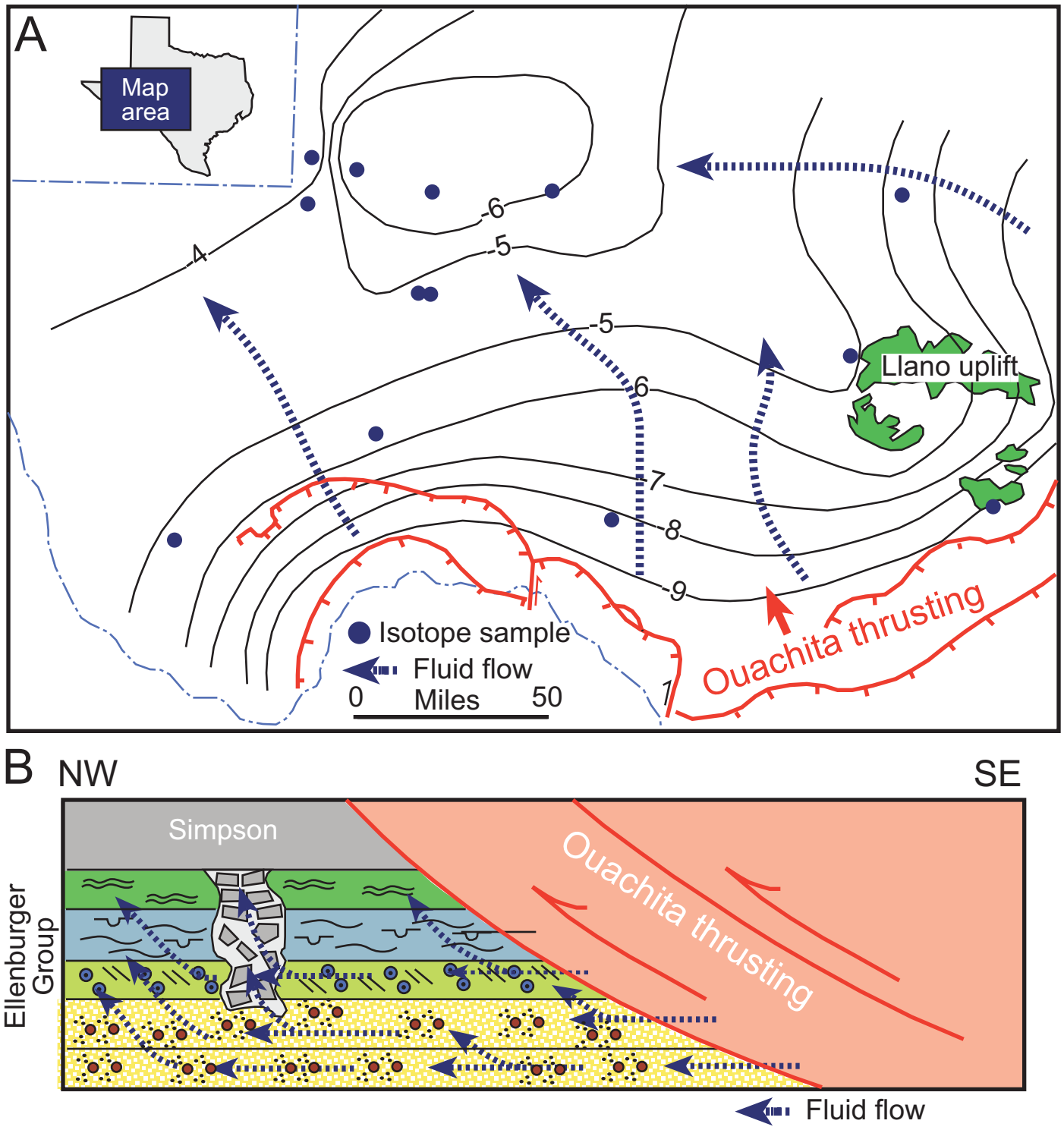

Figure 15. Fluid-flow model of Kupecz and Land (1991) for late-stage replacement Dolomite-L2. Figures from Kupecz and Land (1991). (A) Contour map of delta O^{18} isotopes of the late-stage replacement Dolomite-L2. Hypothetical fluid pathway-flow lines added by present author. The map indicates that hydrothermal fluids moved from the Ouachita Orogeny front in the southeast toward New Mexico to the northwest. (B) Schematic diagram showing the pathways for the hydrothermal fluids expelled by thrusting during the Ouachita Orogeny. The fluids moved along permeable faults, fractures, karst-breccia zones, and matrix pore-rich units.

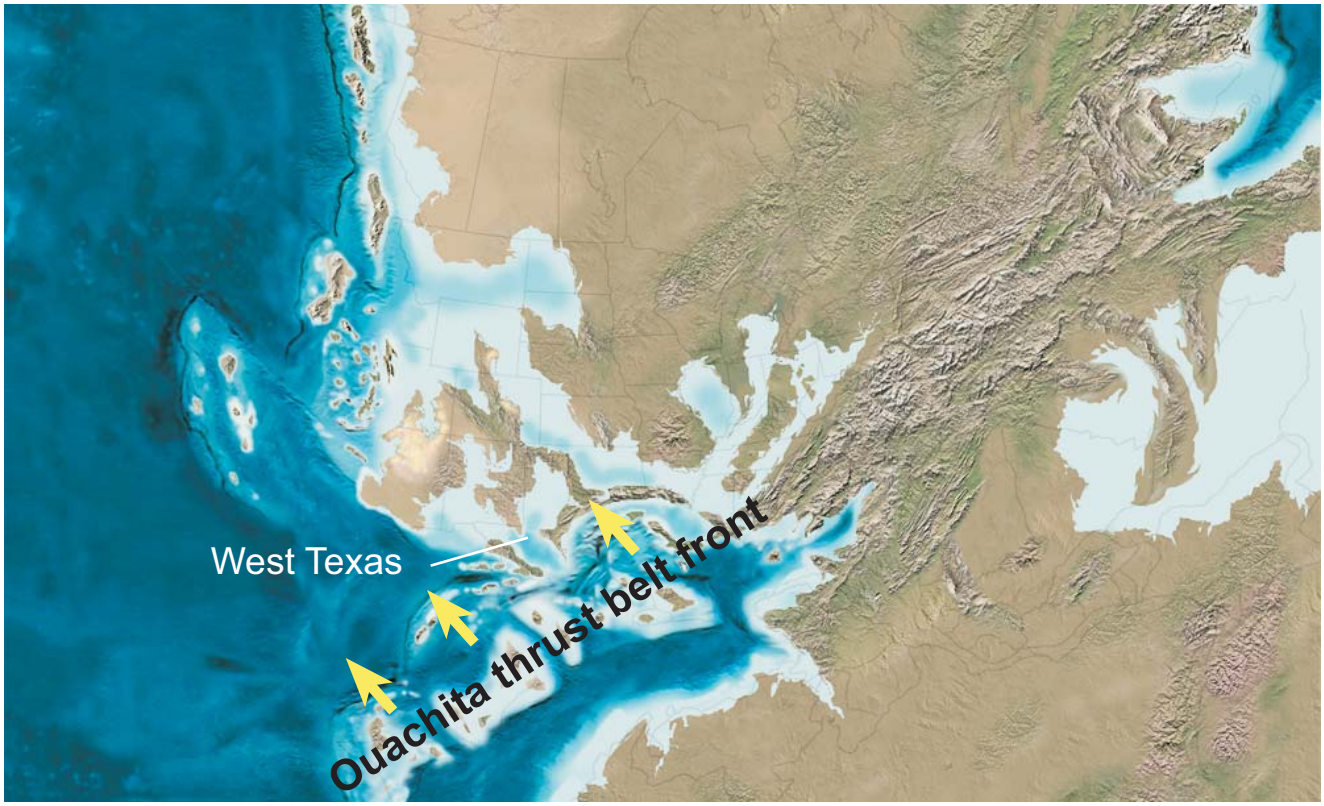

Figure 16. Plate reconstruction map of Early Pennsylvanian (315 Ma) by Blakey (2005b). The Ouachita thrusting injected dolomitizing fluids into the Ellenburger Group in the Central and West Texas areas. The yellow arrows indicate direction of thrust-fault movement.

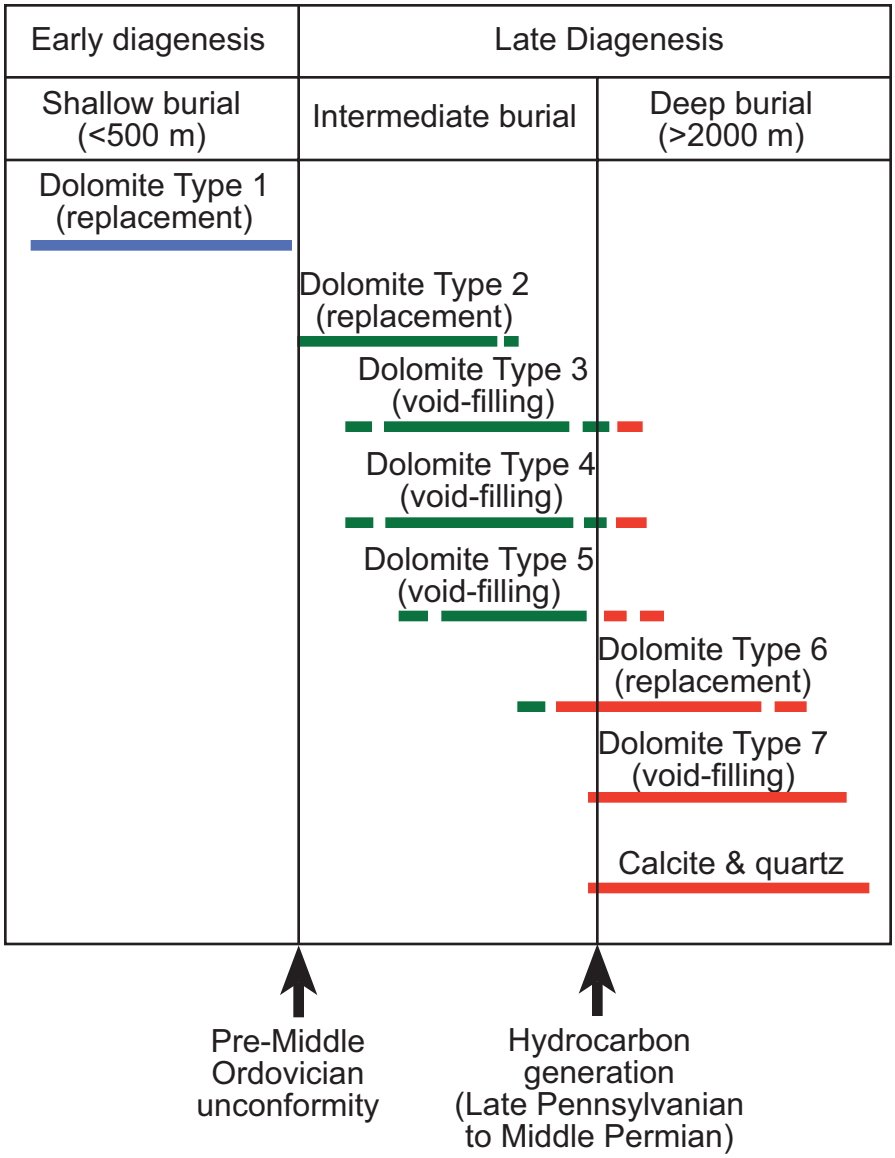

Figure 17. Paragenetic sequence of Amthor and Friedman (1992) for Ellenburger regional diagenetic study. Figure from Amthor and Friedman (1992).

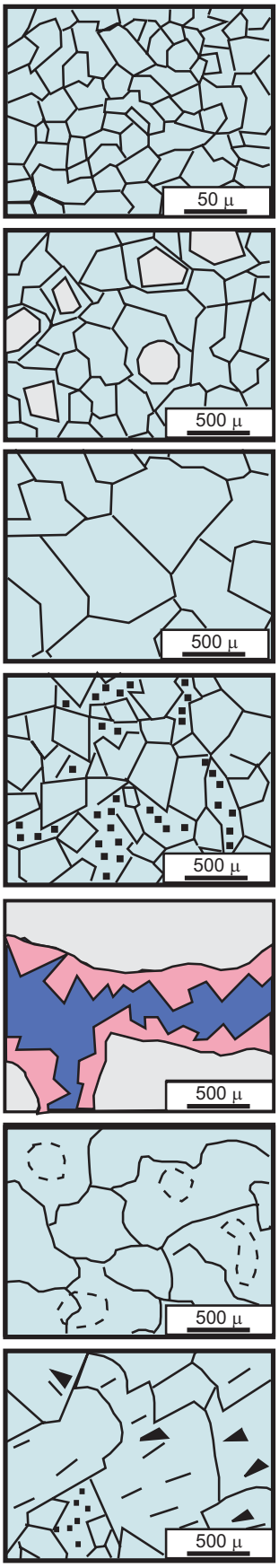

Dolomite type 1: Unimodal, very fine to fine-crystalline planar-s mosaic dolomite; dense, dark mosaics, replacing lime mud, preserving sedimentary structures.

Dolomite type 2: Unimodal, medium- to coarse-crystalline planar-s mosaic dolomite; milky white to clear, or cloudy core, clear rim texture, nonmimic replacement of grains.

Dolomite type 3: Coarse- to very coarse crystalline planar-s dolomite; milky to clear crystals; no replacement features; fills void space and fractures.

Dolomite type 4: Medium- to coarse-crystalline planar-e mosaic dolomite; clear or cloudy core, clear rim texture; not replacement features; occurs in mottles, breccias, or near stylolites.

Dolomite type 5: Medium- to coarse- crystalline planar-e dolomite; clear crystals lining void space and fractures filled by late dolomite and/or calcite.

Dolomite type 6: Coarse- to very coarse crystalline nonplanar-a dolomite; dark, inclusion-rich crystals, with serrated, irregular, curved, or otherwise distinct boundaries; undulose extinction; vague nonmimic replacement of grains.

Dolomite type 7: Coarse- to very coarse crystalline nonplanar-c dolomite milky white to clear crystals with undulose extinction and curved crystals faces (saddle dolomite); void-filling; associated with authigenic quartz and late calcite.

Figure 18. Dolomite textures described by Amthor and Friedman (1992). Figure from Amthor and Friedman (1992).

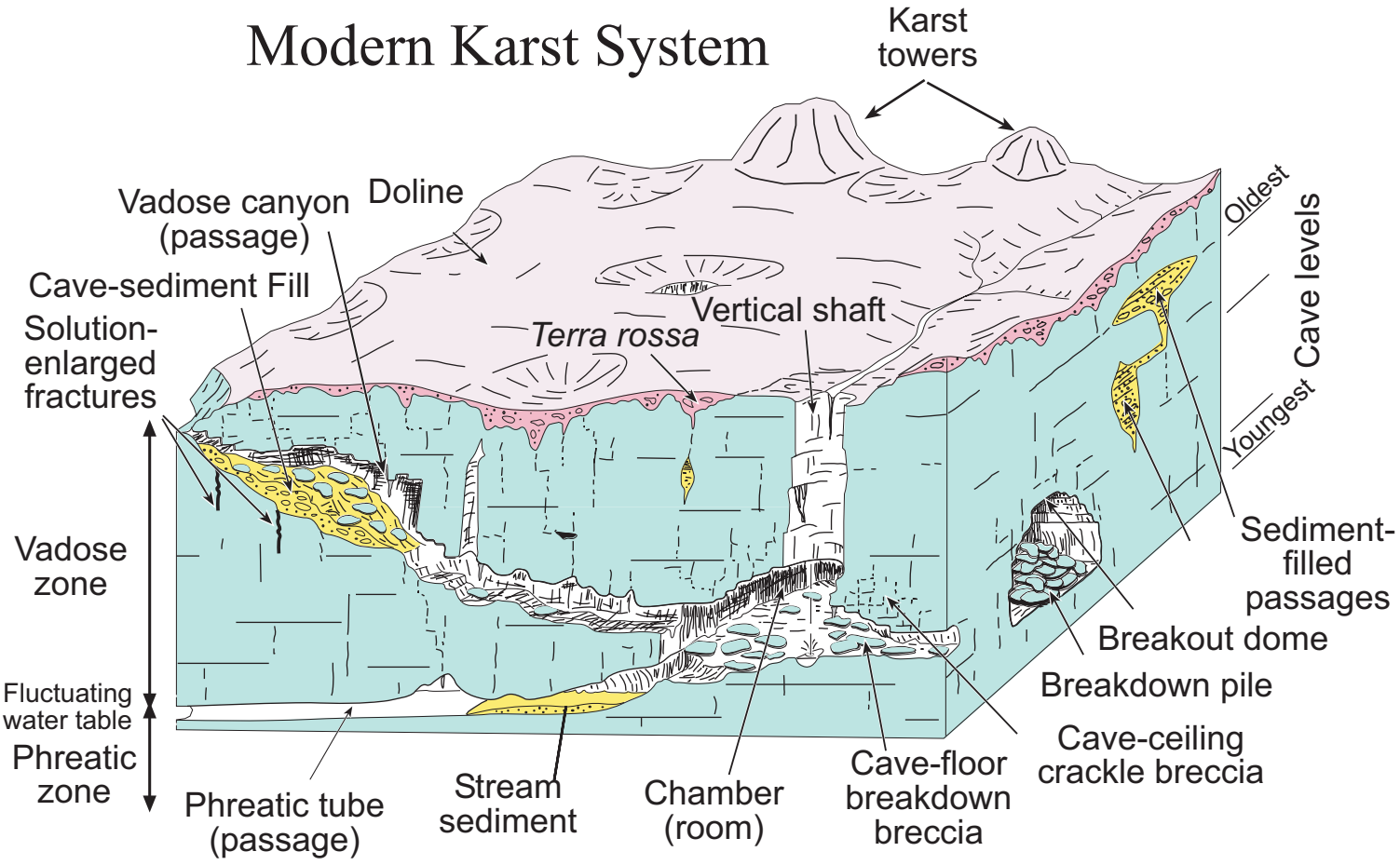

Figure 19. Block diagram of a near-surface modern karst system. The diagram depicts four levels of cave development (upper right corner of block model), with some older passages (shallowest) having sediment fill and chaotic breakdown breccias. Breccia and fracture development begin in a cave system while it is at the surface. As the water table drops, increased stress develops around caverns promoting brecciation and fracturing. Modified from Loucks (1999).

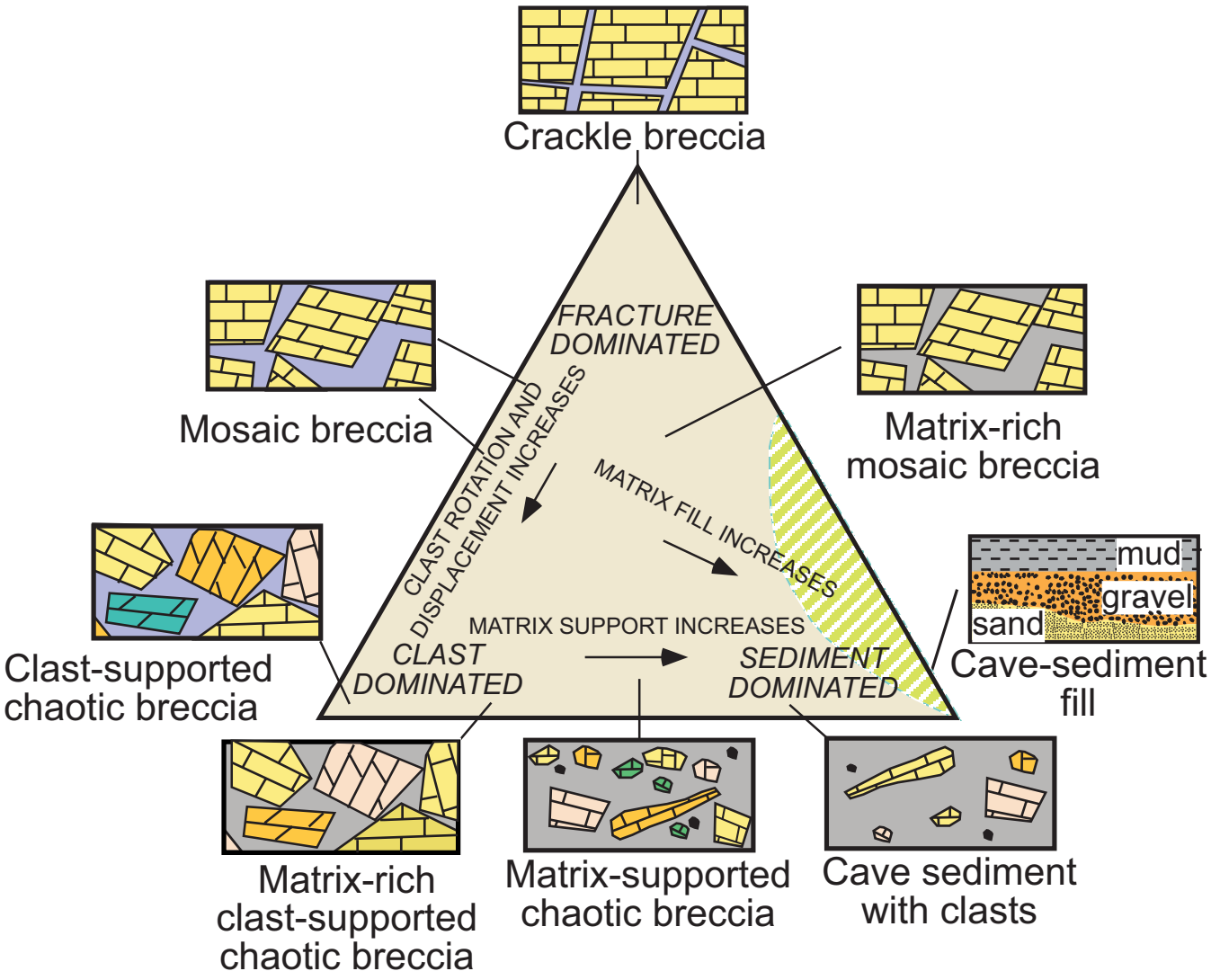

Figure 20. Classification of breccias and cave-sediment fills. Shaded area in the lower right of the diagram indicates that no cave features plot in this area. Cave-sediment fills and breccias can be separated into three end members: crackle breccia, chaotic breccia, and cave-sediment fill. Crackle breccias show slight separation and displacement. Mosaic breccias display some displacement, but they can be fitted back together. Chaotic breccias are composed of displaced clasts that cannot be fitted back together, and they can be composed of clasts of different origins (polymictic). Cave-sediment fill can form a matrix within the breccia, as well as support individual clasts. The best reservoir quality is in the matrix-free breccias. From Loucks (1999).

Evolution of a Cave Passage

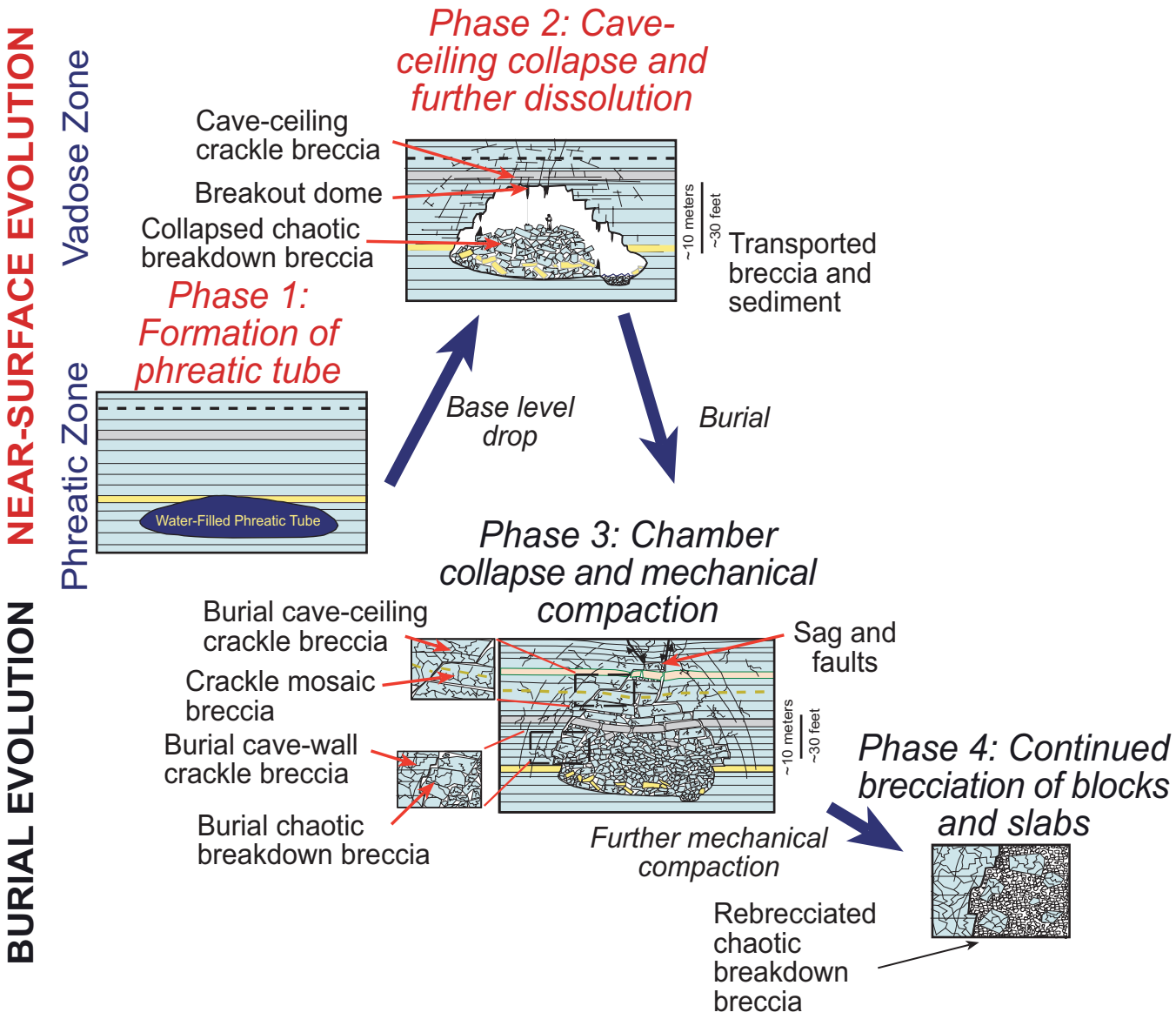

Figure 21. Schematic diagram showing evolution of a single cave passage from its formation in the phreatic zone of a near-surface karst environment to burial in the deeper subsurface. In the near-surface, excavation and associated breakdown are major processes. Many near-surface cave passages contain abundant breccias and cave-sediment fill. Crackle breccia fracturing affects the wall and ceiling rock early in the history of the cave. Excavation solution and cave sedimentation terminate as the cave-bearing strata subside into the subsurface. Mechanical compaction increases and restructures the existing breccias and remaining cavities. Most large voids collapse after several thousand feet of burial, forming more chaotic breakdown breccia. Some large interclast pores may be preserved. Differentially compacted but relatively intact strata over the collapsed chamber are fractured and form burial cave-roof crackle and mosaic breccias with loosely to tightly fitted clasts. Continued burial leads to more extensive mechanical compaction of the previously formed breakdown, thus causing blocks with large void spaces between them to fracture and pack more closely together. The resulting product is a rebrecciated chaotic breakdown breccia composed of smaller clasts. Many of the clasts are overprinted by crackle fracture brecciation.

Evolution of Cave Systems

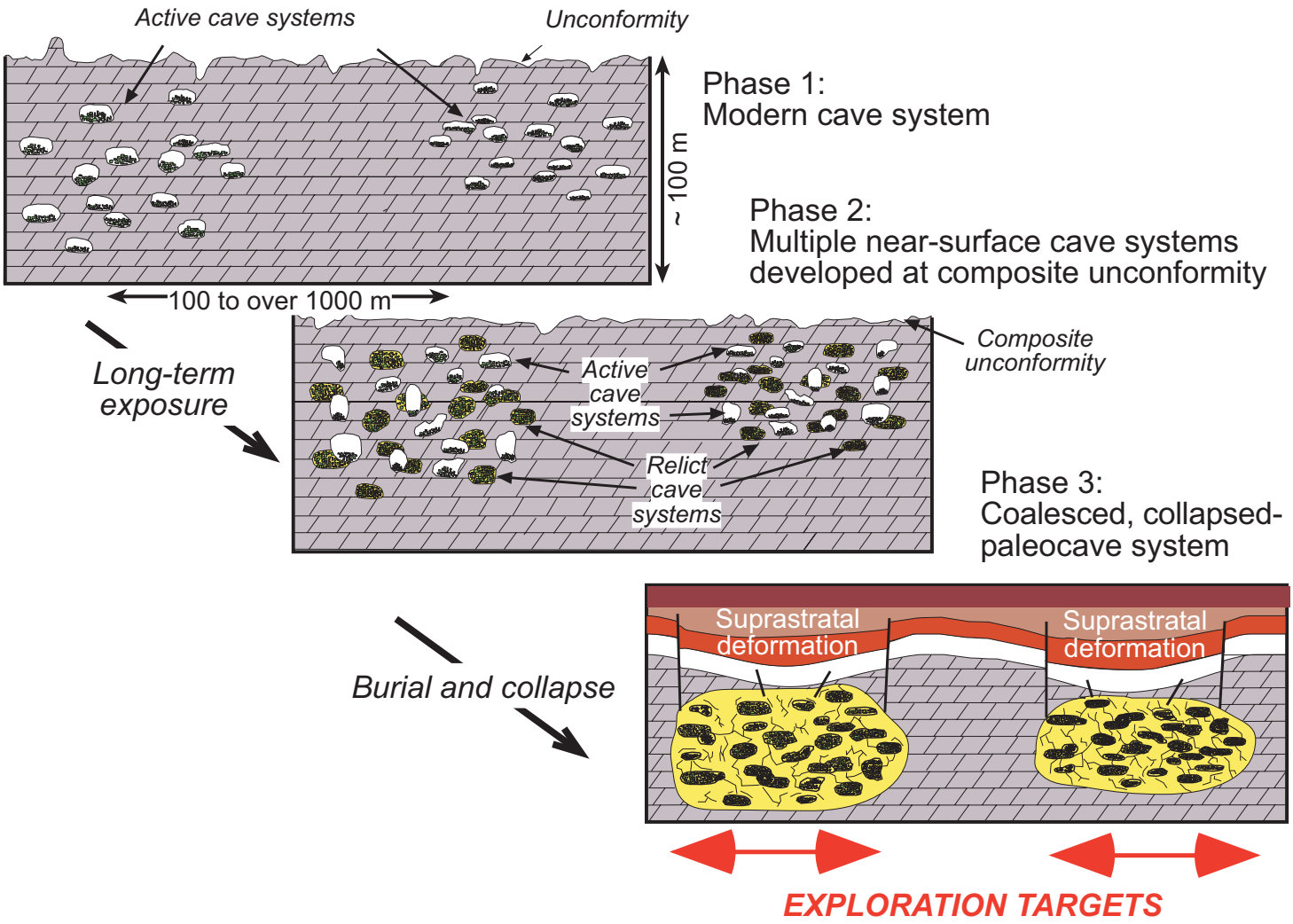

Figure 22. Schematic diagram showing the stages of development of a coalesced, collapsed-paleocave system. The development of a large collapsed-paleocave reservoir is the result of several stages of development. Multiple cave-system development at a composite unconformity may be necessary in order to produce a high density of passages. As the multiple-episode cave system subsides into the deeper subsurface, wall and ceiling rocks adjoining open passages collapse and form breccias that radiate out from the passage, and may intersect with fractures from other collapsed passages and older breccias within the system. The result is the coalescing of the cave system into a spatially complex reservoir system. The resulting coalesced breccia/fractured bodies can be thousands of feet of across, thousands of feet long, and hundreds of feet thick. Strata above the collapsed cave system are deformed by brecciation, faulting, and sagging (suprastratal deformation) Modified from Loucks (1999).

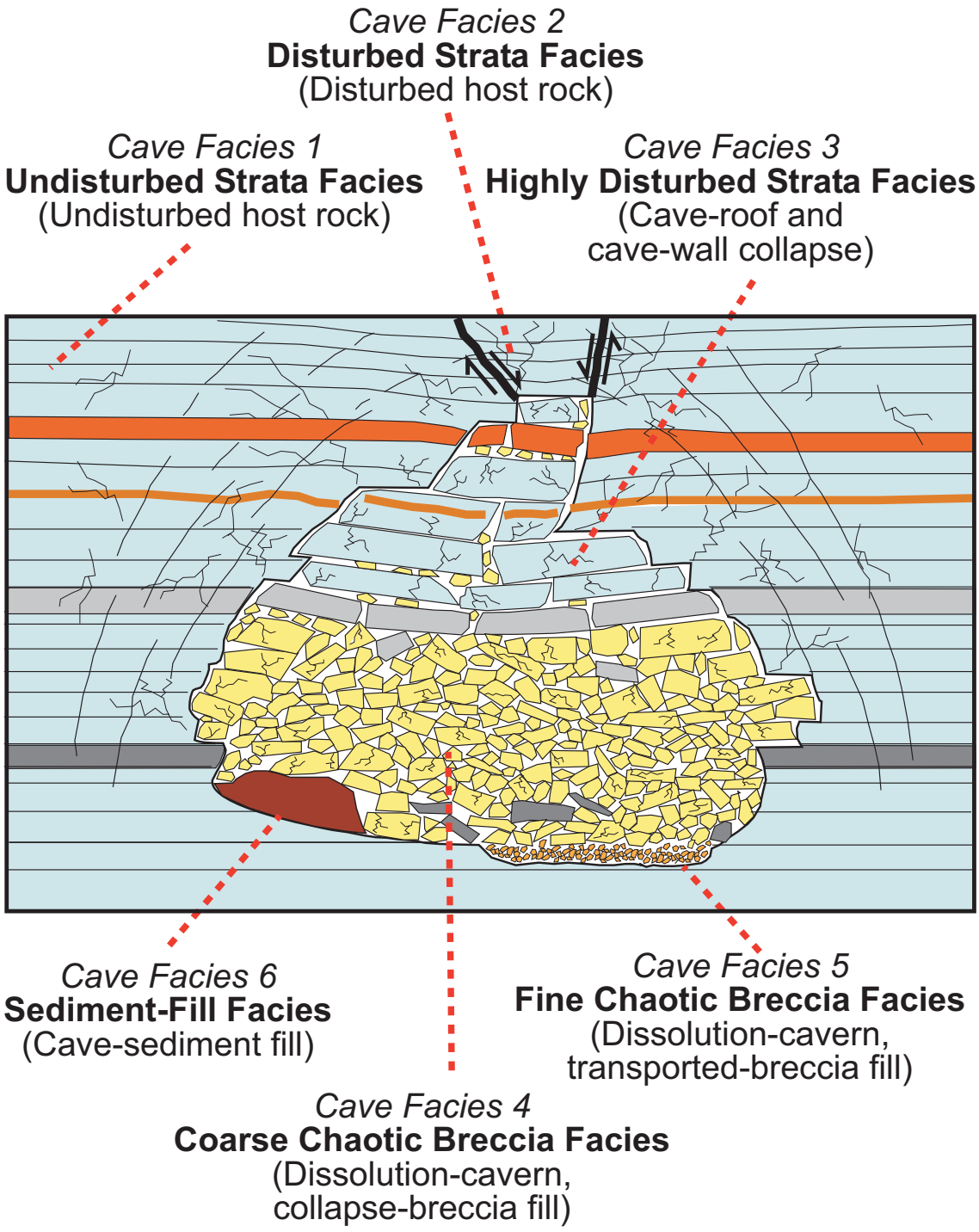

Figure 23. Paleocave facies classification by Loucks and Mescher (2001). See Table 1 for details.

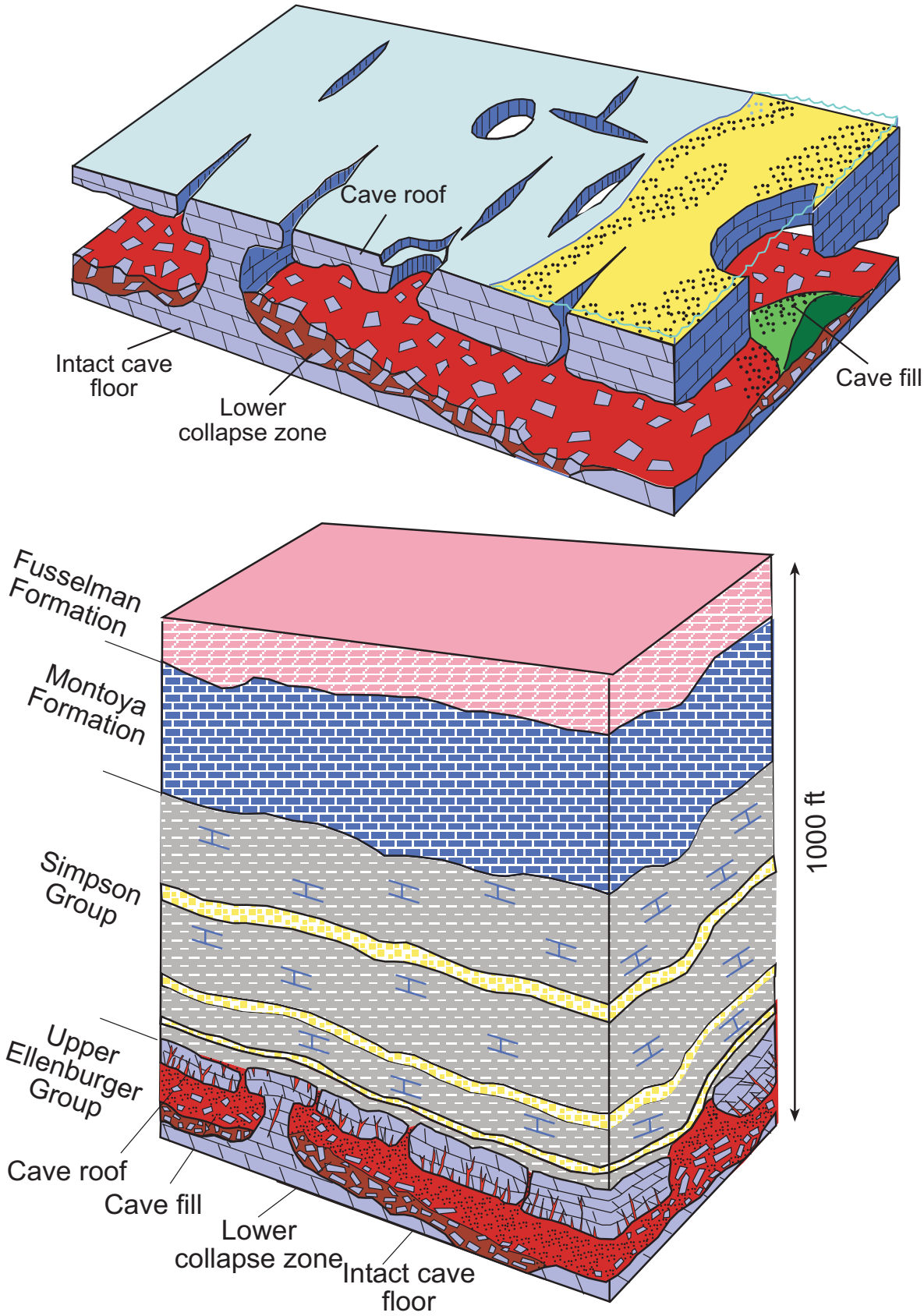

Figure 24. Paleocave models of Kerans (1988, 1989). (A) Schematic block diagram of a cave in the Lower Ordovician of West Texas showing cave floor, cave roof, cave-sediment fill, and collapsed breccia. Simpson siliciclastic material is filling cave during later transgression. (B) Schematic block model showing the collapsed Ellenburger paleocave system buried by successive Ordovician and Silurian deposits. Burial resulted in fracture brecciation of the roof and sagging of later units.

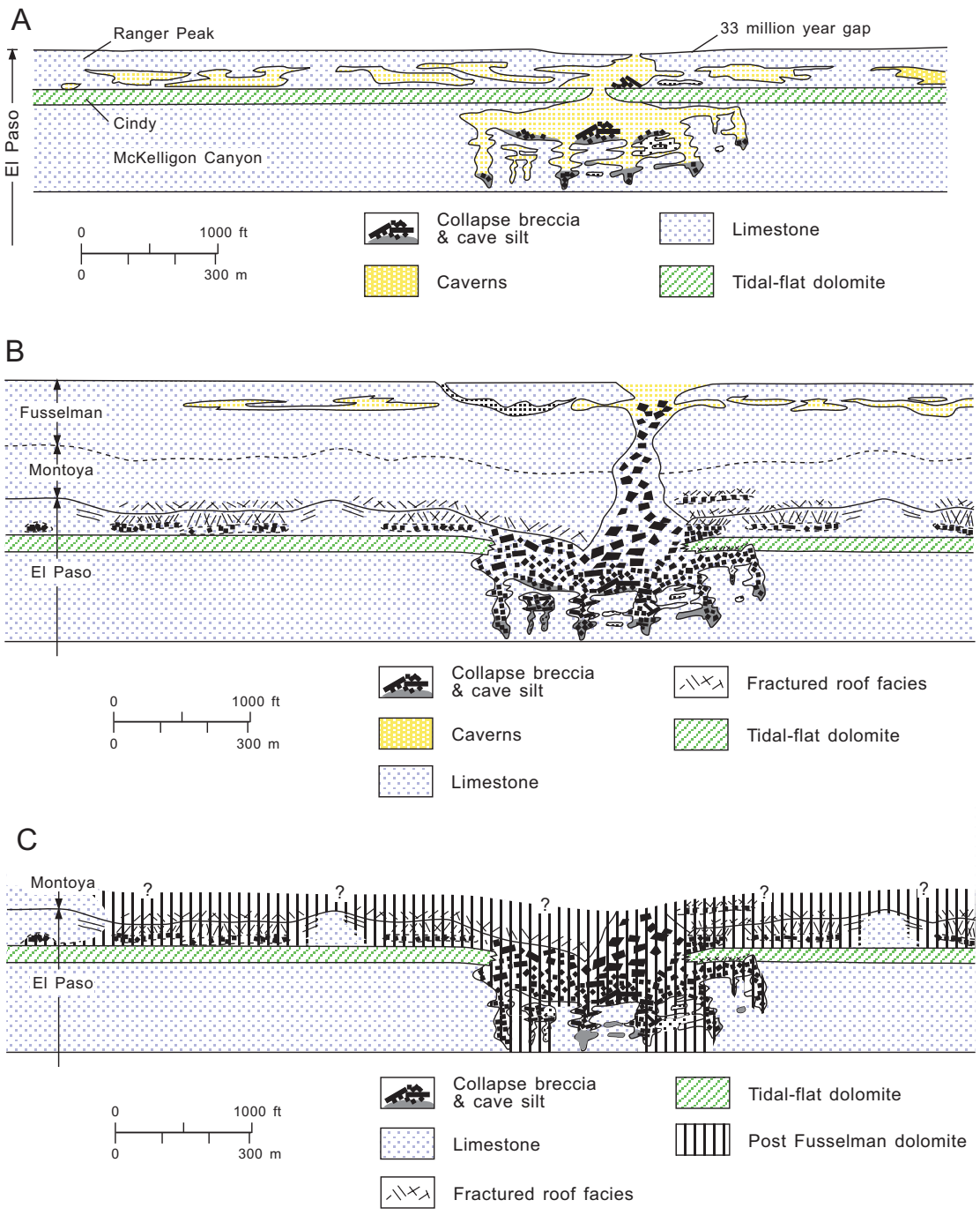

Figure 25. Reconstruction of El Paso paleocave system by Lucia (1995). Figure caption is directly from Lucia (1995). (A) Penecontemporaneous dolomitization of the Cindy Formation and development of tabular, laterally continuous caverns in the Ranger Peak Formation and vertical, laterally discontinuous caverns in the McKelligon Canyon Formation. (B) Collapse of the El Paso caverns showing collapse of the Montoya, development of breccia pipes up into the Fusselman Formation, and development of caverns in the Fusselman Formation. (C) Late-stage dolomitization of the El Paso and Montoya groups controlled by fluid flow through collapse breccia, fractures, and into adjacent carbonates.

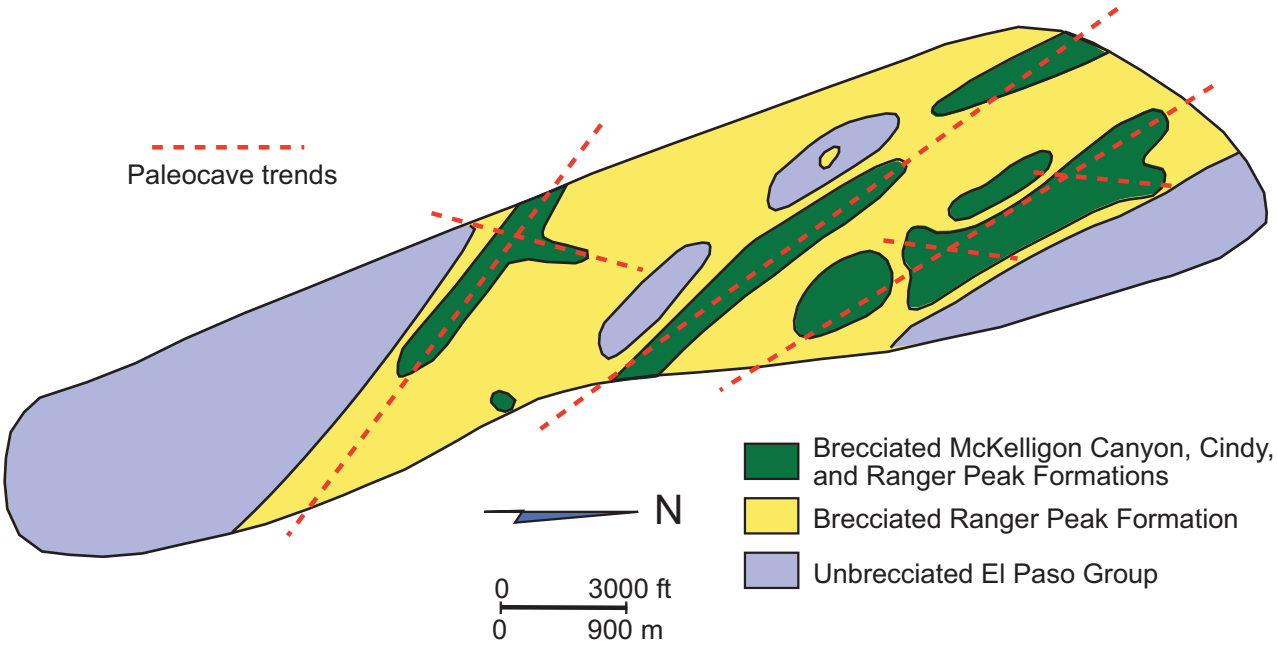

Figure 26. Reconstruction by Lucia (1995) of the different collapsed breccia in the Franklin Mountains, Texas. Paleocave trend lines are by present author.

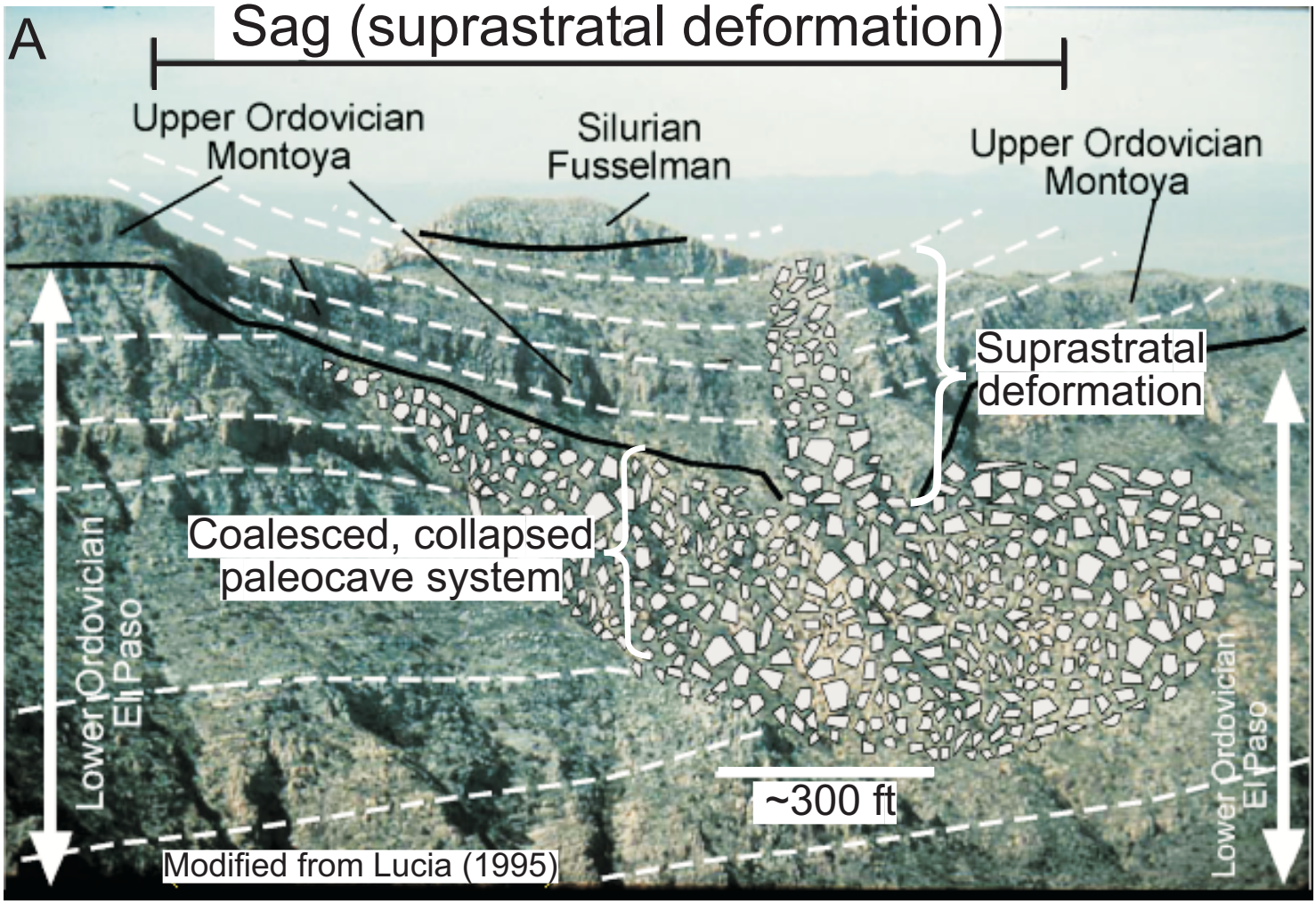

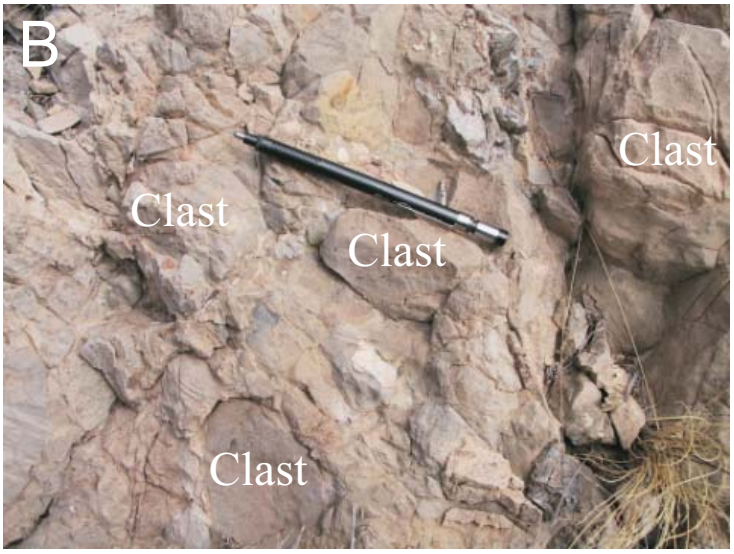

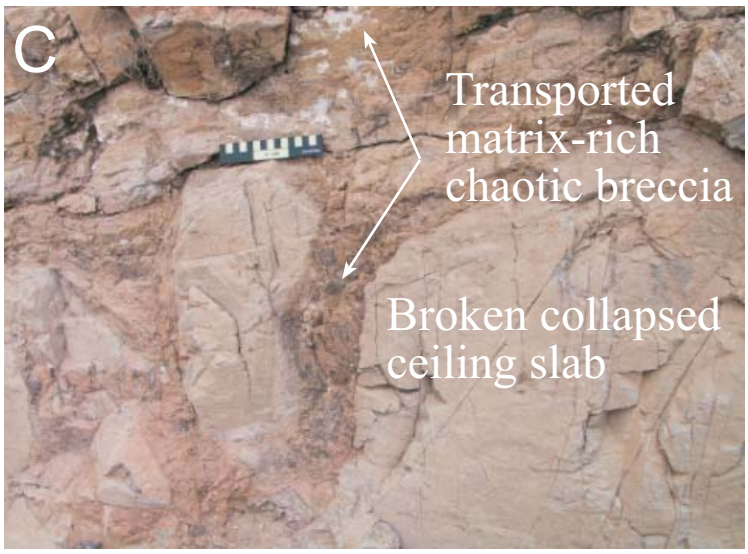

Figure 27. (A) Photograph of the Great McKelligon Sag in the Franklin Mountains of far West Texas. Photograph and general interpretation are from Lucia 1995 but modified by present author. This is an outstanding outcrop example of a coalesced, collapsed paleocave system with associated overlying suprastratal deformation. (B) Transported matrix-rich chaotic breccia. (C) Broken collapsed ceiling slab embedded in transported matrix-rich chaotic breccia.

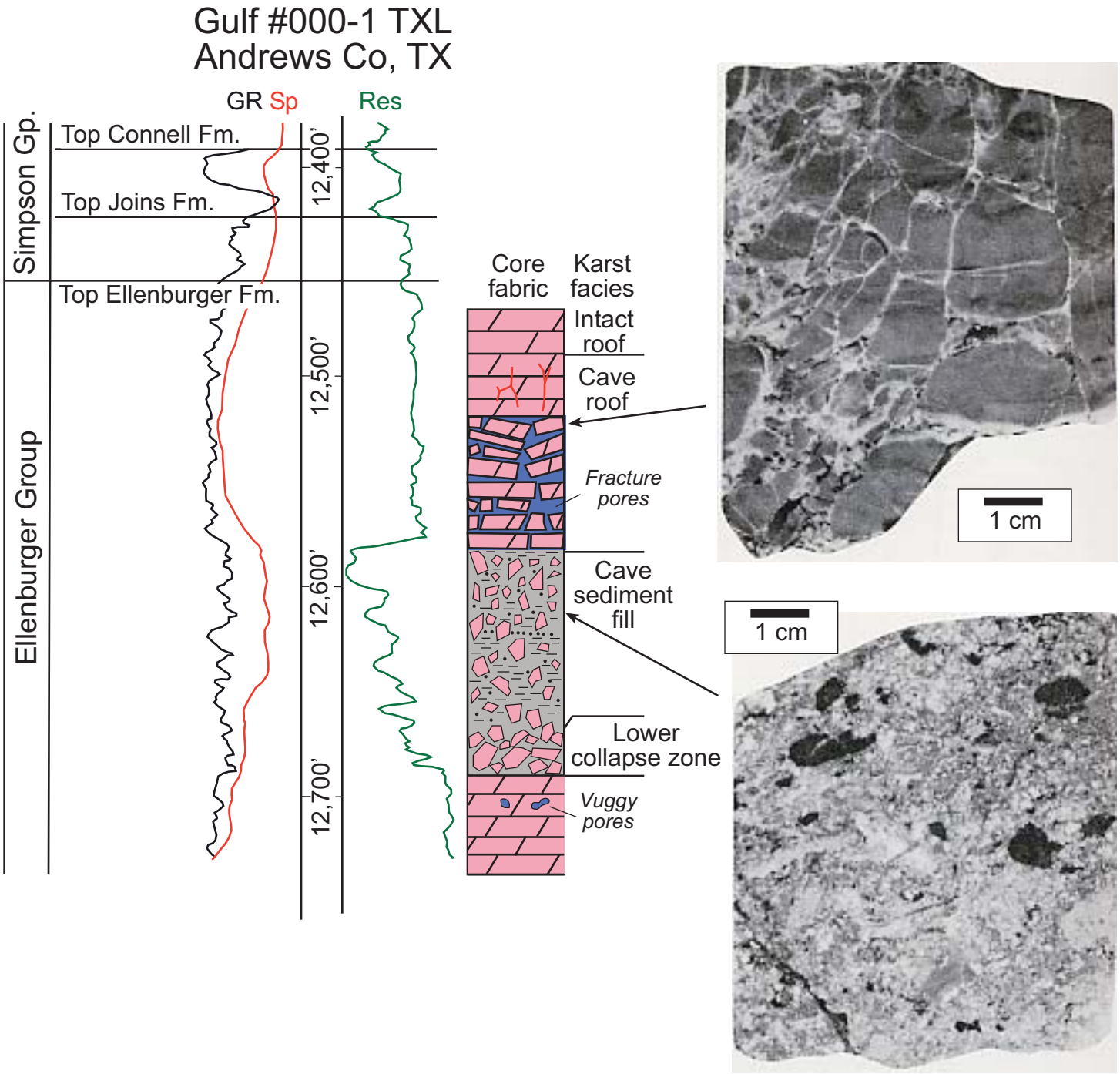

Figure 28. Core and wireline logs form the Gulf #000-1 TXL, Emma reservoir (Andrews County, Texas). Upper photograph from 12,526 ft shows crackle-fracture pores in collapse cave roof. Lower photograph from 12,610 ft shows cave-sediment fill (debris flow) with clasts floating in matrix of chloritic shale and quartz sand. From Kerans (1989).

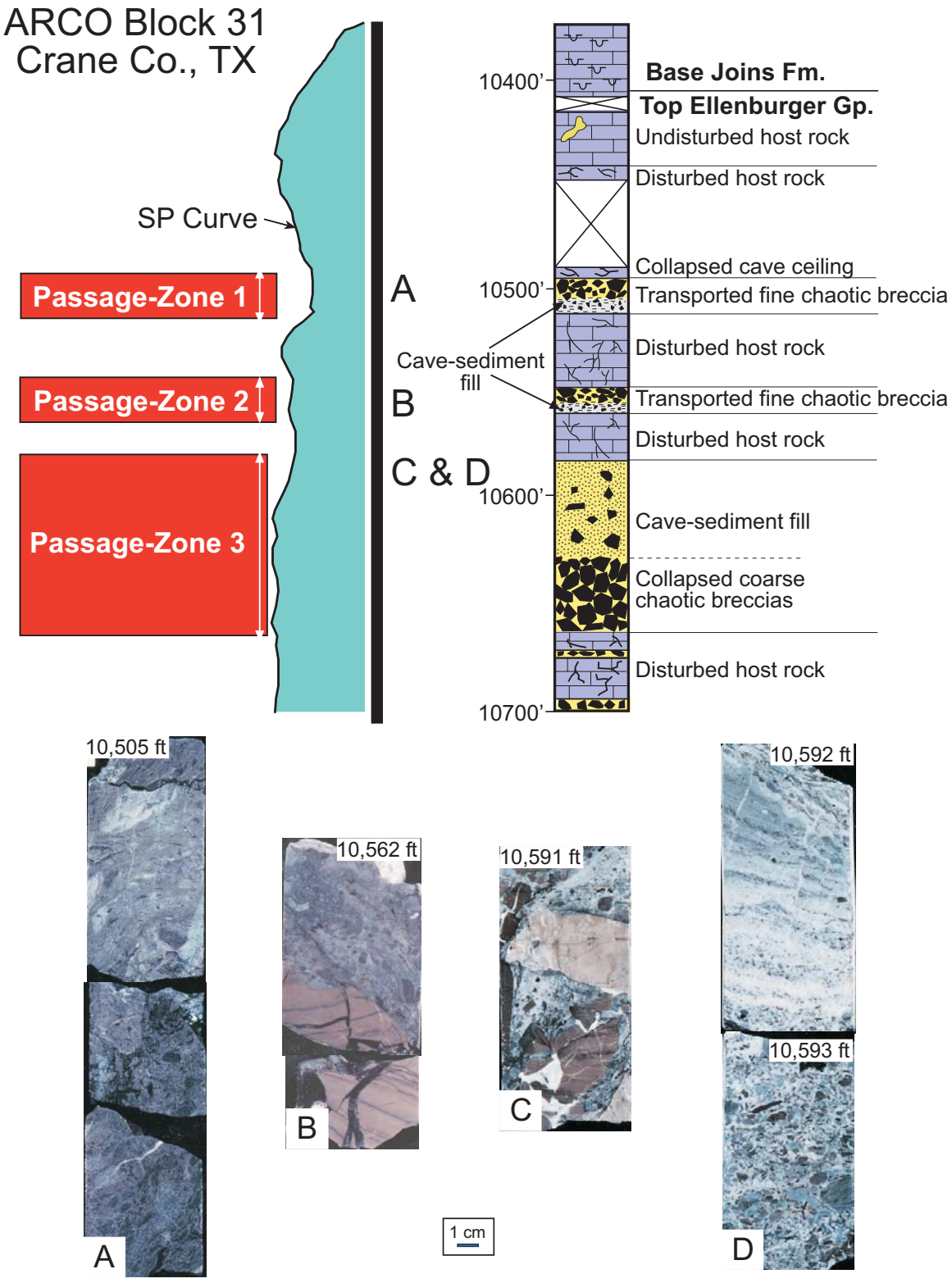

Figure 29. Core description and associated SP log for the Arco Block 31 core in Crane County, Texas. Photograph A is from a debris flow of transported fine chaotic breccia (cave-sediment fill in a passage). Photograph B from a debris flow of transported fine chaotic breccia (cave-sediment fill in a passage). Photograph C is siliciclastic-rich sand and carbonate clast cave-sediment fill (cave-sediment fill in a passage). Photograph D is a debris flow at the base overlain by siliciclastic cross-bedded sandstone (cave-sediment fill in a passage). Modified from Loucks and Handford (1992) and Loucks (2001)

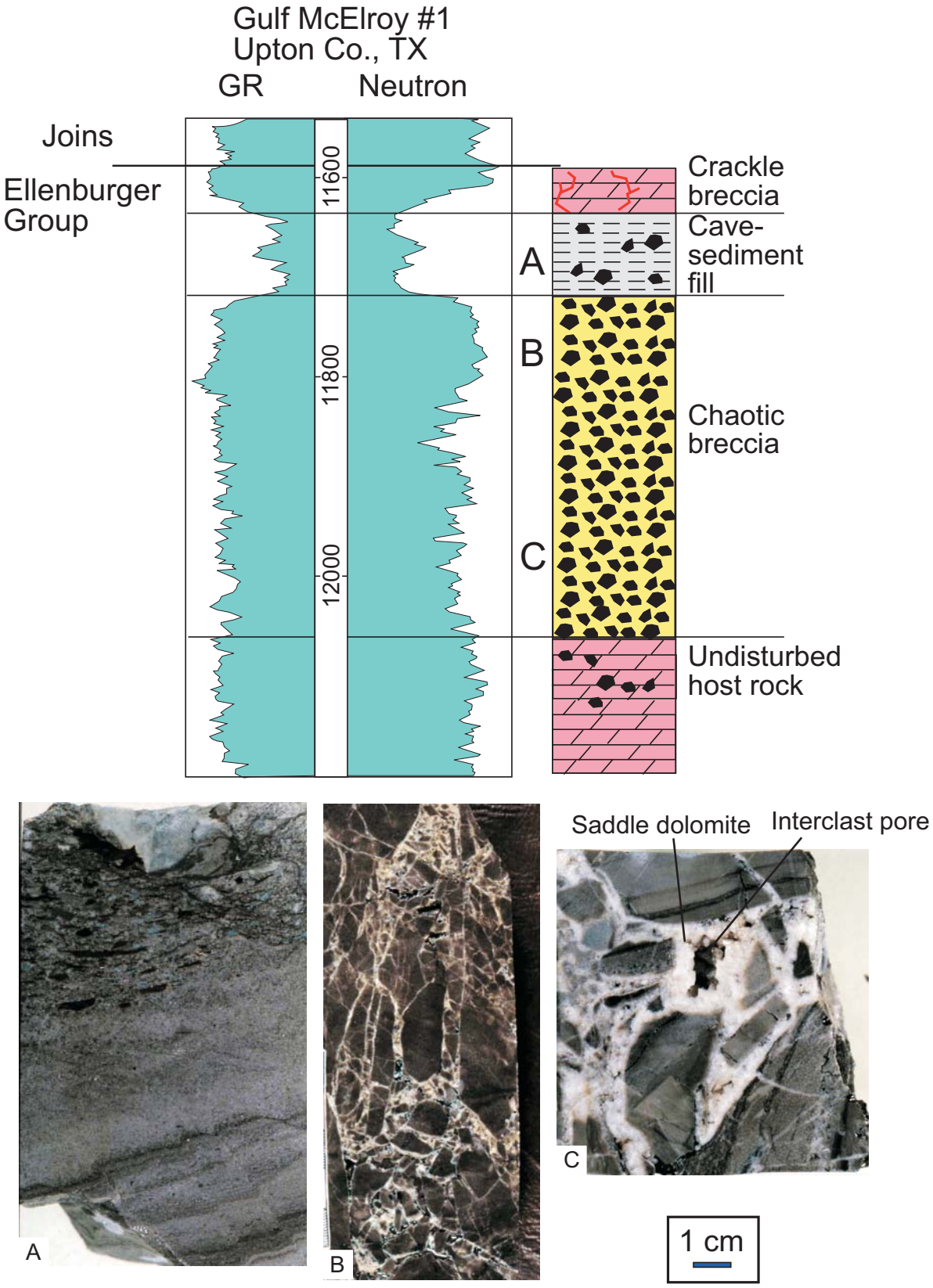

Figure 30. Core description and associated gamma-ray log for the Gulf #1 McElroy core in Upton County., Texas. Photograph A is from the cave-sediment fill in a passage. Photograph B from a chaotic breccia pile in a passage. The clasts show late crackle brecciation. Photograph C from a chaotic breccia pile in a passage. Because of the lack of matrix between the clasts and incomplete filling by saddle dolomite, there are interclast pores present. From Kerans (1989).

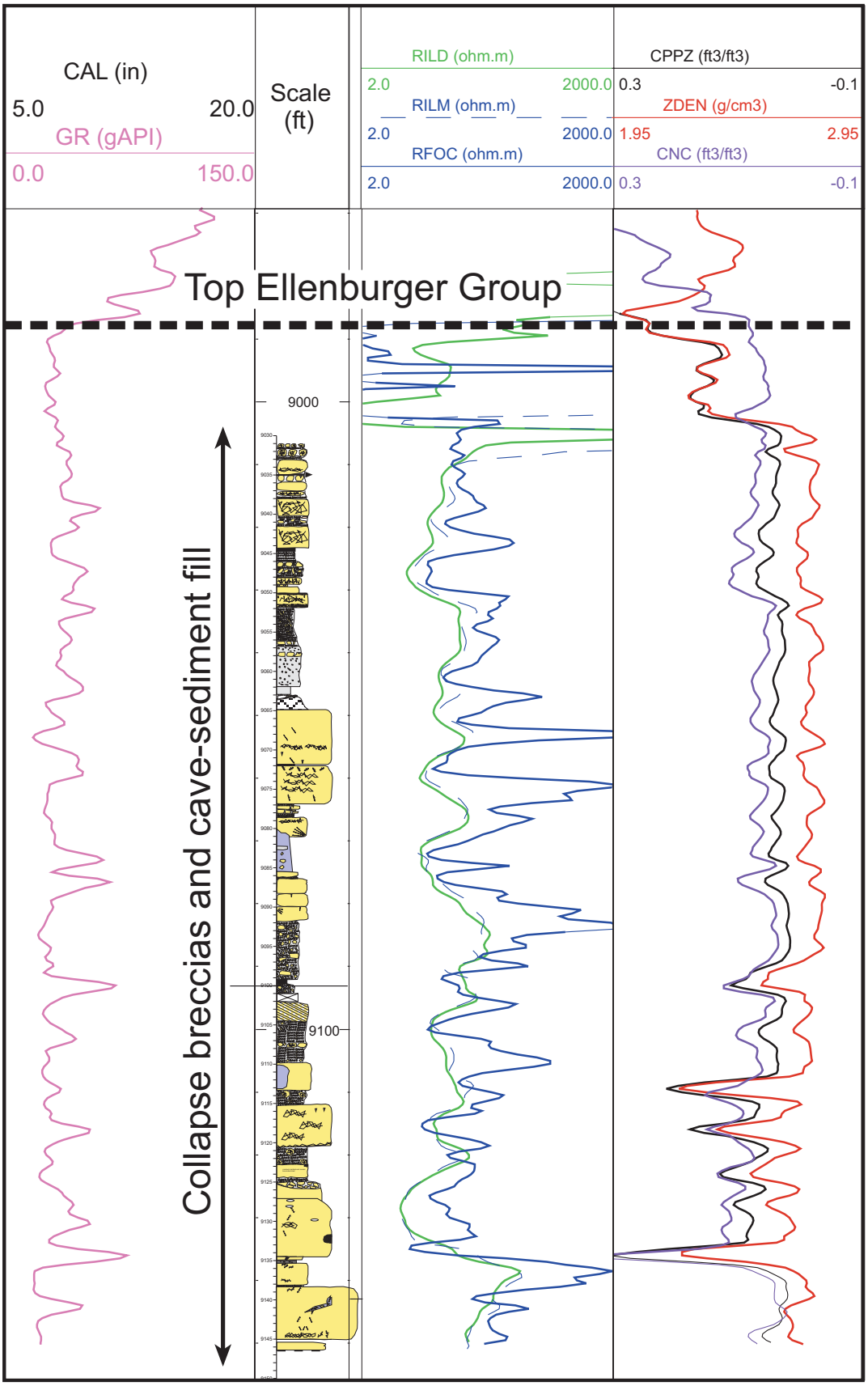

Figure 31. Goldrus Producing Company Unit #3 core and associated wireline logs in Barnhart field (Regan County, Texas) is extensively karsted. See Figure 32 for examples of rock types. From Combs et al. (2003).

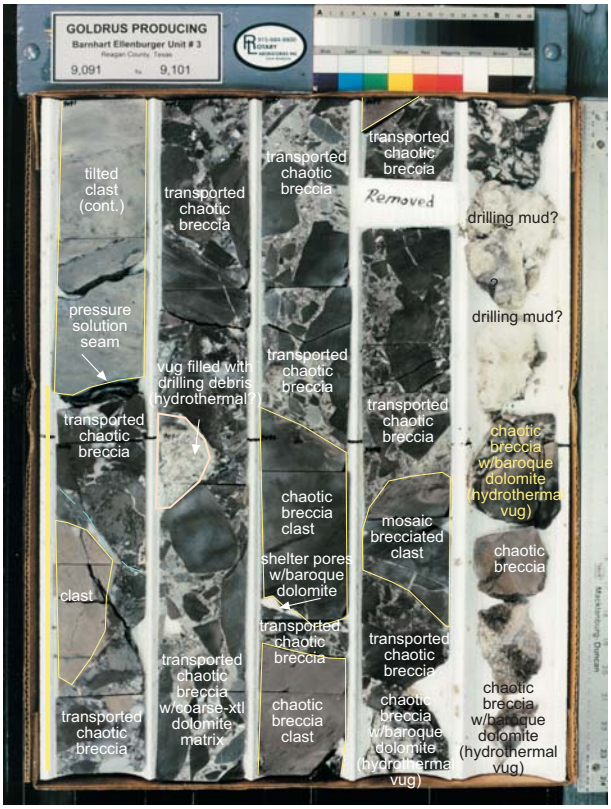

Debris-flow breccia in a paleocave passage. Some of the clasts show crackle brecciation.

Large deformed blocks with crackle breccia overprint interbedded with cave-sediment fill.

Large deformed blocks with crackle breccia overprint.

Large deformed blocks with crackle breccia overprint.

Figure 32. Example of several Ellenburger paleocave facies from the Goldrus Unit #3 Barnhart core in Regan County, Texas. From Combs et al. (2003).

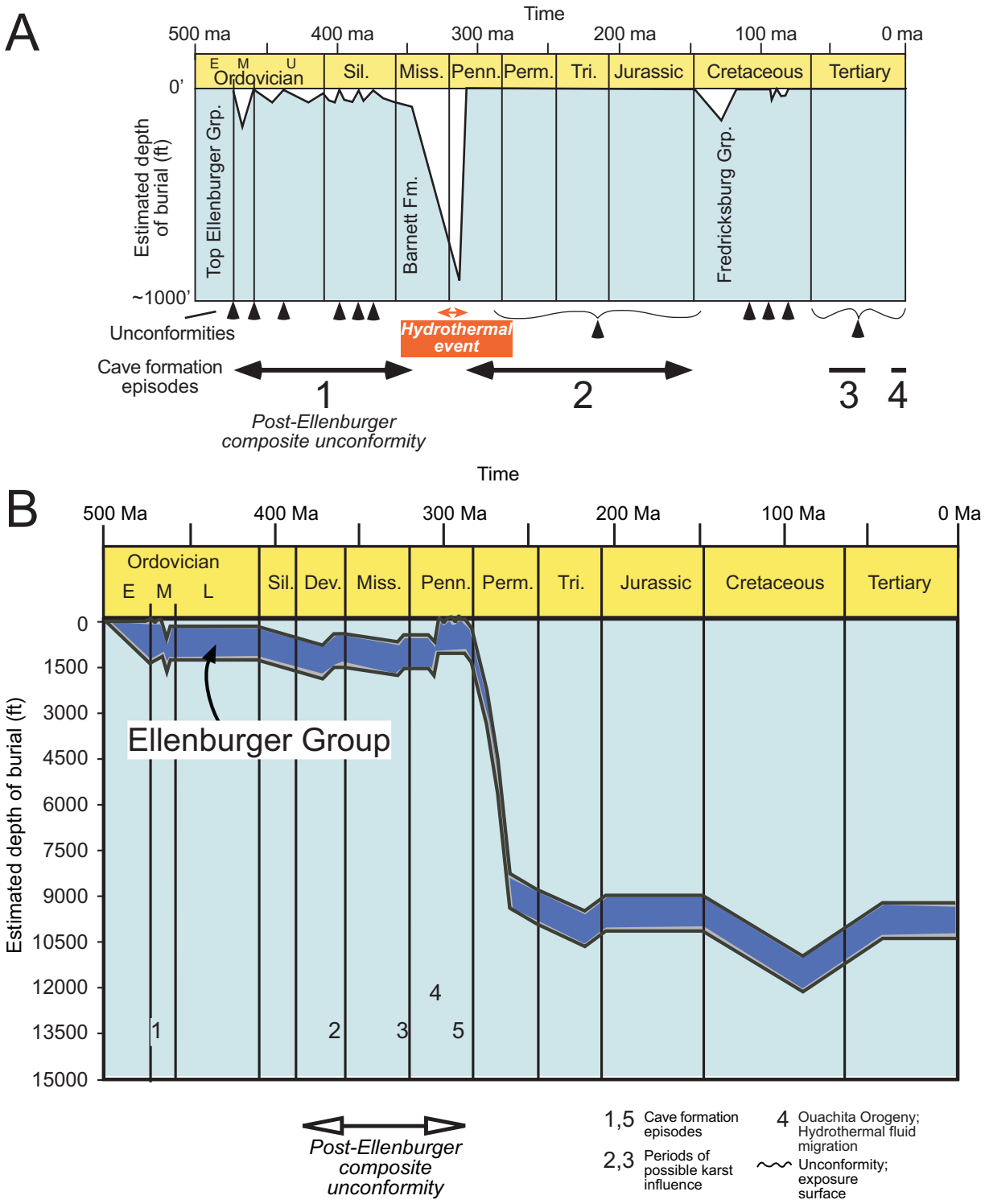

Figure 33. (A) Schematic burial history plot for the Lower Ordovician Ellenburger Group in the Llano Uplift area of Central Texas. From Kupecz and Land (1991). (B) Generalized burial history of the Ellenburger Group within Barnhart field in Regan Co., Texas. Barnhart field underwent several episodes of uplift. At least two of these episodes exposed the Ellenburger Group to karstification and cave formation: (1) Early-Middle Ordovician and, (2) Pennsylvanian times. The Ellenburger Group was also brought close to the surface during the Devonian and Mississippian, and may have experienced some karst influence here. During the Early Pennsylvanian time the Ellenburger Group experienced hydrothermal processes and tectonic uplift related to the Ouachita Orogeny. From Combs et al. (2003).

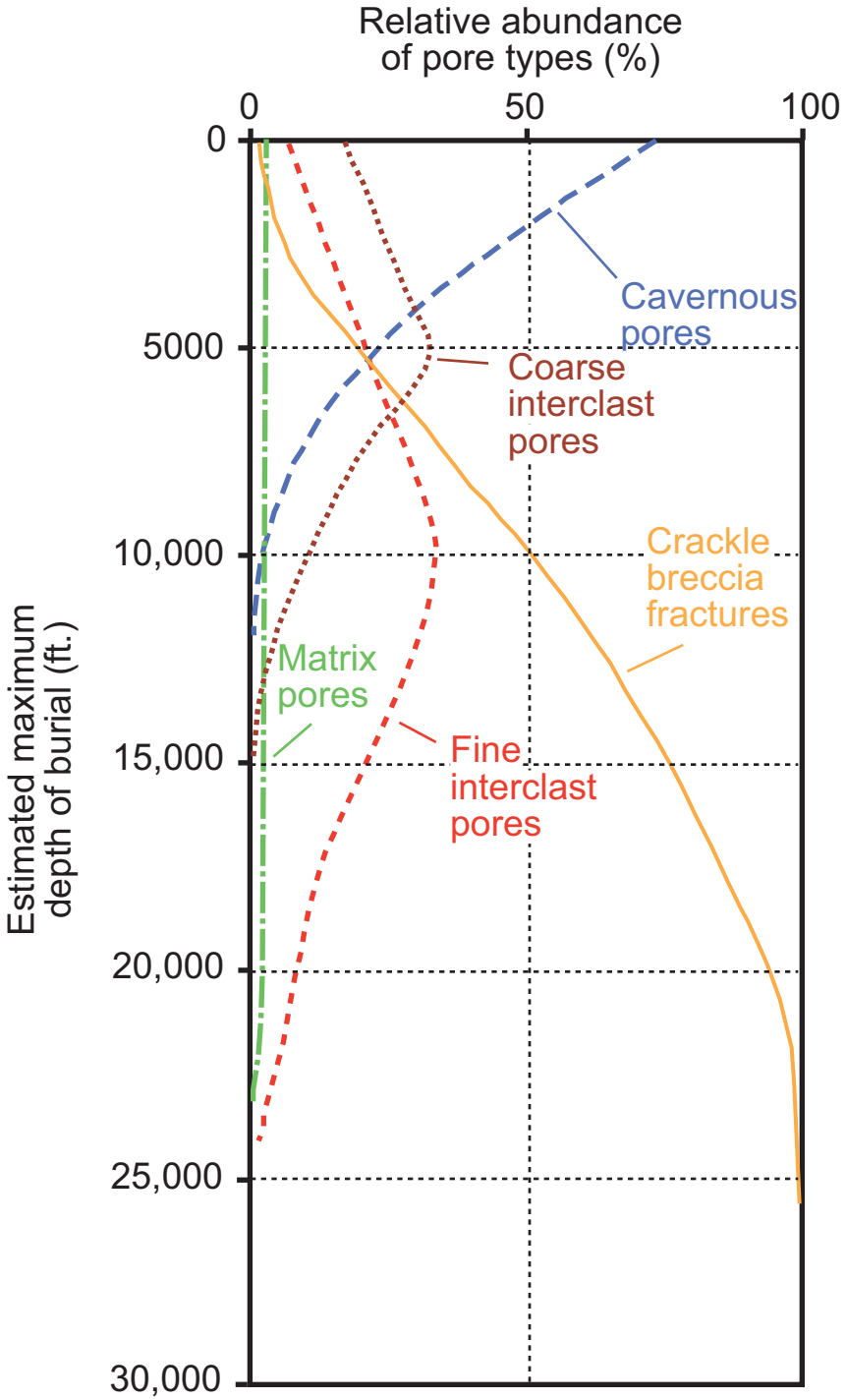

Figure 34. Generalized burial evolution of a cave-system pore network with relative proportions of pore types. The dividing line between fine clast and coarse clasts is 6 cm. The relative abundance of pore types and estimated burial depth are estimates based on review of near-surface and buried paleocave systems presented in Tables 1 and 2 of Loucks (1999). After 20,000 ft of burial, the graph is very speculative. Figure modified from Loucks (1999).

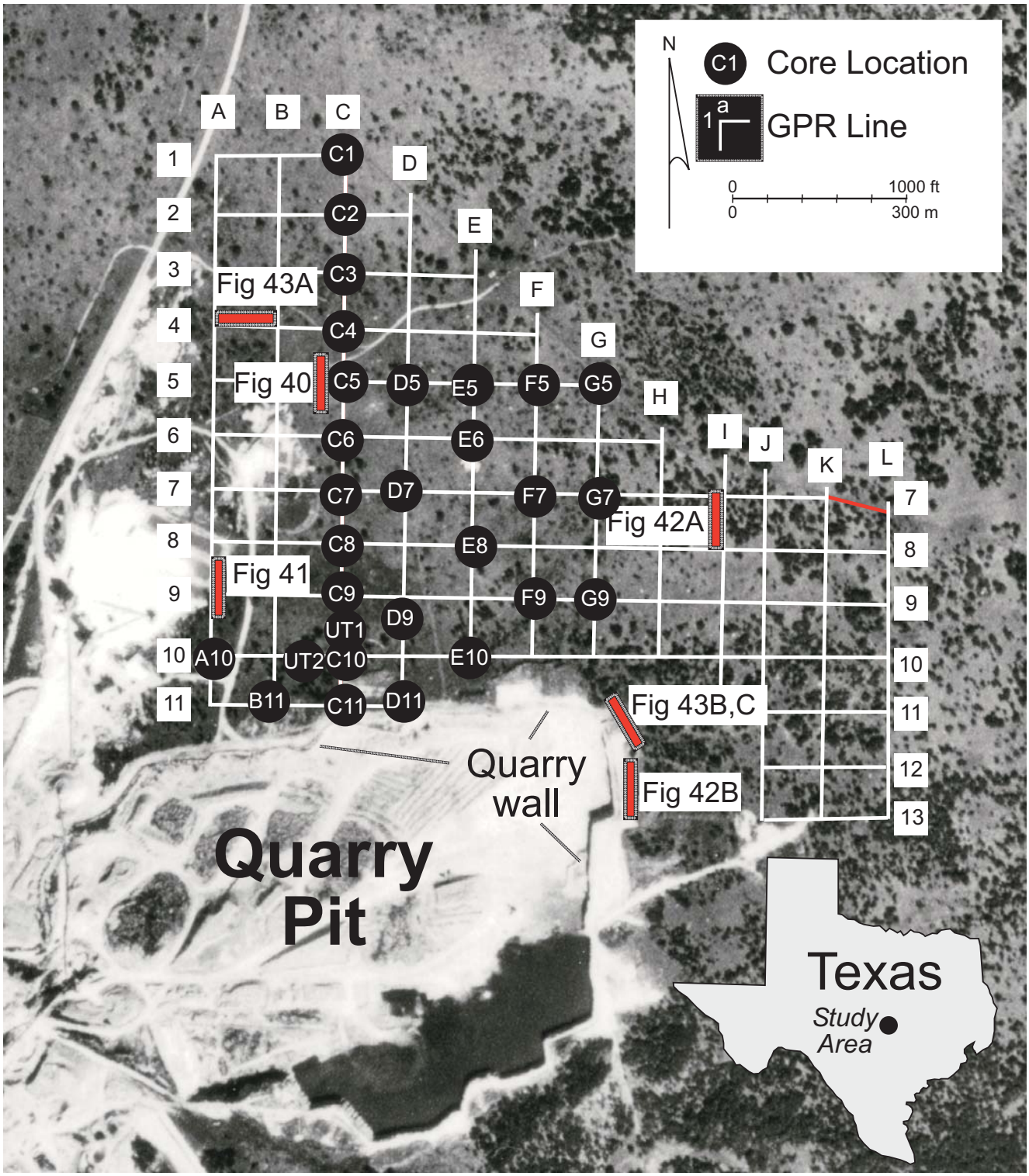

Figure 35. Aerial photograph of Dean Word Quarry showing location of grid of ground-penetrating radar (GPR) lines and cores. Locations of GPR lines illustrated later in the paper are labeled. From Loucks et al. (2004).

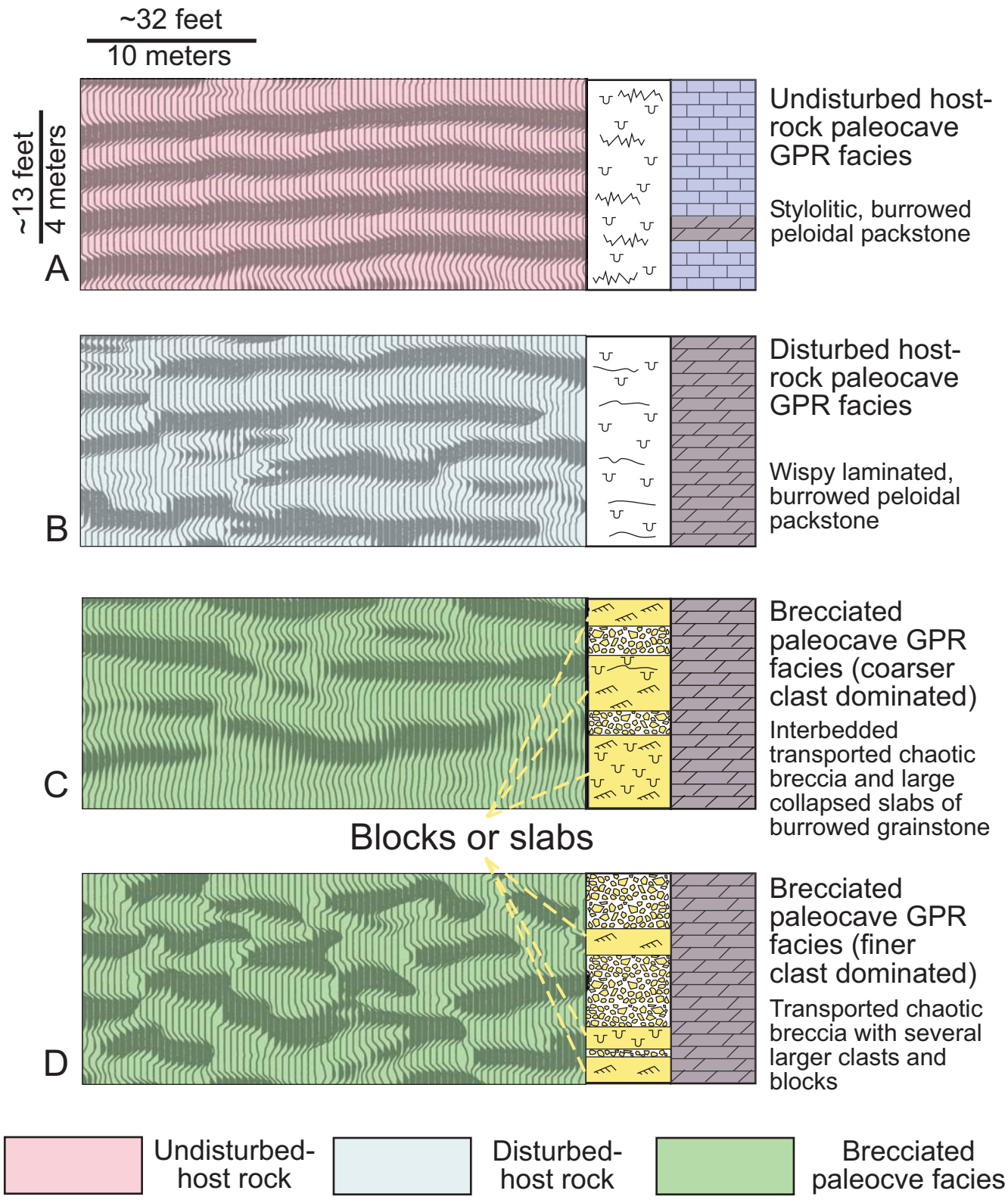

Figure 36. Type ground-penetrating radar reflection patterns for different paleocave facies. Each reflection pattern is matched to core. From Loucks et al. (2004).

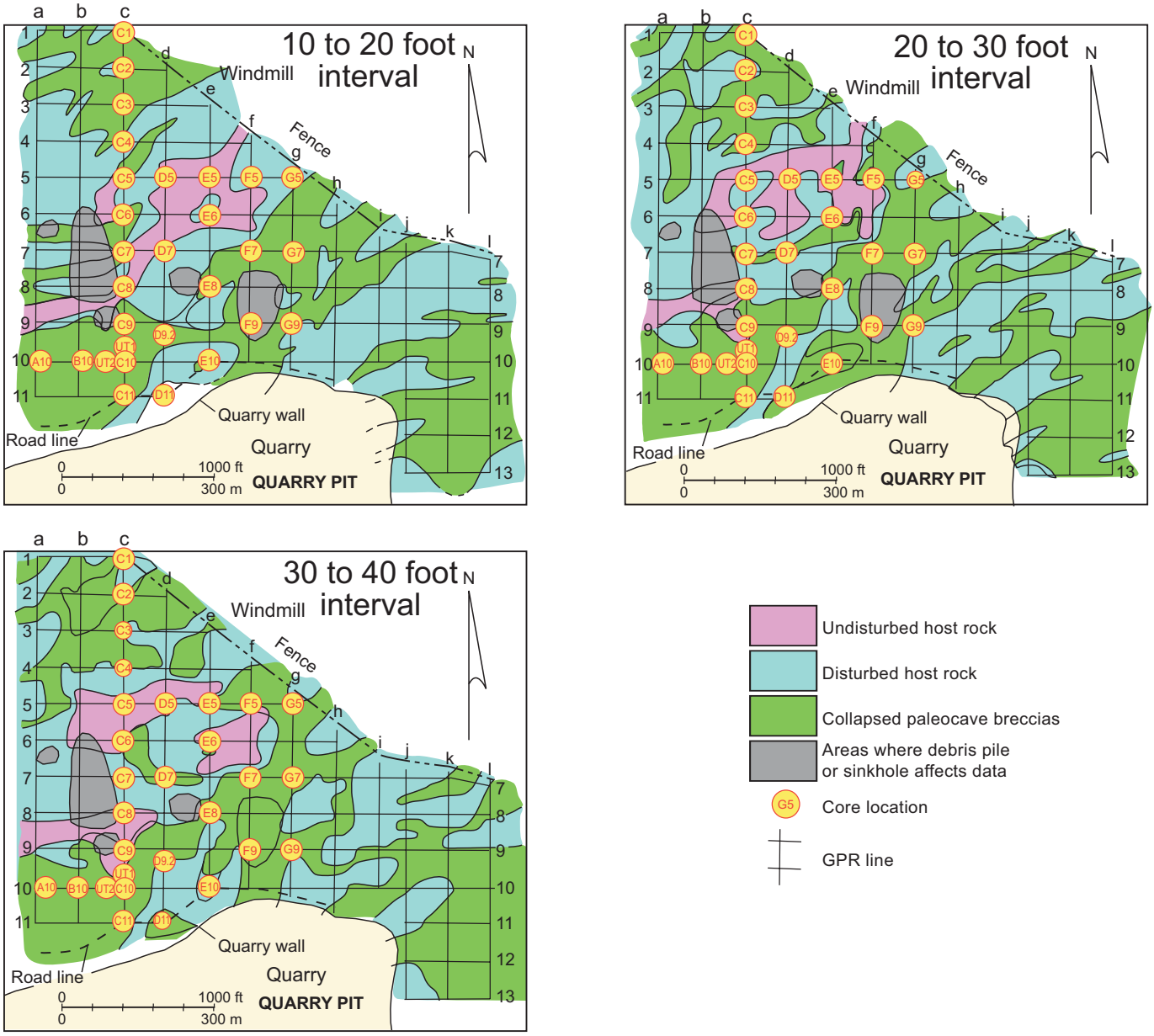

Figure 37. Integration of core and GPR data allows a three-dimensional interpretation of the paleocave system. The mapped volume is divided into three depth zones to display the distribution of paleocave facies. The brecciated bodies, which outline the trends of former passages, are as much as 1100 ft wide. The intervening areas between the breccias are as much as 660 ft wide. From Loucks et al. (2004).

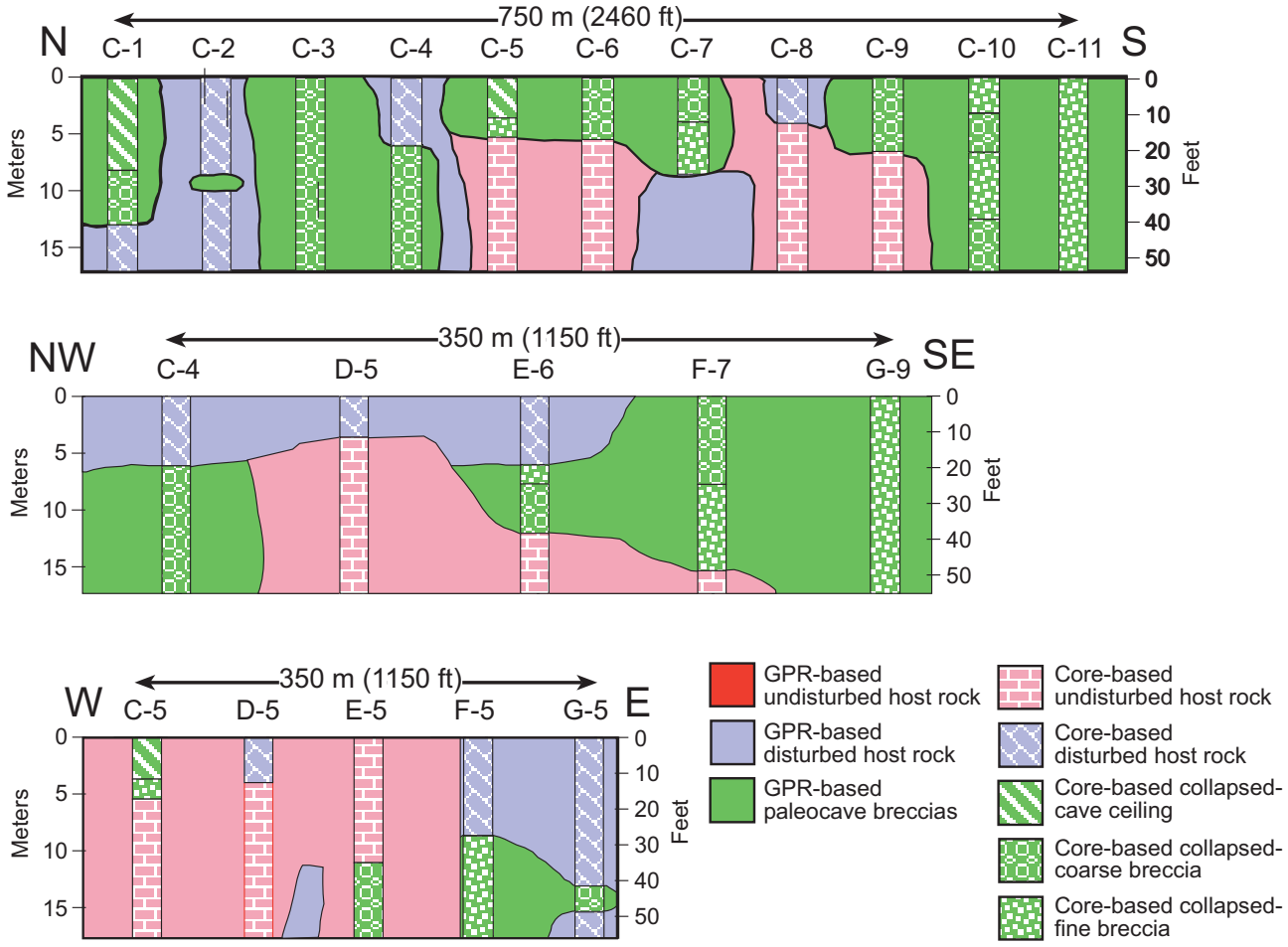

Figure 38. Simplified facies cross sections using core and GPR data. See Figure 35 for location of wells used on lines of sections. From Loucks et al. (2004).

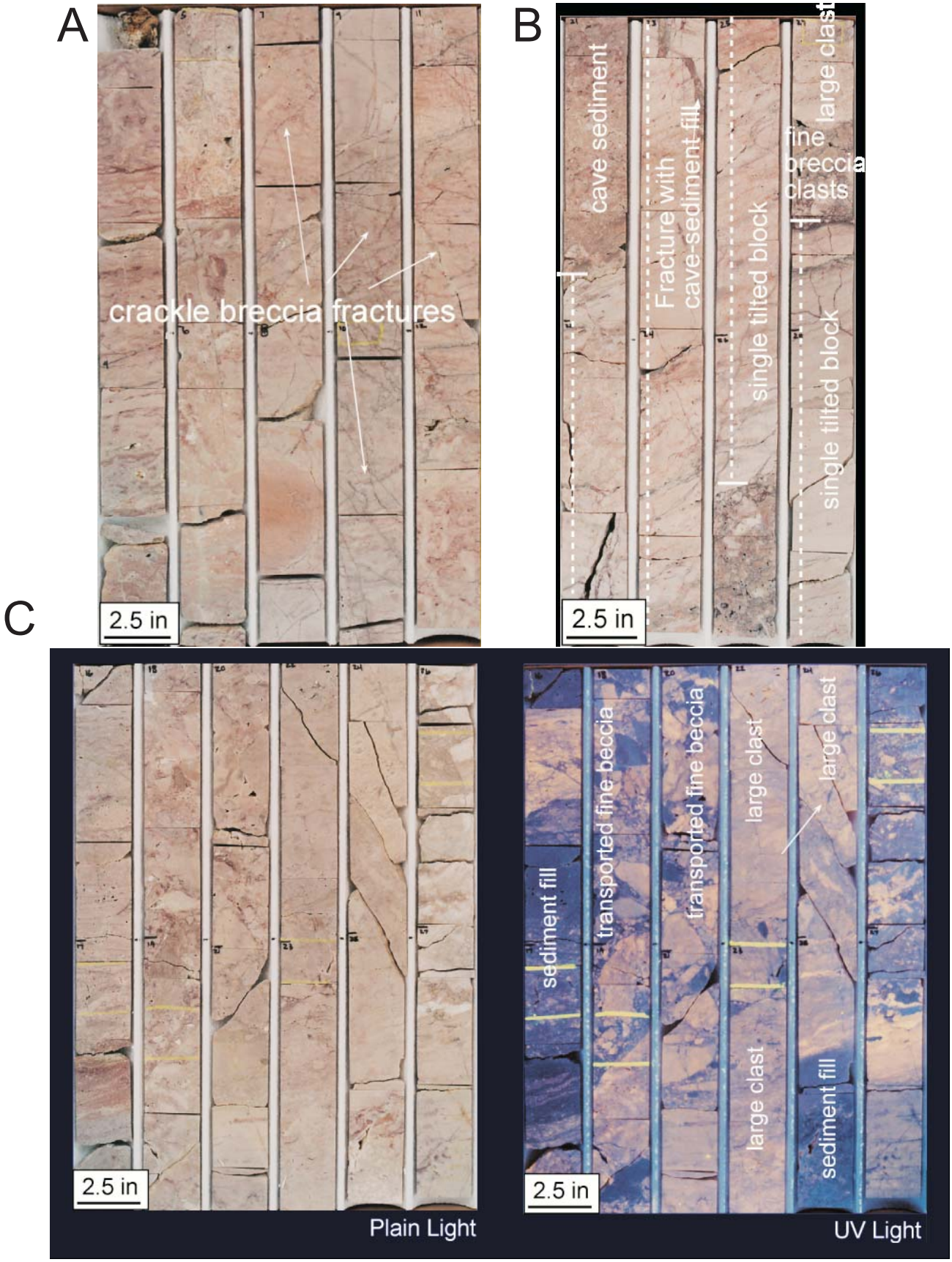

Figure 39. Core examples paleocave facies. (A) Cave roof showing extensive crackle breccia fractures. (B) Cave-passage fill composed of large blocks of chaotic breccia blocks and interbedded cave-sediment fill. (C) Cave-passage fill composed of large blocks of chaotic breccia blocks and interbedded cave-sediment fill. From Loucks et al. (2004).

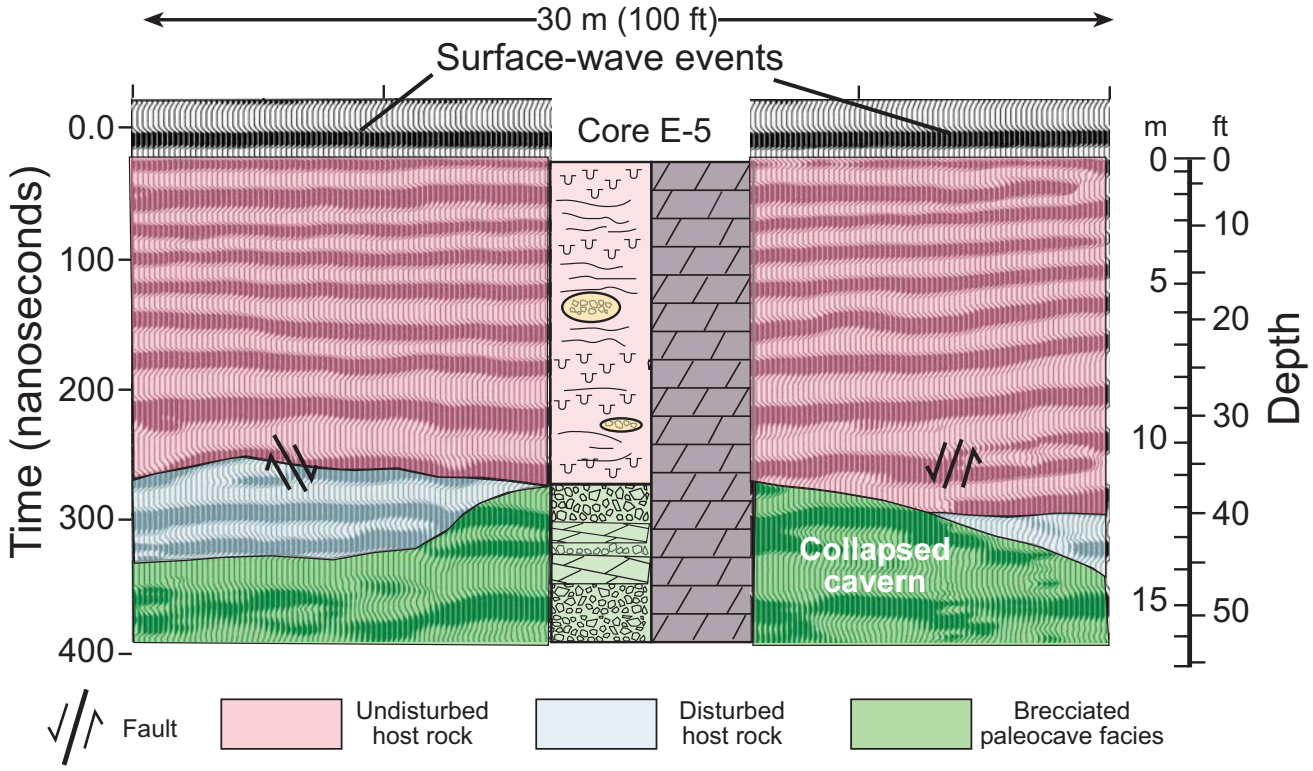

Figure 40. GPR section and core description showing a sequence of cave-fill breccias overlain by undisturbed host rock. A few small faults occur in the host rock above the collapsed cavern. See Figure 35 for location of GPR line and core. From Loucks et al. (2004).

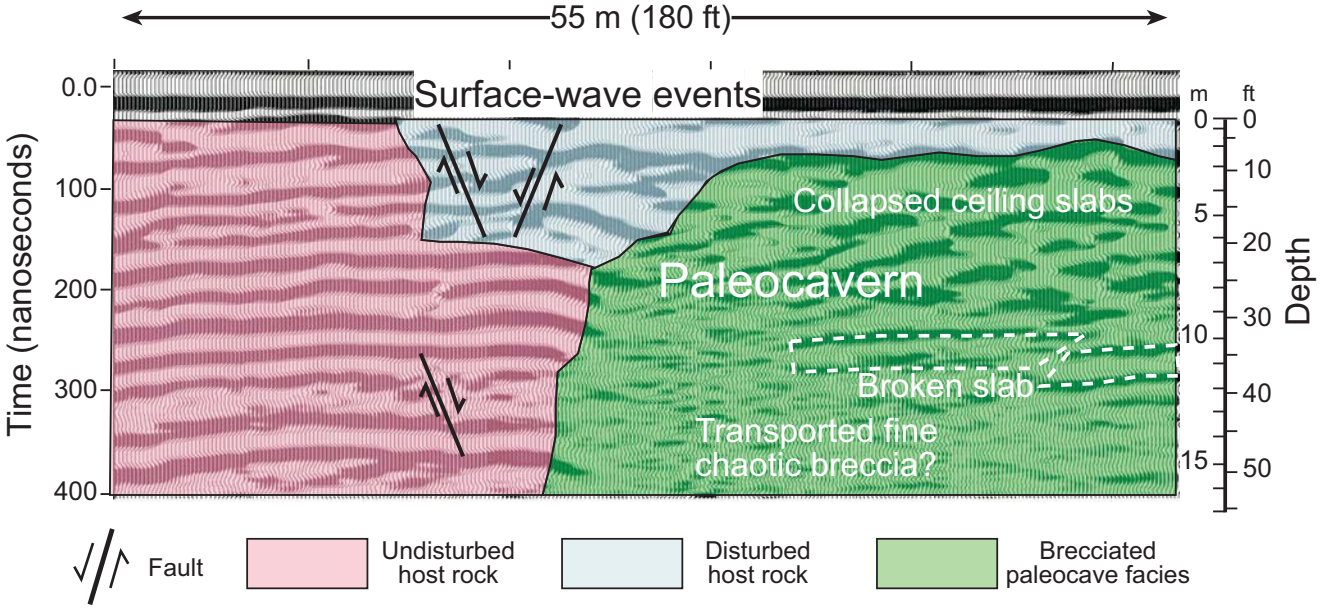

Figure 41. Collapsed paleocavern in contact with undisturbed and disturbed host rock. Several faults occur in the disturbed host rock. Reflection patterns in the collapsed cavern show probable fine breccia in the lower part of the chamber (no reflections) and coarser breccia (slabs) near the top (higher amplitude events). A large broken cave-ceiling slab may also be imaged. See Figure 35 for location of GPR line. From Loucks et al. (2004).

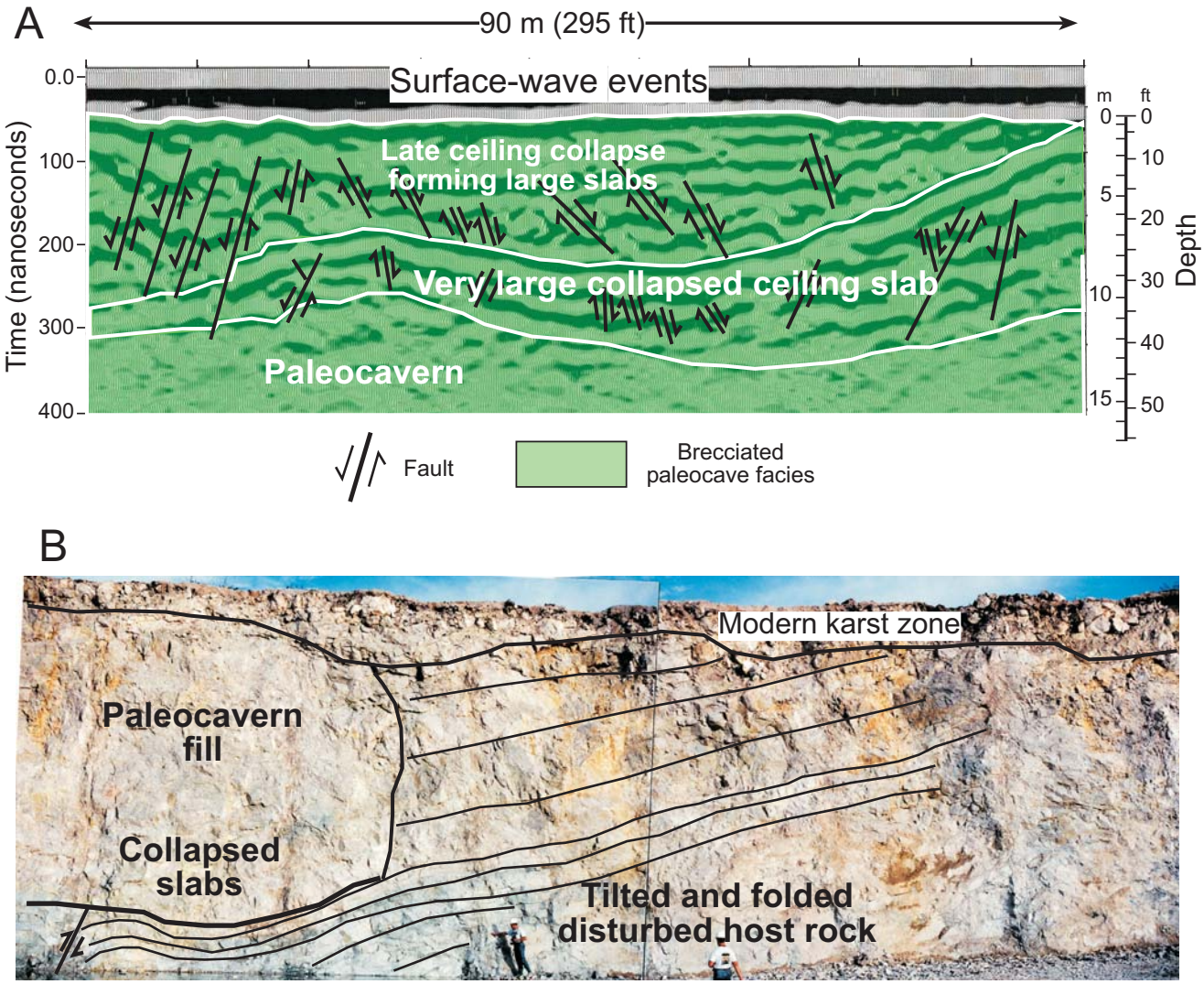

Figure 42. (A) Very large, folded, cave-ceiling slab overlying a paleocavern filled with chaotic breccia. The upper section of the cave ceiling appears to have collapsed after the large slab below on the basis of the onlapping reflection pattern between the two sections. See Figure 35 for location of GPR line. (B) Complex sag and fold feature along east wall in Dean Word Quarry showing features similar to GPR line presented in Figure 42A above. The lower part of the quarry face shows continuous tilted but folded bedding that is interpreted to have sagged or collapsed into a lower paleocavern. The upper part of the tilted block dips into a paleocavern filled with chaotic breccias and slabs. See Figure 35 for location of photograph. From Loucks et al. (2004).

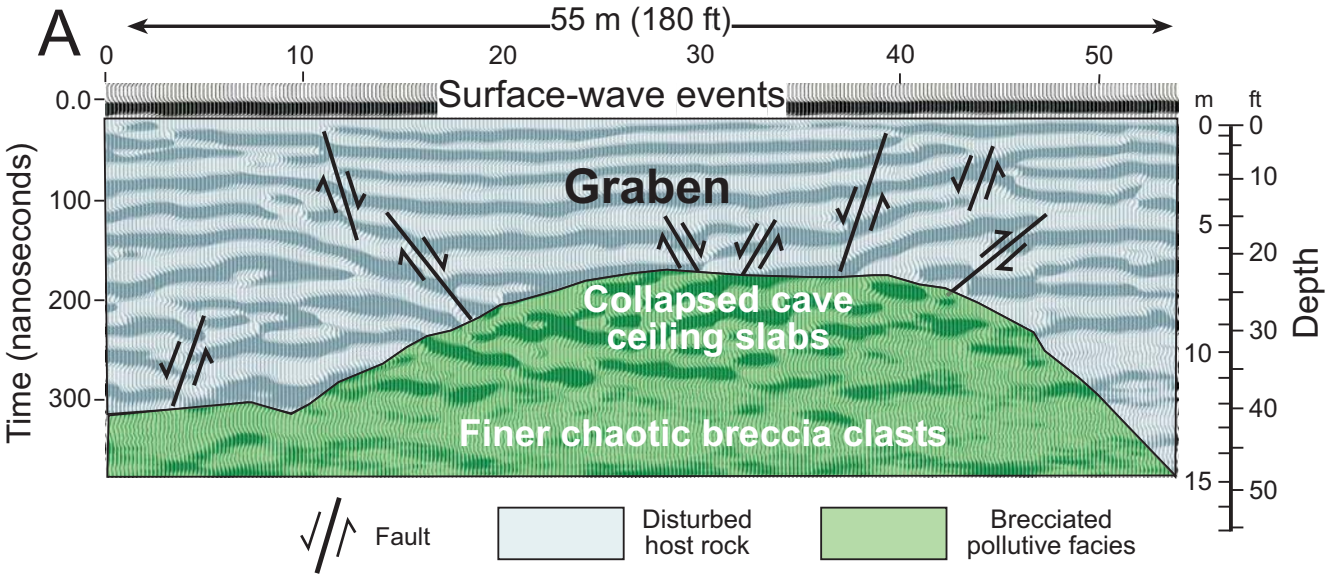

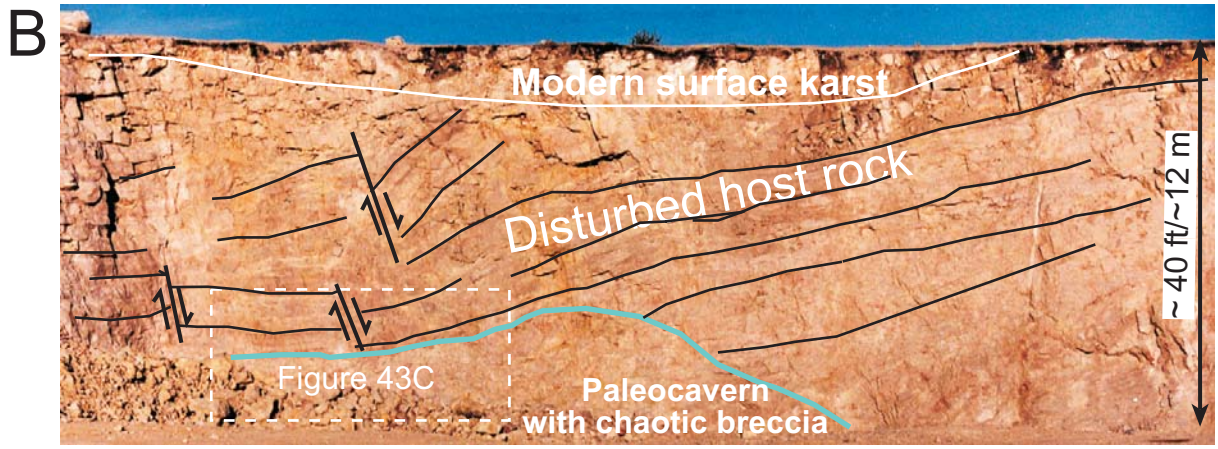

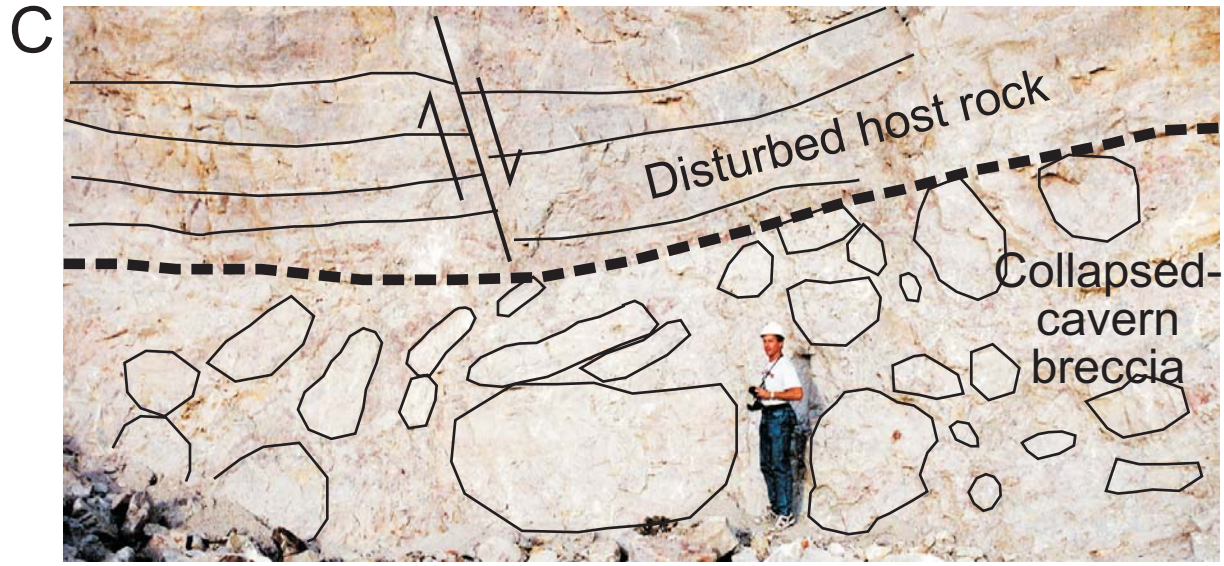

Figure 43. Faults over collapsed paleocaverns. (A) Graben and associated fault system in disturbed host rock overlying a collapsed paleocavern. Within the paleocavern, coarser slabs appear to be at the top and finer breccia at the bottom on the basis of the change in reflection pattern continuity. See Figure 35 for location of GPR line. (B) Example of faulted, disturbed host rock over a collapsed paleocavern similar to GPR line in Figure 43A. Detail of the collapsed paleocavern outlined in dashed box is shown in Figure 43C. (C) Close up of collapsed cavern shown in Figure 43B. Large collapse blocks, up to several meters across, are within the paleocavern (several prominent blocks are outlined). See Figure 35 for location of photographs. From Loucks et al. (2004)

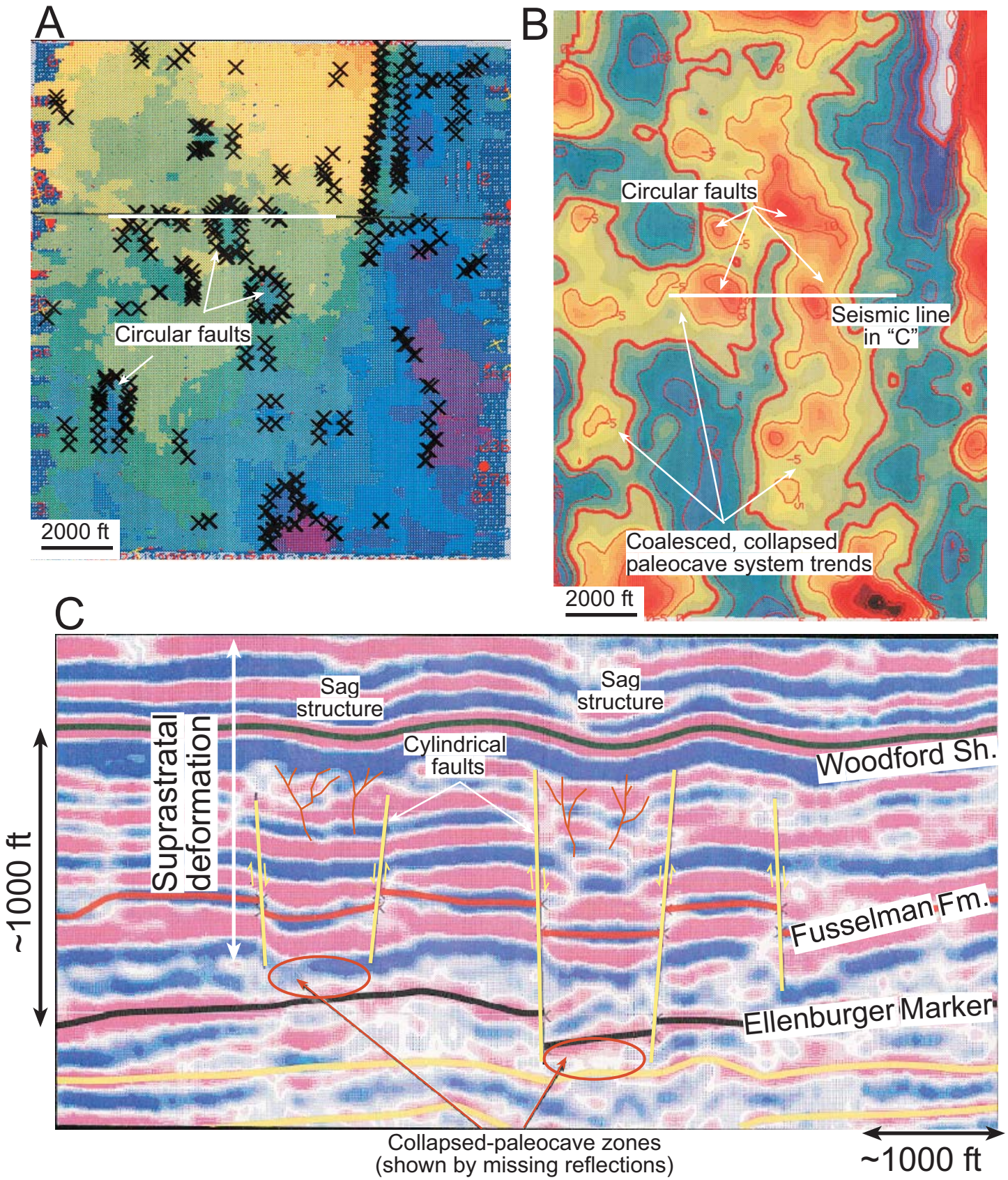

Figure 44. 3-D seismic example over an Ellenburger paleocave system from the Benedune field in West Texas. (A) Structure map on Fusselman Formation showing cylindrical faults produced by burial collapse of the Ellenburger cave system. (B) Second-order derivative map displaying sag zones produced by collapse in the Ellenburger interval. (C) Seismic line showing missing sections (collapse in Ellenburger section), cylindrical faults, and sag structures. Suprastratal deformation is over a thousand feet thick in this section. Modified from Loucks (1999).

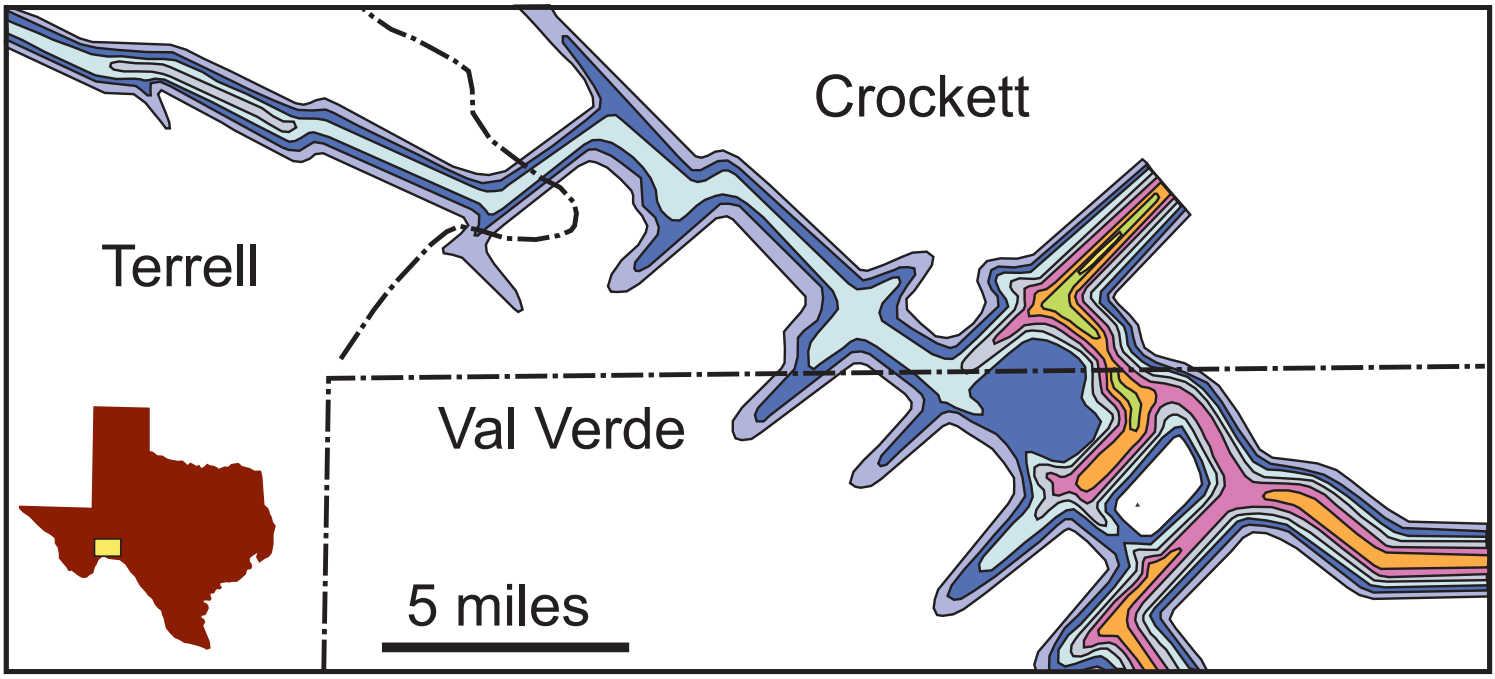

Figure 45. Isopach map of cave-sediment-fill prone interval in Ellenburger Group from wireline logs. The map shows a strong rectilinear pattern that is probably controlled by preSauk unconformity paleofractures. Hot colors are the thicker sections of cave-sediment fill. Figure from Canter et al. (1993).

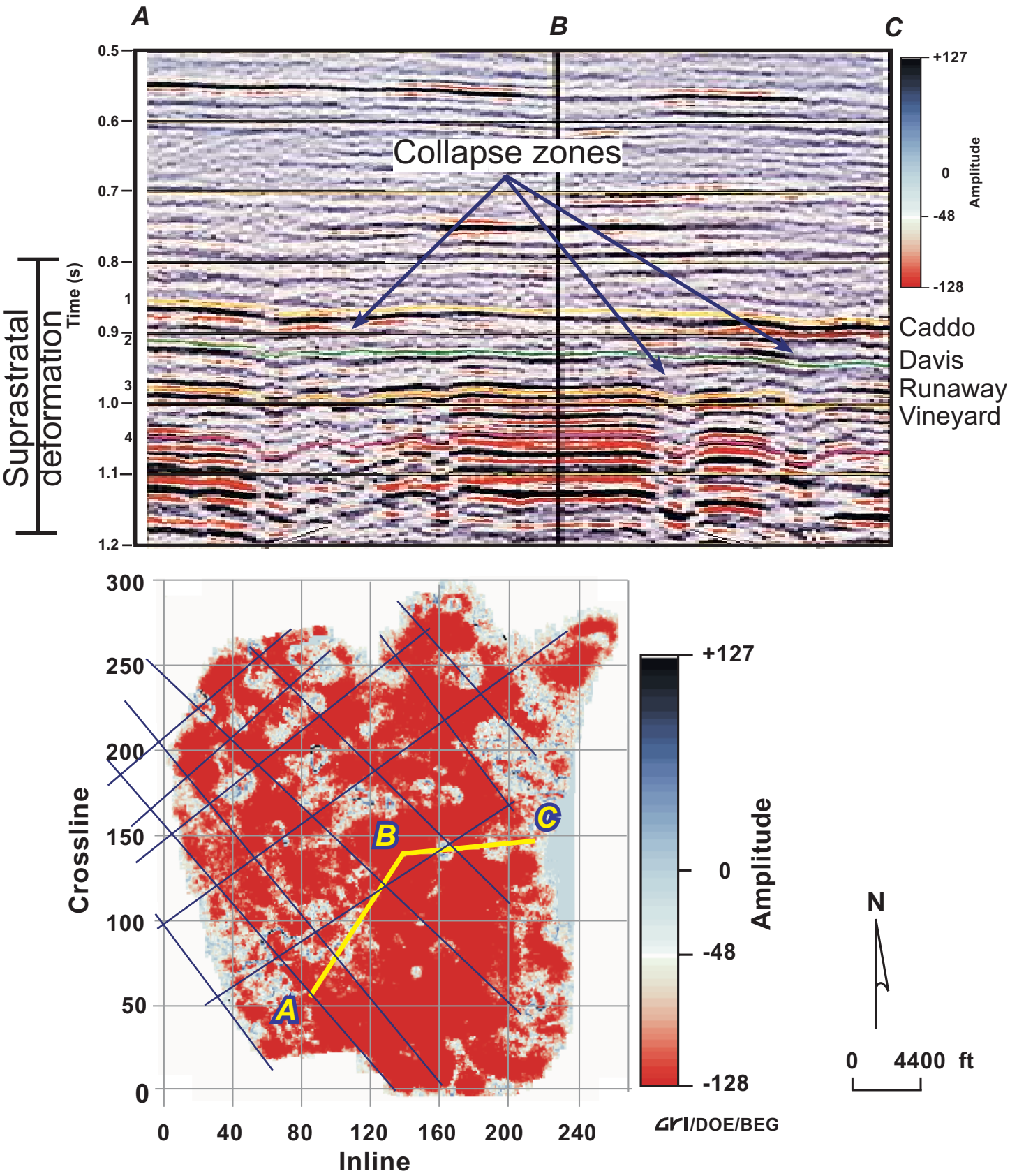

Figure 46. Seismic example of buried collapsed karst features from Boonsville on the line of Jack and Wise Counties in north Texas by Hardage et al. (1996). (A) Seismic profile along line ABC (see figure below), which traverses these collapse zones. Figure was stretched laterally by present author. Zones are up to 2000 ft thick. (B) Seismic reflection amplitude response on the Vineyard surface. The red areas show continuity, whereas the semicircular white areas show disruption of continuity. The white areas are late burial collapse related to karsting of the Ellenburger Group. The blue lines drawn by present author are meant to emphasize the northwest and northeast alignment of the collapse features.

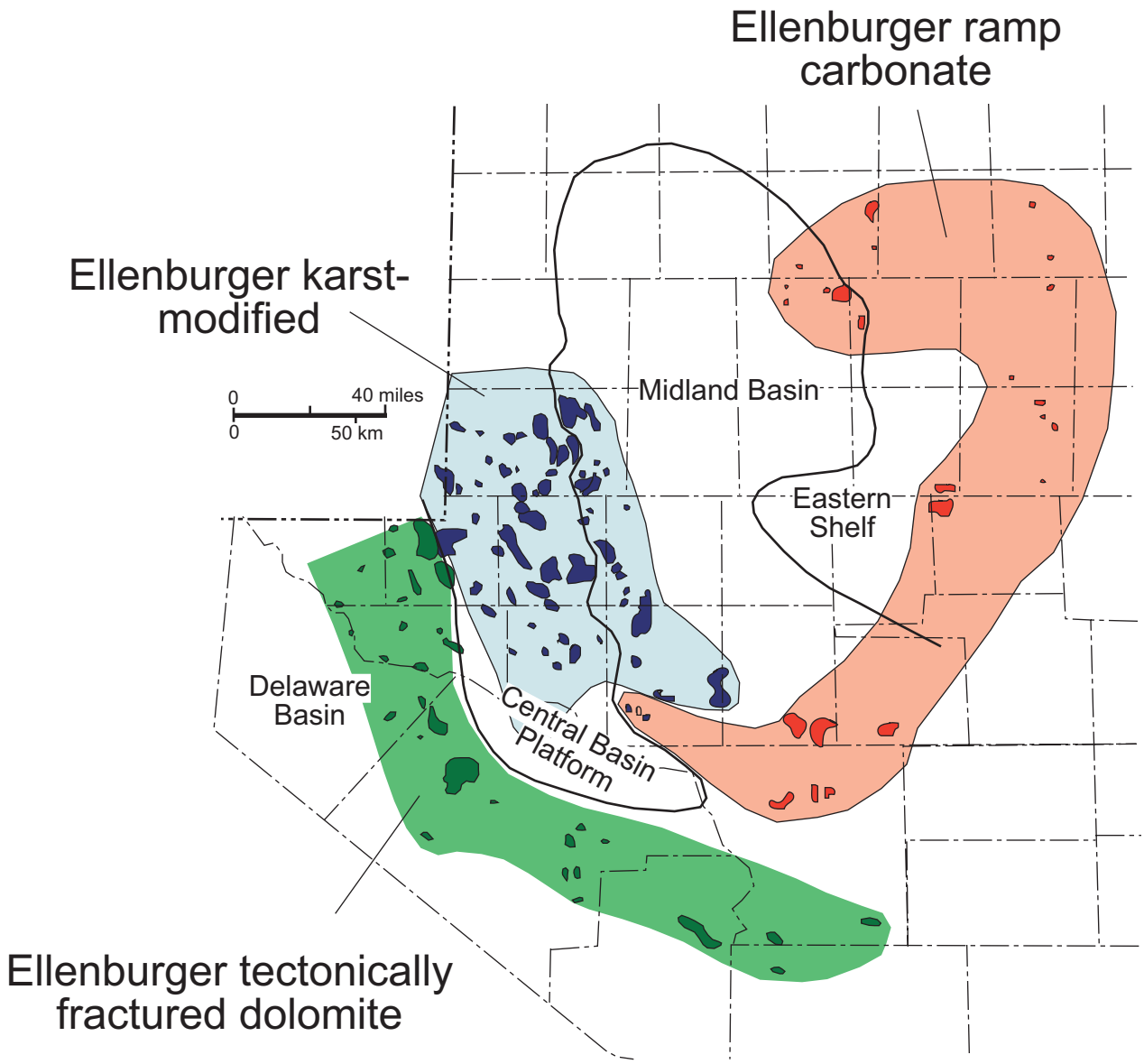

Figure 47. Distribution of Ellenburger Group reservoir types by Holtz and Kerans (1992). Figure modified from Holtz and Kerans (1992).

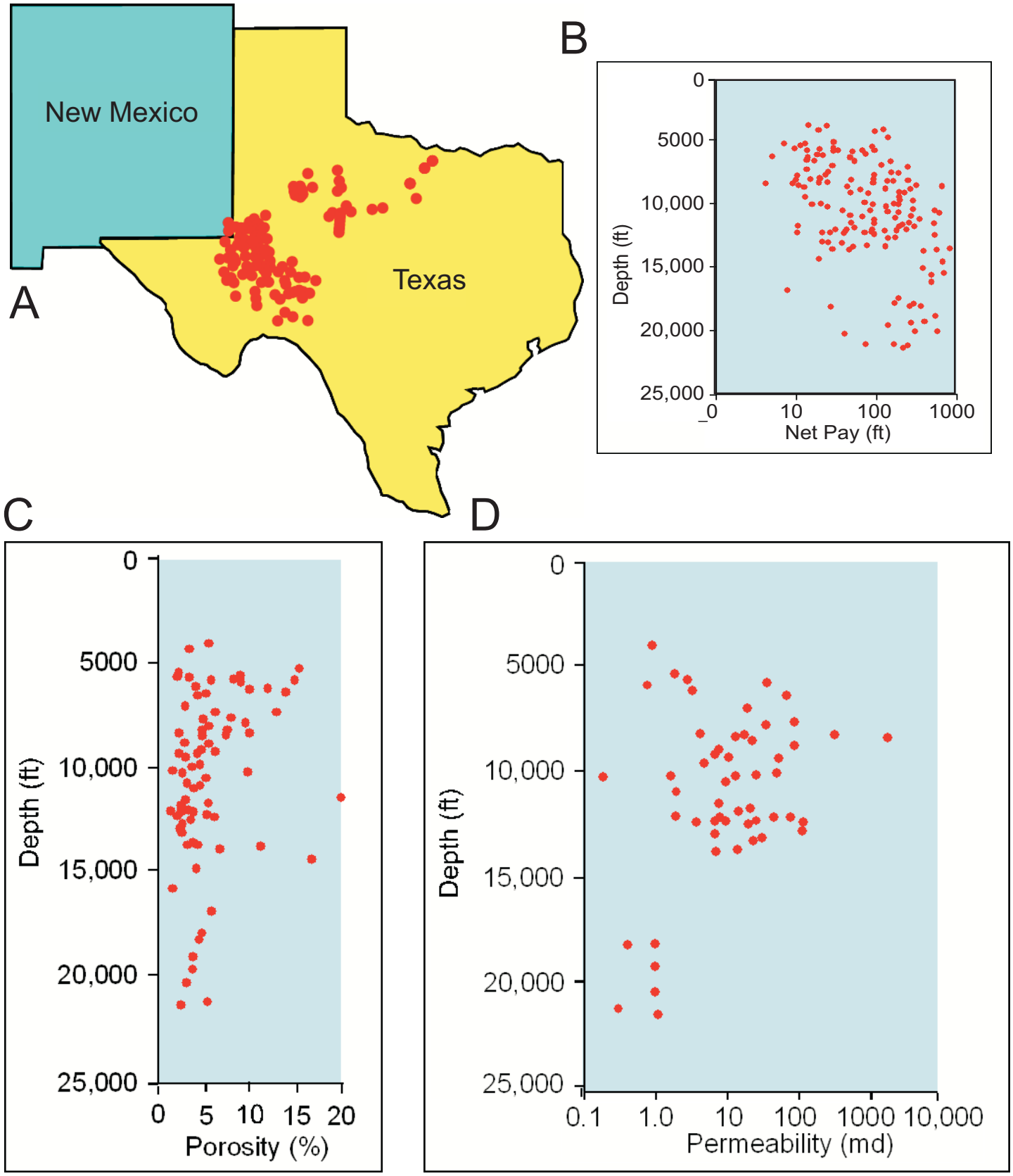

Figure 48. Field data from a 1985 Nerhing database (exact reference not available). (A) Map showing field locations. (B) Thickness of net pay. (C) Average reservoir porosity versus depth. Note most porosity values are 5% of less. (D) Average reservoir permeability versus net pay. Note good permeabilities despite low porosity values.

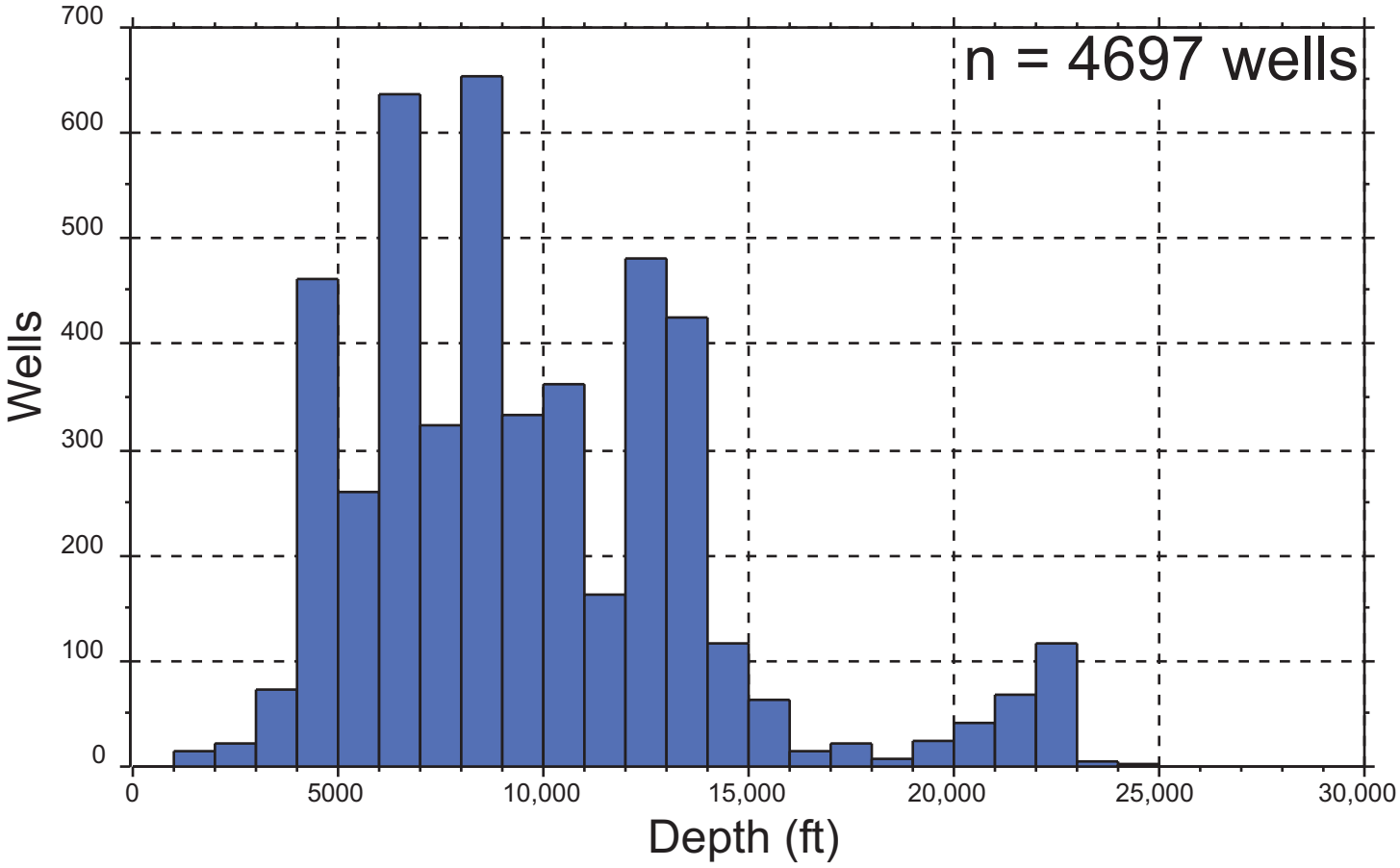

Figure 49. Histogram of productive (past and present) wells drilled into the Ellenburger Group. Producing wells show a range from 856 ft (Originala Petroleum #1 Gensler well in Archer County, Texas) to 25, 735 ft (Exxon Mobil McComb Gas Unit B well in Pecos County, Texas).

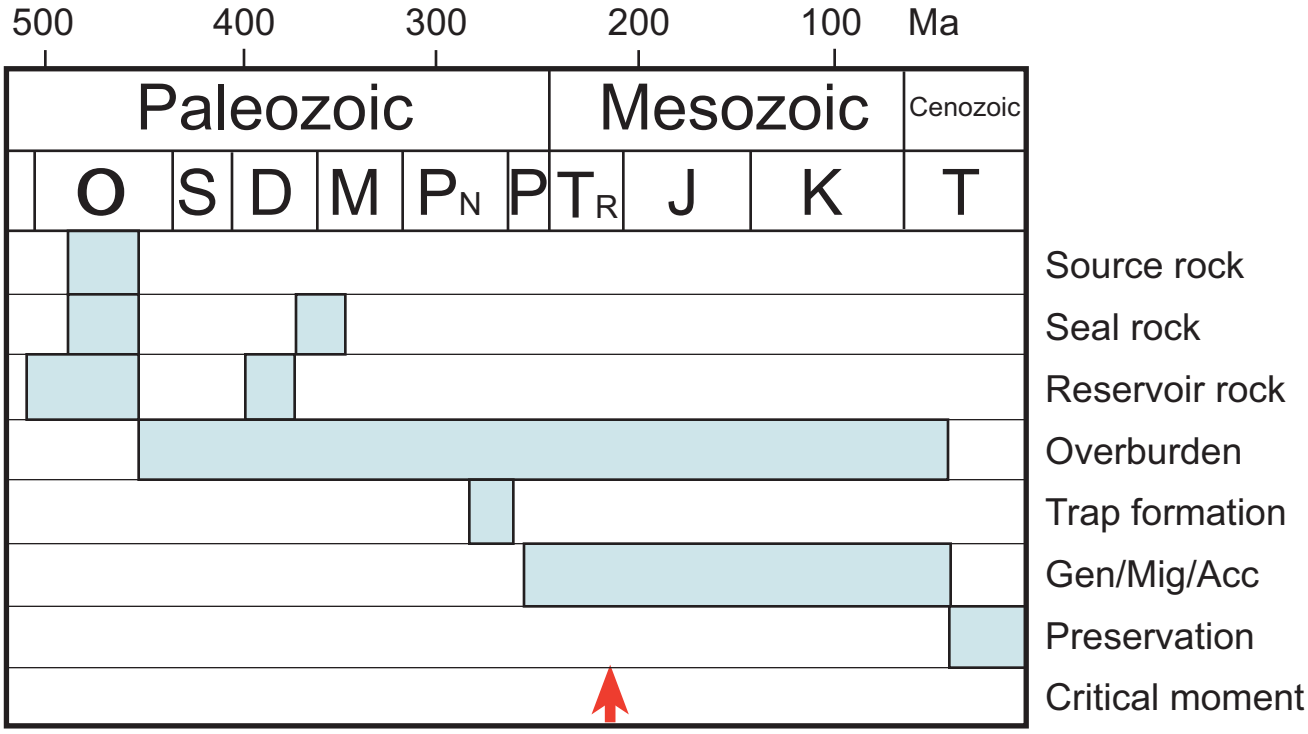

Figure 50. Event chart for the Simpson-Ellenburger petroleum system in the area of the Central Basin Platform showing the temporal relationships of the essential elements and processes. From Katz et al. (1994).

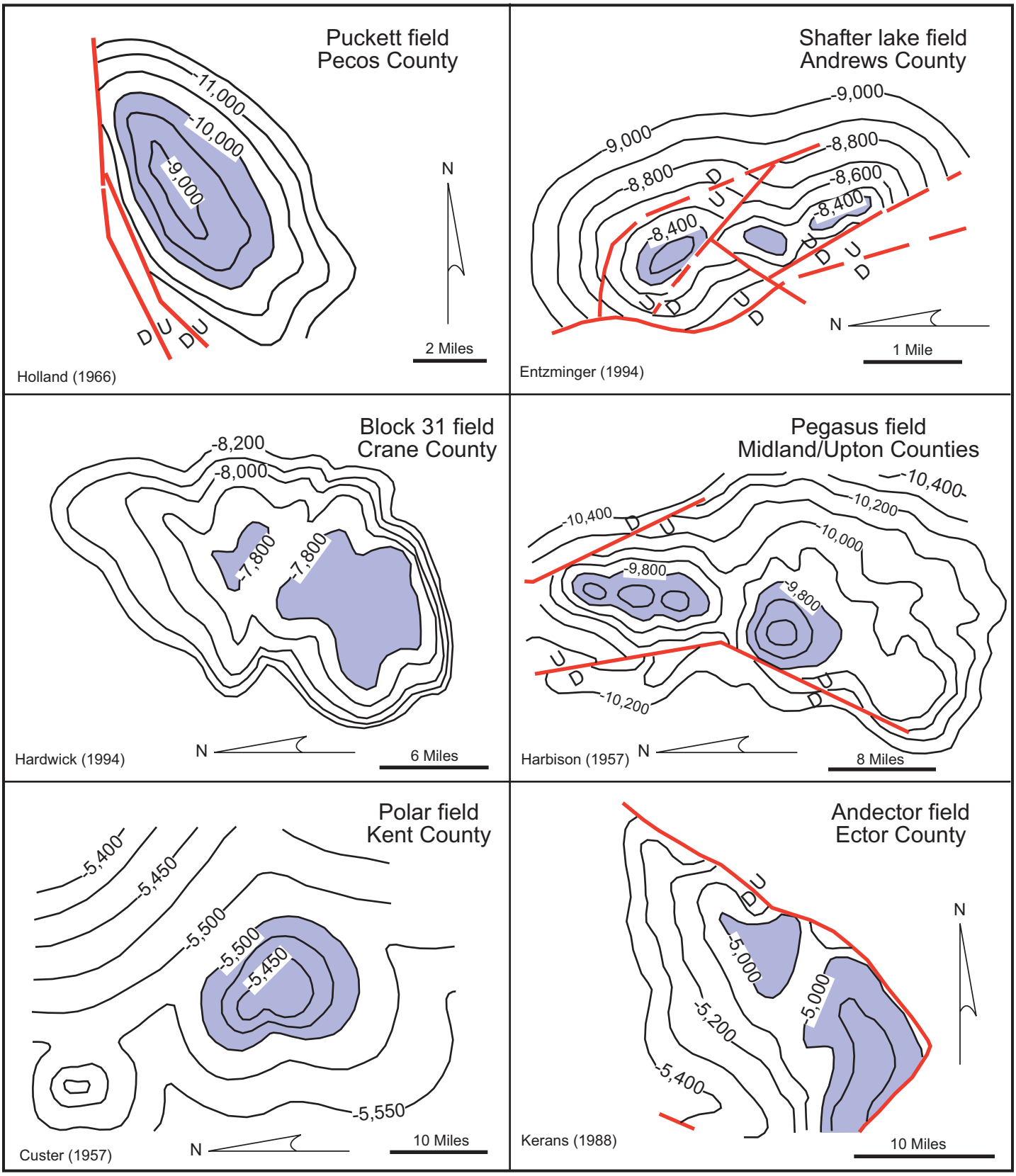

Figure 51. Example of structural trapping geometries of Ellenburger reservoirs. Structures are relatively simple anticlines or faulted anticlines.

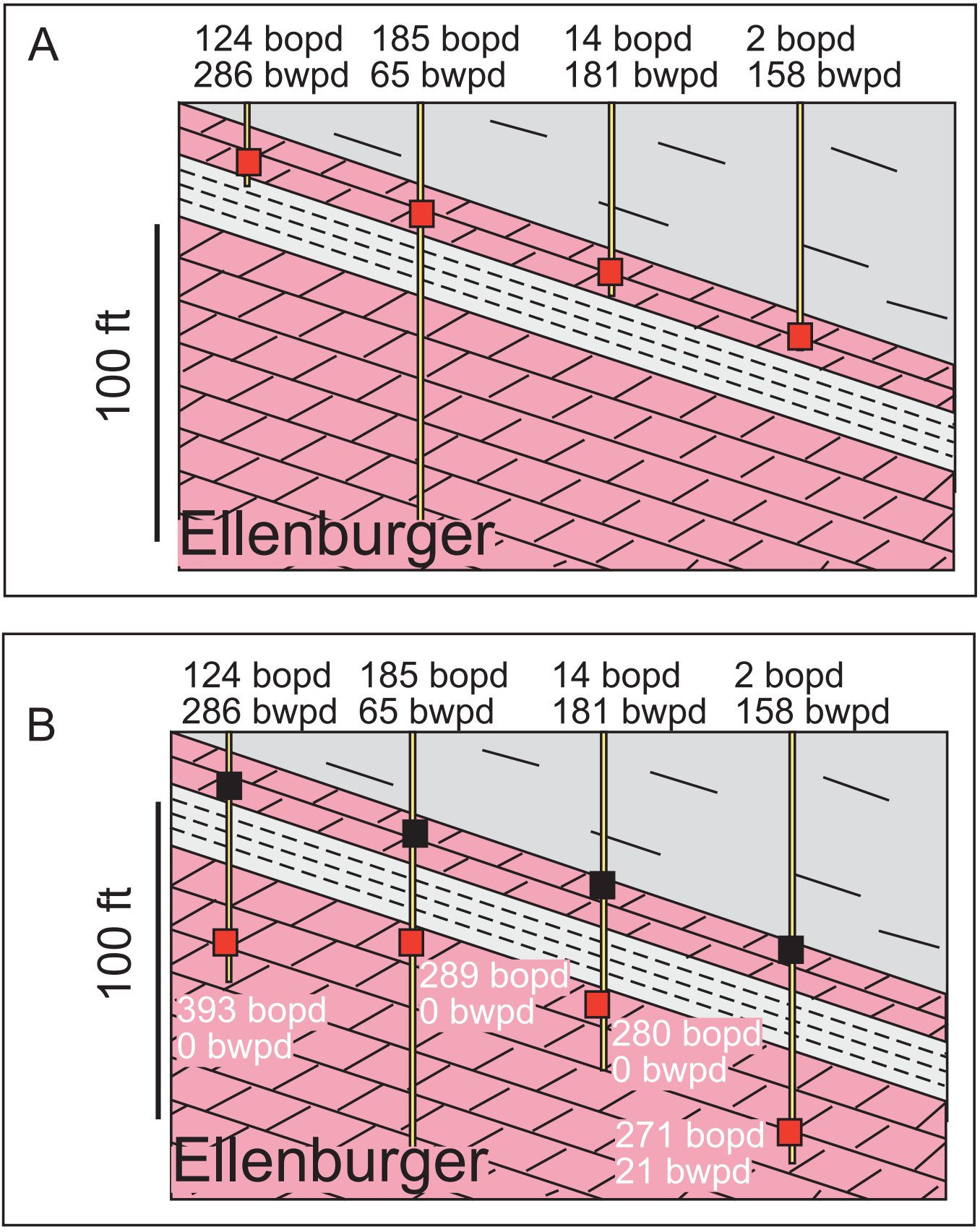

Figure 52.University Block 31 field example form Kerans (1988) that shows permeability barrier within the upper part of the Ellenburger. (A) Initial completions (pre-1977) were above the cave-sediment-prone zone. (B) The wells were deepened after 1977 and new hydrocarbon intervals were encountered.